MASTERARBEIT | MASTER'S THESIS

Titel | Title

HRM and pyrosequencing-based identification of *Apis mellifera carnica* mtDNA in honey for product authentication and subspecies conservation

verfasst von | submitted by

Andrea Bevilacqua BSc

angestrebter akademischer Grad | in partial fulfilment of the requirements for the degree of

Master of Science (MSc)

Wien | Vienna, 2026

Studienkennzahl lt. Studienblatt | Degree programme code as it appears on the student record sheet:	UA 066 659
Studienrichtung lt. Studienblatt | Degree programme as it appears on the student record sheet:	Masterstudium Lebensmittelchemie
Betreut von | Supervisor:	Univ.-Prof. Mag. Dr. Margit Cichna-Markl

ABSTRACT

Honey is susceptible to fraud, including false declarations of origin. Since honey contains environmental DNA (eDNA), molecular approaches can be used to assess its authenticity. In particular, *Apis mellifera* DNA recovered from honey provides information on the entomological source of the product, can indirectly indicate its geographic provenance, and is relevant for the protection of native honeybee subspecies. Mitochondrial DNA (mtDNA) is especially suitable for this purpose due to its high copy number, stability, maternal inheritance, and high mutation rate.

This study aimed to develop a method to identify *A. mellifera* subspecies in honey, with particular focus on *A. m. carnica*, a subspecies native to Austria and protected in four Austrian federal states. Honey samples were selected to represent diverse geographic origins and subspecies distributions, focusing on Austrian honeys, as well as relevant European and non-European samples. Bee specimens were also collected for analysis and used as a reference. DNA extraction was optimized for both honey and bees, including the Alpine and Pannonian variant of *A. m. carnica*. Highly variable mtDNA regions were then investigated. In the ND4 gene, a region containing six diagnostic SNPs was identified and targeted using a newly designed assay (BEE 3_2), involving a biotinylated reverse primer to enable pyrosequencing (PSQ). Real-time quantitative PCR (qPCR) followed by high-resolution melting (HRM) analysis was conducted, with subsequent PSQ to confirm the results.

Using this method alone, the Alpine variant of *A. m. carnica* could be distinguished from the other subspecies commonly used by European beekeepers. However, the development of a second assay (BEE 6), targeting a single diagnostic SNP, was necessary for the more challenging discrimination of the Pannonian variant from *A. m. ligustica*. Nevertheless, BEE 6 still requires further validation. The combined HRM and PSQ approach, using these two assays together with a third assay (BEE 2_1) already established in our research group, showed promising results in distinguishing honey containing only *A. m. carnica* DNA (Alpine, Pannonian, or a mixture of both) from samples containing other subspecies. This approach may therefore support consumer protection, verification of honey authenticity, assessment of geographic origin, and conservation of this protected subspecies.

ZUSAMMENFASSUNG

Honig ist anfällig für Betrug, einschließlich falscher Herkunftsangaben. Da Honig Umwelt-DNA (eDNA) enthält, können molekulare Ansätze zur Überprüfung seiner Authentizität eingesetzt werden. Insbesondere liefert aus Honig gewonnene DNA von *Apis mellifera* Informationen über die entomologische Quelle des Produkts, kann indirekt auf die geografische Herkunft hinweisen und ist für den Schutz einheimischer Honigbienen-Unterarten relevant. Mitochondriale DNA (mtDNA) eignet sich besonders für diesen Zweck aufgrund ihrer hohen Kopienzahl, Stabilität, maternalen Vererbung und hohen Mutationsrate.

Ziel dieser Studie war die Entwicklung einer Methode zur Identifizierung von *A. mellifera*-Unterarten in Honig, mit besonderem Fokus auf *A. m. carnica*, einer in Österreich heimischen und in vier Bundesländern geschützten Unterart. Honigproben wurden ausgewählt, um unterschiedliche geografische Herkunftsgebiete und Unterartenverteilungen abzudecken, mit Schwerpunkt auf österreichischen Honigen sowie relevanten europäischen und außereuropäischen Proben. Auch einzelne Bienen wurden für die Analyse gesammelt und als Referenz verwendet. Die DNA-Extraktion wurde sowohl für Honig- als auch für Bienenproben optimiert, einschließlich der alpinen und pannonischen Variante von *A. m. carnica*. Anschließend wurden hochvariable mtDNA-Regionen untersucht. Im ND4-Gen wurde eine Region mit sechs diagnostischen SNPs identifiziert, die mit einem neu entwickelten Assay (BEE 3_2), unter Verwendung eines biotinylierten Reverse-Primers für die Pyrosequenzierung (PSQ) gezielt analysiert wurde. Es wurde eine real-time quantitative PCR (qPCR) gefolgt von einer High-Resolution-Melting (HRM)-Analyse durchgeführt, wobei anschließend die PSQ zur Bestätigung der Ergebnisse und zur weiteren Differenzierung der Subspezies eingesetzt wurde.

Mit dieser Methode allein konnte die alpine Variante von *A. m. carnica* von den anderen, in der europäischen Imkerei häufig verwendeten Unterarten unterschieden werden. Für die schwierigere Abgrenzung der pannonischen Variante von *A. m. ligustica* war hingegen die Entwicklung eines zweiten Assays (BEE 6), das auf einen einzelnen diagnostischen SNP abzielt, erforderlich. BEE 6 benötigt jedoch eine weitere Validierung. Der kombinierte HRM- und PSQ-Ansatz unter Verwendung dieser beiden Assays zusammen mit einem weiteren, in unserer Arbeitsgruppe bereits etablierten Assay (BEE 2_1) zeigte vielversprechende Ergebnisse bei der Unterscheidung von Honigproben, die nur *A. m. carnica*-DNA (alpine, pannonische oder eine Mischung beider Varianten) enthalten, von Proben mit anderen Unterarten. Dieser Ansatz könnte somit zum Verbraucherschutz, zur Überprüfung der Honig-Authentizität, zur Bewertung der geografischen Herkunft sowie zur Erhaltung dieser geschützten Unterart beitragen.

ACKNOWLEDGEMENTS

Before proceeding with the discussion, I would like to dedicate a thought to the people who have been close to me throughout this journey.

First of all, my heartfelt gratitude goes to Univ.-Prof. Mag. Dr. Margit Cichna-Markl for accepting me into her research group and for guiding me through the writing of this paper with clarity and expertise. I would also like to thank Andrijana Marijan for patiently introducing me to the laboratory methods used in this thesis, and Katharina Pühringer MSc for her precious advice and support.

Above all, I would like to thank my parents, Cristina and Romeo, who have supported me tirelessly despite the distance that separates us. You have always put me and my education first, surrounding me with encouragement and opportunities. This is not something to be taken for granted, and I am therefore immensely grateful to you for everything you have done for me. I could not ask for a better family.

Finally, I want to express my gratitude to Karl, who has always given me hope, teaching me that life always finds a way to move forward and set things right. Thank you for every sacrifice, for your humanity and generosity and for sharing with me every victory and every defeat throughout these years. You are a unique and irreplaceable person, and I feel blessed and proud to have you by my side.

Once again, thank you to all of you. This wonderful achievement is as much yours as it is mine.

TABLE OF CONTENTS

1. INTRODUCTION

Honey is a sweet substance naturally produced by honeybees from nectar or other plant secretions and is widely appreciated for its nutritional value. Its high market demand has made honey one of the most frequently adulterated food products, through sugar addition, mixing with lower-quality honey, or false declarations of botanical and geographic origin. While sugar addition has traditionally been the main focus of authenticity studies, false claims about geographic and botanical provenance are also common and relevant for consumers, who select honey based on organoleptic properties (Honrado et al., 2022) such as color, taste, and nutritional composition, closely linked to the floral and geographic source (Dodd et al., 2025).

Analysis of environmental DNA (eDNA) – a mixture of genetic material derived from pollen, honeybees, microorganisms, and other environmental sources acquired during nectar collection – has emerged in recent years as a very promising method for assessing the authenticity and quality of honey (Pathiraja et al., 2023). This complex DNA composition represents a valuable source of information that can support the determination of botanical, entomological, and geographic origin, as well as provide insights into environmental conditions (Soares et al., 2023).

Among honeybee species, *A. mellifera* is the most widespread and productive worldwide (Soares et al., 2018). The species comprises multiple subspecies distributed across defined evolutionary lineages, whose geographic distribution can, in principle, contribute to the assessment of honey origin, although this relationship may be influenced by anthropogenic activities such as queen bee trade (Honrado et al., 2022). In Europe, the Central and Eastern European lineage (C) includes two subspecies widely used in apiculture: *A. m. ligustica*, native to Italy, and *A. m. carnica*, native to Central Europe, including Austria, and parts of the Balkans (Moškrič et al., 2022; Utzeri et al., 2022). The identification and preservation of native subspecies are considered crucial to ensure genetic diversity, local adaptation, and colony survival (Fontana et al., 2018; Momeni et al., 2021).

Since honey contains degraded and low-quantity DNA, molecular analyses require genetic markers that allow highly sensitive detection. Mitochondrial DNA (mtDNA), characterized by high copy number, maternal inheritance, and relative structural stability, represents a suitable target for subspecies identification (Shokolenko & Alexeyev, 2015; Soares et al., 2018). Single nucleotide polymorphisms (SNPs) within mtDNA regions can differentiate evolutionary lineages and, in some cases, closely related subspecies (Momeni et al., 2021). Molecular approaches such as qPCR (Alexander et al., 2005; Bustin & al., 2009), HRM analysis (Druml & Cichna Markl, 2014), and PSQ (Ghemrawi et al., 2023) allow detection and confirmation of polymorphisms, enabling reliable subspecies assignment even from complex matrices such as honey.

2. AIMS

The aim of this study was to develop and evaluate molecular methods for the detection and identification of *A. mellifera* subspecies DNA in honey. Particular emphasis was placed on *A. m. carnica*, a subspecies native to Austria and legally protected in several federal states. The study should investigate whether subspecies-specific DNA signatures present in honey could be used as an indirect indicator of geographic origin and as a tool to support honey authenticity and labeling verification.

To achieve this objective, mtDNA regions with high haplotype variability should be selected and used to design and optimize molecular assays based on qPCR, HRM analysis, and PSQ. Because honey represents a challenging matrix characterized by low DNA yield and degradation, two different extraction kits should be tested and compared in order to improve DNA recovery and ensure reliable downstream molecular analyses. The study further aimed to assess the discriminatory power, robustness, and practical applicability of these methods for analyzing both honey-derived DNA and DNA extracted from individual bees.

Selected nuclear DNA (nDNA) targets should also be explored for comparison with mtDNA-based approaches. Finally, the study sought to assess whether characteristic genetic patterns in honey could be linked to geographic origin, thereby contributing to the development of analytical tools supporting the authentication of honey and the conservation of protected *A. mellifera* subspecies.

3. THEORETICAL PART

3.1. Environmental DNA (eDNA) in honey

Environmental DNA (eDNA) consists of genetic material released into the environment by living organisms and recoverable from environmental matrices, including honey. Honey represents a particularly informative eDNA reservoir due to the extensive ecological interactions of honeybees while collecting nectar. While pollen constitutes the main contributor to honey-derived eDNA, additional DNA originates from honeybees, other pollinating insects, microorganisms such as bacteria, fungi, and viruses, as well as parasites and environmental contaminants (Pathiraja et al., 2023; Soares et al., 2023).

The analysis of honey eDNA provides several layers of information. Pollen DNA can be used to determine floral sources and verify botanical origin. DNA derived from honeybees enables the identification of subspecies and may contribute to tracing entomological and geographic provenance. Microbial DNA can further reflect environmental conditions and hive health status (Soares et al., 2023).

Despite its potential, eDNA analysis in honey presents technical challenges. DNA is often highly fragmented due to enzymatic activity, honey processing, and storage conditions. Moreover, the honey matrix contains compounds capable of inhibiting polymerase chain reaction (PCR). Advances in DNA extraction protocols and sensitive molecular techniques have significantly improved the reliability of eDNA-based analyses, enabling the use of honey as a complex but informative biological matrix (Soares et al., 2023).

3.2. *A. mellifera* taxonomy and subspecies

A. mellifera is the most widespread and economically important honeybee species globally and comprises 33 described subspecies grouped into five evolutionary lineages, four of which are present in Europe: African (A), Central and Eastern European (C), Western and Northern European (M), Near Eastern and Central Asian (O) (Ilyasov et al., 2020). The last lineage (Y) consists of only *A. m. jemenitica*, which is not native to Europe (Momeni et al., 2021).

The C lineage includes two subspecies of great importance for honey production: *A. m. ligustica* and *A. m. carnica*. The latter, also known as the Carniolan honeybee, is native to southern Central Europe and the Balkan region and comprises the Alpine and the Pannonian ecotypes, both morphologically and genetically distinguishable from each other (Balazs et al., 2025; Moškrič et al., 2022; Utzeri et al., 2022).

Human-mediated breeding practices, particularly queen bee trade and crossbreeding, have altered the natural distribution of subspecies. Although these practices can enhance productivity, they may reduce genetic diversity and compromise local adaptation. Locally adapted populations generally exhibit improved survival rate, highlighting the importance of conserving endemic subspecies (Momeni et al., 2021).

Several European countries have implemented legal measures to protect native *A. m. carnica* populations, reflecting the broader EU emphasis on conserving honeybee biodiversity (Fontana et al., 2018). As for Austria, the subject of beekeeping falls under the legislative competence of the individual federal states, so each of them has its own dedicated law. To date, only four Austrian federal states have specific laws regarding this matter: Styria (explicitly allowing only the use of *A. m. carnica*), Lower Austria (no explicit ban, but practice oriented towards *A. m. carnica*), Vienna and Carinthia (only the use of *A. m. carnica* is allowed, other subspecies only with prior authorization) (Land Kärnten, 1992; Land Niederösterreich, 2014; Land Steiermark, 1998; Land Wien, 2000).

Understanding *A. mellifera* taxonomy and subspecies distribution is therefore essential for verifying the entomological origin of honey and for informing conservation strategies aimed at maintaining genetic diversity and colony fitness.

3.3. mtDNA and SNP analysis

It should be noted that some subspecies of *A. mellifera* have so far been described only based on morphology (body parts measurement and wings shape assessment), and therefore a confirmation at the molecular level is necessary. The same applies to the classification of the subspecies within the aforementioned evolutionary lines (Ilyasov et al., 2020).

To assess the taxonomic closeness between subspecies at the molecular level, methods based on mtDNA are applied, in which it is possible to highlight single nucleotide polymorphism (SNPs) (Ilyasov et al., 2020). SNPs are single-base variations in the genome that represent a widespread and stable form of genetic diversity. In *A. mellifera*, phylogenetic informative SNPs are an excellent source of information for distinguishing population structure and subspecies differentiation, allowing the identification of genetic lineages and patterns of admixture among them. Due to their abundance and discriminatory power, SNPs are widely used to infer genetic structure and ancestry relationships in bee populations (Momeni et al., 2021).

In this study, it was preferable to focus on mtDNA for several reasons. First of all, honey is a complex matrix in which DNA tends to fragment and degrade (Soares et al., 2018). However, mtDNA inside the mitochondria of eukaryotic cells is enclosed in structures called nucleoids (Bogenhagen, 2012), which are attached to the folds of the inner membrane of these organelles. Within the nucleoids, mtDNA is organized in a very compact manner, much more so than nDNA in the cell nucleus. This makes mtDNA more stable (Shokolenko & Alexeyev, 2015).

Furthermore, mtDNA is present in a remarkably high number of copies per cell (Shokolenko & Alexeyev, 2015; Soares et al., 2018), reaching hundreds or even thousands of copies of this genome of about 16 kb. This considerable number of copies is essential for the organism so that any mutations do not affect the phenotype, unless the mutant mtDNA reaches a threshold value of about 70% of the total (Shokolenko & Alexeyev, 2015).

Another important aspect is the fact that mtDNA has a higher evolutionary rate than nDNA (Allio et al., 2017; Dong et al., 2021; Soares et al., 2018). This means that mtDNA has a higher frequency of mutations, with a ratio of mtDNA to nDNA mutation rates ranging from 2 to 6 in insects. This has led to mtDNA becoming the marker of choice for phylogenetic studies (Allio et al., 2017).

Finally, a fundamental point: mtDNA is inherited exclusively through the maternal line, so a queen bee passes it entirely to all her offspring (Soares et al., 2018). This uniparental inheritance appears to confer an evolutionary advantage, as mechanisms have evolved to exclude paternal mitochondria from the zygote (Lee et al., 2023), preventing heteroplasmy and limiting potentially negative consequences of mixed mtDNA (Veeraragavan et al., 2024). Multi-parental mtDNA copies, being genetically divergent, might interact inefficiently with nDNA and fail to provide adequate cellular energy (Lee et al., 2023). In higher eukaryotes, mtDNA encodes 13 of the ~80 structural subunits of the electron transport chain (Veeraragavan et al., 2024).

SNPs have proven useful for assigning individual bees to their subspecies, but while differentiating the five lineages of *A. mellifera* is relatively easy, distinguishing closely related subspecies within the same lineage remains more challenging (Momeni et al., 2021).

Molecular methods combining qPCR and HRM analysis allow amplification of mtDNA fragments containing informative SNPs and detection of sequence variation through melting temperature (Tm) differences (Bustin et al., 2009; Druml & Cichna Markl, 2014). PSQ can then be used to confirm polymorphisms by determining the exact nucleotide sequence of targeted regions (Alexander et al., 2005; Ghemrawi et al., 2023).

The integration of these molecular approaches enables reliable assignment of honeybee subspecies even from degraded honey-derived DNA and supports investigations of honey authenticity, geographic provenance, and conservation of native *A. mellifera* populations (Soares et al., 2018; Utzeri et al., 2022).

3.4. Primer design

Primer design is a critical step in the development of PCR-based assays, as it directly affects specificity, sensitivity, and overall robustness of amplification (Bustin & Huggett, 2017; Sharma, 2020). Primers are short single-stranded DNA sequences designed to bind specifically to a target sequence, providing the starting point for DNA polymerase during PCR (Beyene, 2014; Elkins, 2013). PCR requires two primers – a forward (5') primer (hereafter referred to as Fw primer) and a reverse (3') primer (hereafter referred to as Rev primer) – that anneal to opposite strands of the target DNA and define the length of the amplified region, known as the amplicon (Beyene, 2014; Elkins, 2013).

High-quality primers bind exclusively to the target sequence, avoiding non-specific amplification, which can be verified using alignment tools such as Nucleotide BLAST (Sharma, 2020). Primer design can be broadly divided into three main phases: identification of the target sequence, *in silico* evaluation of primer properties, and experimental optimization and validation.

3.4.1. Identification of the target sequence

The first phase involves selecting an appropriate target sequence for amplification. For qPCR applications, short amplicons are preferred (ideally ≤200 bp, up to 500 bp), while sequencing-based applications typically use products of lengths suitable for the chosen platform, with primers flanking the region of interest (Elkins, 2013). However, sequencing efficiency has been shown to decline substantially beyond 140 bases (Ghemrawi et al., 2023).

For SNP genotyping techniques such as HRM analysis or PSQ, the selected amplicon must contain the polymorphic site of interest. At the same time, primer binding regions should not overlap with SNPs, as mismatches at primer annealing sites may reduce amplification efficiency and compromise genotype assignment (Piriyapongsa et al., 2009; Słomka et al., 2017).

Target sequences are typically retrieved from public databases using alignment tools such as Nucleotide BLAST, which allow verification of sequence identity and specificity by aligning candidate sequences against genomic databases. The use of accession numbers from published studies enables direct retrieval of well-characterized sequences, particularly for conserved or extensively studied genes (Ye et al., 2012).

3.4.2. *In silico* evaluation of primer properties

Once the target sequence has been identified, candidate primers are evaluated *in silico* using computational tools to predict their behavior during PCR. Key parameters include primer length, GC (guanine–cytosine) content, Tm, and the potential formation of secondary structures (such as hairpins), homodimers, or heterodimers (Elkins, 2013).

Optimal primer pairs generally exhibit similar Tm – typically between 55 and 72°C, with minimal differences between Fw and Rev primers – and a moderate GC content (40–60%) to ensure stable annealing without excessive secondary structure formation (Elkins, 2013; Sharma, 2020). Primer length usually ranges between 18 and 30 nucleotides, or more restrictively between 18 and 24 nucleotides when stringent optimization is required (Sharma, 2020).

Runs of identical bases, strong self-complementarity, and primer–primer interactions should be avoided, as they can reduce amplification efficiency and assay specificity (Elkins, 2013; Sharma, 2020).

Several online tools are commonly used for these analyses, including the Oligonucleotide Properties Calculator (oligocalc.eu), which provides estimates of Tm, GC content, primer length, and potential dimer formation (Owczarzy et al., 2008), as well as the RNAfold Webserver, which predicts secondary structures such as hairpins or self-complementary regions (Lorenz et al., 2011).

PSQ primers differ from standard PCR primers in both function and design: they initiate a linear sequencing reaction rather than exponential amplification, requiring only a single primer without matched Tm values. Nevertheless, they must still meet key criteria for reliable sequencing: adequate specificity, appropriate length and Tm, and minimal stable secondary structures (e.g., hairpins or 3' self-complementarity), which can interfere with annealing and extension (Buck et al., 1999).

3.4.3. Experimental optimization and assay robustness

Although *in silico* analyses provide valuable predictive insights, they cannot fully replicate experimental conditions. Consequently, *in vitro* optimization of PCR assays – including annealing and extension temperatures, primer concentration, and cycling parameters – is widely recognized as an essential, empirical step in assay development to ensure specificity, efficiency, and robustness of amplification (Elkins, 2013; Bustin & Huggett, 2017).

At the assay level, primer performance must remain stable under variable experimental conditions. Therefore, careful documentation of target sequences and accession numbers, followed by systematic testing of different reaction conditions, is critical to confirm the reliability and reproducibility of the amplification. This iterative process of validation is considered standard practice in PCR assay development and is widely reported in method-focused publications (Elkins, 2013; Bustin & Huggett, 2017).

In summary, successful primer design relies on accurate target selection, thorough *in silico* evaluation of primer properties, avoidance of polymorphisms in binding sites, and experimental optimization to ensure robust and reproducible PCR-based genotyping.

3.5. DNA extraction

DNA extraction consists in the purification of DNA from a biological sample, during which other cellular components such as proteins, lipids and membranes are removed in order to obtain DNA of sufficient quality for downstream analyses (Elkins, 2013; Gupta, 2019). This process requires careful handling to prevent sample contamination (Elkins, 2013).

In eukaryotic organisms, including animals and plants, DNA is contained within cells that possess an outer lipid bilayer membrane and a cytoplasm rich in proteins, sugars, lipids and inorganic ions. In addition, these cells contain membrane-bound organelles such as the nucleus, which houses the chromosomes, and mitochondria, which contain circular DNA; together, these genetic elements regulate protein synthesis. DNA molecules are highly negatively charged due to their phosphate backbone and are stabilized intracellularly by magnesium ions (Elkins, 2013).

Despite the diversity of available protocols, most DNA extraction methods share a common conceptual framework and rely on a limited number of fundamental steps (Gupta, 2019). In particular, DNA extraction generally follows three main stages: cell lysis, separation, and isolation (Elkins, 2013).

However, honey is a complex matrix that requires a sample preparation step before DNA extraction. The high sugar content and the presence of compounds such as organic acids, polyphenols, and enzymes can indeed inhibit extraction and molecular analyses if not removed (Soares et al., 2015). Furthermore, DNA in honey is present in small amounts and often degraded, making a preliminary step necessary to concentrate the biological material and reduce contaminants (Kek et al., 2018). Previous studies show that steps such as solubilization, heating, and centrifugation improve DNA yield and purity before lysis and purification steps (Lalhmangaihi et al., 2014).

After sample preparation, the first step in DNA extraction is cell lysis, which allows genetic material to be released from the cells contained in the sample. Lysis is achieved through a combination of mechanical, chemical, and thermal stimuli. In the case of a solid sample, the first step is to break it down mechanically so that the lysis buffer can subsequently act on a larger surface area. However, it should be noted that this mechanical action can also fragment the DNA itself into smaller pieces if shear forces are applied. To prevent this and obtain DNA as intact as possible, a bead-beating device is used today (Matissek et al., 2018).

Chemical lysis based on the combined action of cationic detergents like CTAB (cetyltrimethyl-ammonium bromide) (Matissek et al., 2018), chaotropic salts, and proteinase K digestion is one of the most widely used strategies for DNA extraction (Boom et al., 1990; Elkins, 2013; Tan & Yiap, 2009). Detergents disrupt lipid membranes, chaotropic agents denature proteins and inactivate nucleases, and proteinase K digests protein contaminants, thereby improving DNA purity and yield (Elkins, 2013; Wilson, 1997). In samples containing low amounts of target DNA, the addition of carrier RNA is commonly employed to enhance nucleic acid recovery and protect DNA from loss during extraction (Elkins, 2013; Hoff-Olsen et al., 1999).

Finally, DNA extraction generally proceeds through two final phases: separation and isolation. During the separation step, DNA is separated from proteins, lipids, and other cellular components. This can be achieved using organic solvent extraction, in which phenol and chloroform partition proteins and lipids into an organic phase while DNA remains in the aqueous phase (Tan & Yiap, 2009). Alternatively, DNA can be selectively bound to a solid-phase matrix, such as silica or SPE (solid phase extraction) membranes, under chaotropic conditions, while contaminants are washed away (Katevatis et al., 2017; Vandeventer et al., 2013). Some extraction protocols combine both approaches, using chemical separation followed by adsorption onto a solid phase to maximize purity and yield. Finally, during the isolation step, DNA is recovered from the solid phase or aqueous phase via elution with an appropriate buffer (Vandeventer et al., 2013).

3.6. Fluorimetry

After DNA extraction, the concentration of the recovered nucleic acids is measured. Fluorimetry relies on the principle of fluorescence to quantify specific molecules. In fact, certain compounds can absorb incoming light when it falls within a defined region of the spectrum, causing the target molecule to enter an excited state. This is immediately followed by emission of light at a longer wavelength. Fluorescence, by definition, occurs when this emission happens almost instantaneously, typically within 10^{-8} seconds after the excitation source is removed (Matissek et al., 2018).

However, DNA itself does not naturally fluoresce, so to measure its concentration via fluorimetry, specific fluorescent dyes are required, such as SYBR Green I. This dye selectively binds to double-stranded DNA by intercalating into the minor groove of the helix, and this interaction greatly increases its fluorescence. Consequently, the intensity of the emitted fluorescent signal is directly proportional to the amount of double-stranded DNA (dsDNA), which can be quantified using an external calibration curve derived through linear regression (Matissek et al., 2018).

3.7. Polymerase chain reaction (PCR)

PCR is a molecular technique developed by Kary Mullis in 1983 and used for the specific amplification of a DNA fragment from a target sequence. PCR selectively copies the sequence of interest while excluding contaminating DNA from other organisms, such as fungi, bacteria, plants, or unrelated animal DNA present in the sample. After amplification, the PCR products are detected and analyzed, allowing further characterization or quantification (Elkins, 2013; Matissek et al., 2018).

PCR involves a series of essential steps that take place in a device called a thermocycler. Initially, the double-stranded DNA is heated to 95°C to separate it into its complementary single strands in a process called denaturation. When the reaction mixture cools to around 50-60°C, the primers (described in Section 3.1.) bind to their specific target sequences, thereby defining the boundaries of the amplicon. During the subsequent elongation phase, DNA polymerase synthesizes the DNA segment located between the primers, effectively doubling the amount of DNA. These cycles are repeated multiple times, typically up to 40, as further repetitions do not increase yield due to substrate depletion, accumulation of by-products, and reduced activity of the polymerase enzyme. Thanks to this exponential amplification (ideally 2^n, with n representing the number of cycles), the target DNA is amplified to dominate over the background DNA (Matissek et al., 2018). All of these steps are shown in Figure 1.

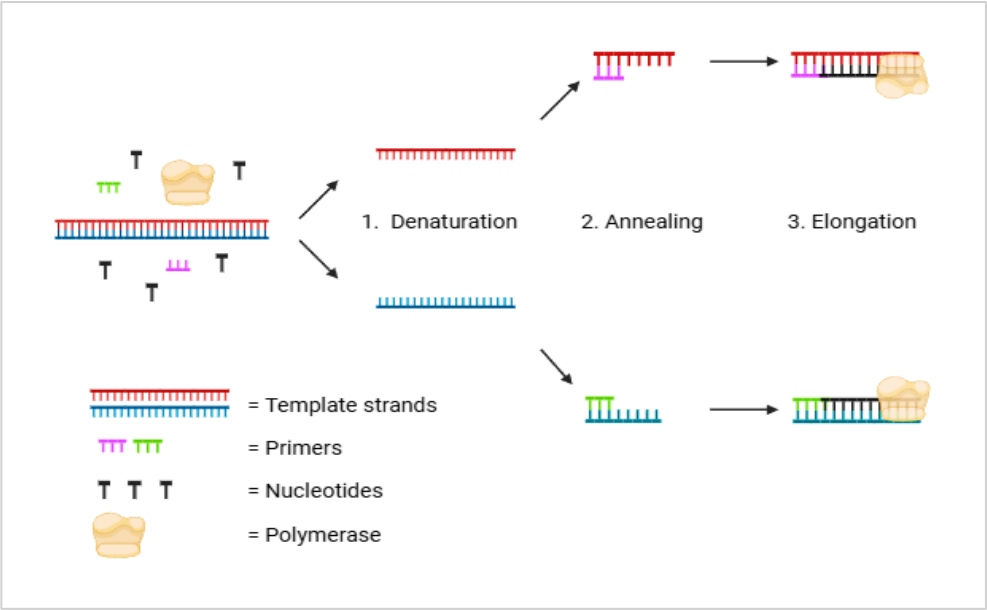

Figure 1
Schematic representation of one single PCR cycle (created with BioRender.com)

For PCR to work, the following components are required (Elkins, 2013).

1. A buffer, typically Tris-HCl, which adjusts the reaction pH to approximately 8.3 under standard conditions (25°C), providing optimal chemical conditions for the reaction. At higher temperatures, the pH decreases to around 6.8, a condition that favors Taq DNA polymerase activity and fidelity (Elkins, 2013; Evans, 2009).
2. $MgCl_2$, as Mg^{2+} ions act as essential cofactors for Taq DNA polymerase and play a critical role in catalytic activity, DNA–primer binding, and reaction specificity (Bermek et al., 2011).
3. Deoxyribonucleoside triphosphates (dNTPs), namely 2'-deoxyadenosine 5'-triphosphate (dATP), 2'-deoxycytidine 5'-triphosphate (dCTP), 2'-deoxyguanosine 5'-triphosphate (dGTP) and 2'-thymidine 5'-triphosphate (dTTP), which constitute the fundamental building blocks required for DNA synthesis during the elongation phase (Evans, 2009).
4. Taq DNA polymerase, an enzyme originally isolated from the thermophilic bacterium *Thermus aquaticus*, which catalyzes the formation of phosphodiester bonds through the stepwise incorporation of dNTPs into the growing DNA strand (Elkins, 2013).
5. DNA primers (Fw and Rev), as discussed in Section 3.1.
6. Template DNA previously extracted from the sample of interest, which serves as the substrate to which primers anneal and on which the polymerase synthesizes complementary strands.

Except for the primer and the template DNA, which must be added by the operator, the other listed components are usually already included in commercially available master mix solutions. Some master mixes also include KCl, which stabilizes the reaction, and bovine serum albumin (BSA), which can bind PCR inhibitors (Elkins, 2013).

Furthermore, in qPCR, fluorescent reporters, such as dyes that bind to double-stranded DNA (e.g., SYBR Green I) or sequence-specific fluorescent probes, are also included in the reaction mixture (Bustin et al., 2009).

3.7.1. Real-time PCR (qPCR)

qPCR is a molecular amplification technique that extends conventional PCR by allowing quantitative measurement of DNA during the amplification process itself, enabling the analysis of relative gene expression or DNA copy number in real time. This is achieved through fluorimetric detection of the amplified DNA as the reaction progresses, which requires the use of a thermocycler equipped with an optical detection system capable of monitoring fluorescence throughout the PCR cycles (Elkins, 2013; Matissek et al., 2018). The result is an amplification curve as shown in Figure 2.

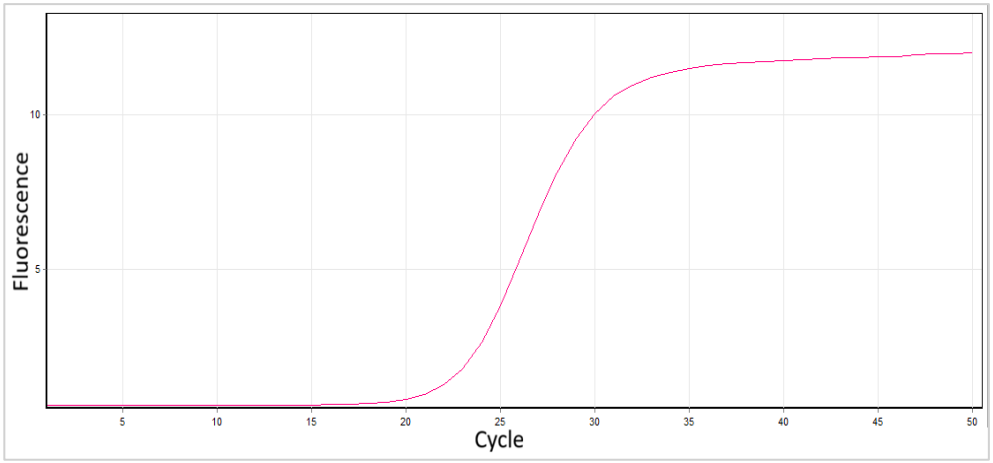

Figure 2

Example of an amplification curve in qPCR (screenshot from Rotor-Gene Q software)
Fluorescence increases with the number of cycles, with an exponential amplification phase and a final plateau.

To enable quantification, the amplification must be made optically detectable. Two main detection strategies are commonly employed. In the first approach, intercalating fluorescent dyes, such as SYBR Green I, bind to double-stranded DNA, resulting in an increase in fluorescence proportional to the total amount of dsDNA present in the reaction. Because this method detects all dsDNA non-specifically, including potential amplification byproducts, a melting curve analysis is recommended to verify product specificity (Matissek et al., 2018).

The second approach relies on sequence-specific fluorescent probes or primers. These probes are oligonucleotides that hybridize to a target sequence located between the primer binding sites and are typically labeled with a fluorophore at the 5' end and a quencher at the 3' end. When the probe is intact, fluorescence emission is suppressed due to the proximity of the quencher. During the elongation phase of PCR, the DNA polymerase degrades the hybridized probe via its 5'→3' exonuclease activity, separating the fluorophore from the quencher and generating a fluorescence signal. The resulting increase in fluorescence is directly proportional to the amount of specific PCR product formed (Matissek et al., 2018).

As amplification proceeds, qPCR enables determination of the threshold cycle (Ct), defined as the cycle number at which the fluorescence signal crosses a predefined threshold. The Ct value provides quantitative information about the initial amount of target DNA present in each sample (Elkins, 2013).

Overall, qPCR allows real-time monitoring of DNA amplification, providing both qualitative and quantitative data. Its main advantages include high sensitivity and specificity, a wide dynamic range, and the ability to quantify targets during the exponential phase without post-PCR analysis. qPCR is versatile, suitable for gene quantification, expression studies, and high-throughput analyses. However, qPCR also has limitations: it requires expensive equipment and reagents, careful primer/probe design, and skilled operators. Results can be affected by sample quality or inhibitors, and the method is limited to known target sequences, making it unsuitable for discovering unknown or highly variable sequences (Smith & Osborn, 2009).

3.8. High resolution melting (HRM) analysis

High-resolution melting (HRM) analysis is a fast, straightforward, and resource-efficient method for detecting genetic variation and is widely applied in genotyping and mutation scanning workflows (Kim et al., 2023). The technique was first developed in 2003 and is based on PCR amplification of a target sequence in the presence of a fluorescent intercalating dye, generating dsDNA amplicons (Wittwer et al., 2003). These amplicons may harbor genetic variants such as SNPs, which directly influence their thermal denaturation behavior (Kim et al., 2023).

HRM analysis relies on the gradual dissociation of PCR products from dsDNA into single-stranded DNA (ssDNA) as temperature is progressively increased in a qPCR thermocycler. During this process, dye release from the DNA duplex causes a decrease in fluorescence that is continuously monitored (Ririe et al., 1997). Melting behavior is primarily determined by the nucleotide sequence of the amplicon, with GC content and fragment length as the main determinants of duplex thermodynamic stability (Erali et al., 2008; Tong & Giffard, 2012).

Because guanine–cytosine (GC) base pairs are stabilized by three hydrogen bonds, whereas adenine–thymine (AT) pairs have two, GC-rich and longer amplicons exhibit higher thermal stability and melt at higher temperatures than AT-rich or shorter fragments (Druml & Cichna-Markl, 2014; Tong & Giffard, 2012). This relationship between Tm, nucleotide composition, and fragment length underlies HRM sensitivity to sequence variation. Even a single base substitution, such as an AT-to-GC transition, alters duplex stability and produces a measurable shift in melting behavior, enabling discrimination of single-nucleotide differences (Tong & Giffard, 2012).

By monitoring fluorescence as a function of temperature, HRM detects sequence variation through differences in melting curve shape and position, enabling discrimination of small variants such as SNPs, unlike conventional melting curve analysis, which mainly reveals nonspecific products. Genotyping is performed by comparing melting profiles: homozygous genotypes typically show Tm shifts, whereas heterozygous genotypes produce characteristic curve shape changes due to heteroduplex formation (Erali et al., 2008; Kim et al., 2023). Thus, HRM integrates sequence-dependent DNA melting with real-time fluorescence detection for sensitive and precise variant discrimination.

After PCR amplification, the analysis is commonly performed by plotting fluorescence intensity as a function of temperature, producing a characteristic sigmoidal curve as the DNA duplex progressively denatures and fluorescence decreases (Ririe et al., 1997). An example is shown in Figure 3. The Tm is defined as the temperature at which approximately 50% of the DNA molecules are denatured and 50% are still double-stranded; this corresponds to the point of maximal rate of fluorescence decrease, which can be identified as the inflection point of the fluorescence–temperature curve (Wittwer et al., 2003).

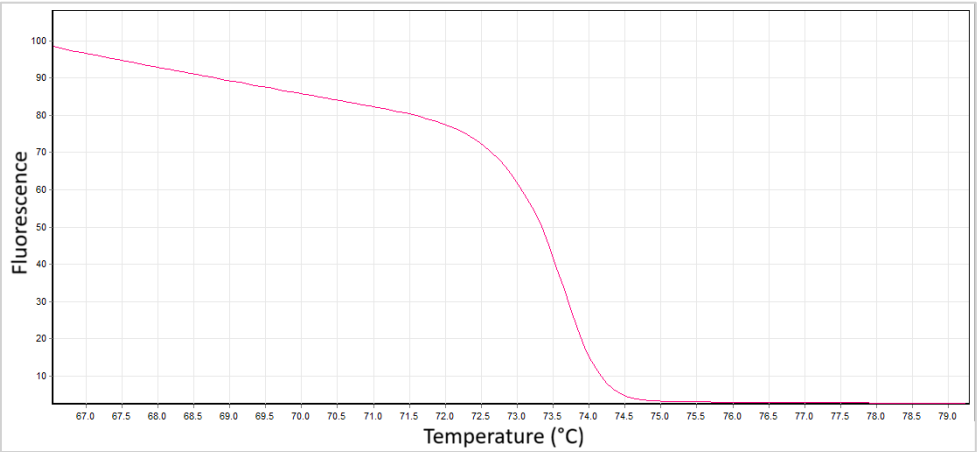

Figure 3

Example of a melting curve (fluorescence intensity vs. temperature)
Fluorescence decreases with increasing temperature, and the inflection point of the curve corresponds to the Tm.

For improved visualization and comparison of melting behavior across samples, fluorescence data are commonly transformed into the negative first derivative of fluorescence with respect to temperature (−dF/dT). In derivative melting plots, DNA melting transitions appear as distinct peaks, whose maxima correspond to the Tm of the respective amplicons (Wittwer et al., 2003; Van der Meulen & Hellemans, 2021). An example is shown in Figure 4. Raw fluorescence curves and derivative plots therefore provide complementary representations of the same denaturation process, with derivative plots enhancing the detection and discrimination of subtle melting differences and being widely adopted in qPCR-based HRM analyses (Wittwer et al., 2003; Van der Meulen & Hellemans, 2021).

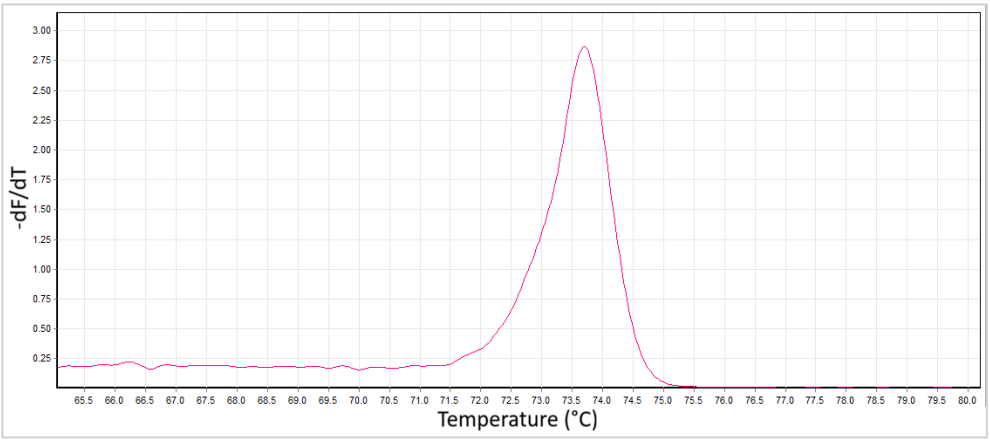

Figure 4

Example of a derivative melting plot (negative first derivative of fluorescence vs. temperature)
The peak maximum corresponds to the Tm.

In specific applications, such as the analysis of mtDNA regions, HRM profiles may reflect the presence of multiple DNA sequences within a sample. When samples derive from multiple individuals, distinct melting profiles arise due to variation among mtDNA haplotypes. In honey, for example, the coexistence of mtDNA from multiple *A. mellifera* individuals – each homoplasmic within its own cells – generates complex HRM profiles that may resemble heterozygous patterns. Importantly, these profiles result from mixtures of homoplasmic mtDNA originating from different maternal lineages, rather than from true heterozygosity at a single genetic locus (Rocha et al., 2018; Parakatselaki & Larsson, 2021). The differences between homozygous and heterozygous patterns are shown in Figure 5 and Figure 6.

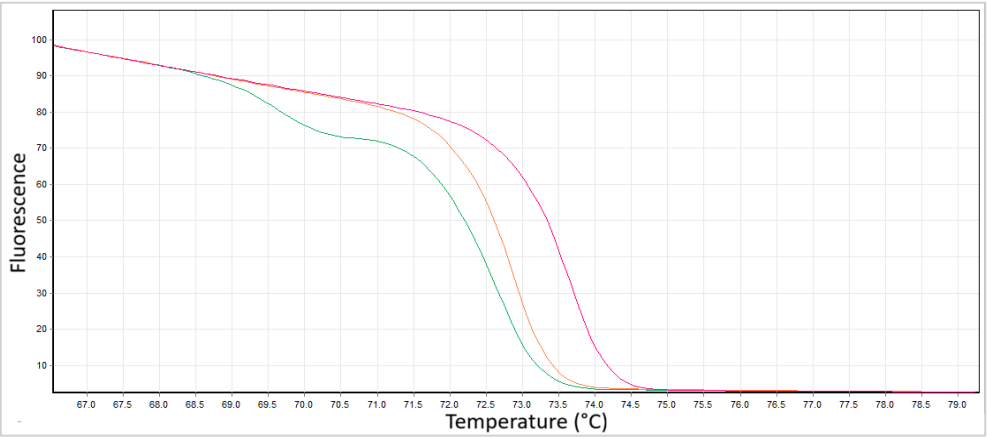

Figure 5

Comparison of three melting curves

The pink curve (sample PBF18.3) and the orange curve (sample PBF7.2) belong to mtDNA extracts from two different subspecies of *A. mellifera* and are therefore homozygous, while the green curve (sample P91) belongs to an mtDNA extract from a honey sample, which contains mtDNA from multiple different *A. mellifera* individuals and therefore represents a mix of homozygotes. This simulates a heterozygous pattern, which can show a more complex melting curve compared to the perfectly sigmoidal melting curves of homozygous patterns.

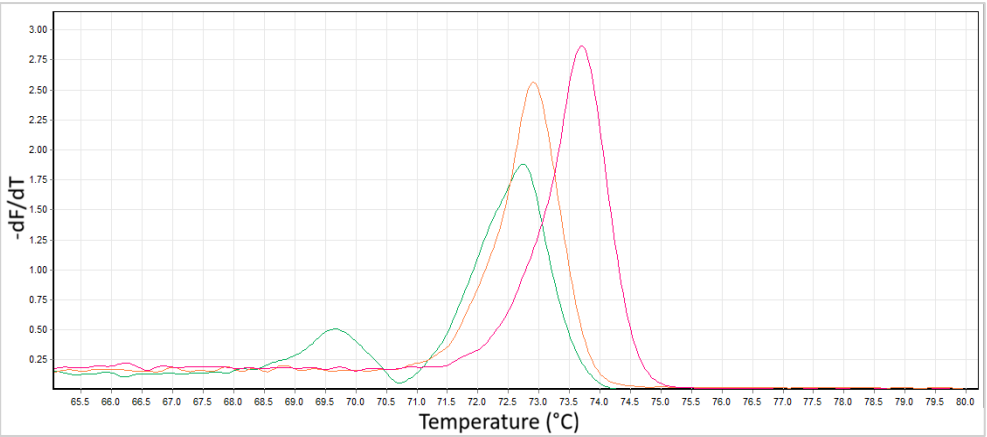

Figure 6

Comparison of three derivative melting plots

The pink plot (sample PBF18.3) and the orange plot (sample PBF7.2) belong to mtDNA extracts from two different subspecies of *A. mellifera* and are therefore homozygous, while the green plot (sample P91) belongs to an mtDNA extract from a honey sample, which contains mtDNA from multiple different *A. mellifera* individuals and thus represents a mix of homozygotes. This simulates a heterozygous pattern, which can show a broader/asymmetric peak or even more than one peak, as in this case.

A key step in HRM data processing is normalization, which involves adjusting the raw fluorescence data so that all melt curves are scaled to a common range, typically with pre-melting fluorescence set near 100% and post-melting fluorescence near 0% (Erali et al., 2010). This process minimizes technical variability arising from differences in DNA concentration, dye incorporation, or instrument sensitivity, ensuring that differences in melting curve shape and position reflect true sequence differences rather than artifacts of signal intensity or PCR efficiency. The use of normalized fluorescence data as a prerequisite for further analysis remains standard practice in modern HRM applications (Zappe & Cichna-Markl, 2024).

Beyond genotyping, HRM analysis allows the identification and exclusion of non-specific amplification products, such as primer dimers, based on their characteristic melting profiles. These non-specific products typically exhibit lower Tm than target amplicons and can be readily distinguished in HRM curves, for example by the presence of melting peaks below approximately 75°C, which are excluded from downstream analysis (Fraser et al., 2023).

Overall, HRM analysis provides a cost-effective, rapid, and closed-tube approach for genotyping and mutation scanning, enabling high-throughput analysis with minimal post-PCR handling. However, its accuracy and discriminatory power depend strongly on experimental factors such as DNA quality, primer design, and instrument resolution, which may limit the reliable distinction of closely related variants and must therefore be carefully optimized to ensure robust HRM performance (Słomka et al., 2017).

3.9. Pyrosequencing (PSQ)

PSQ is a sequencing-by-synthesis approach that monitors nucleotide incorporation through chemiluminescent signals generated by inorganic pyrophosphate (PPi) release, enabling real-time acquisition of sequence information. It is widely used in genetic and epigenetic studies. Before sequencing, extracted DNA is amplified by PCR using a pair of primers, one of which is modified with a biotin molecule at the 5' end. The resulting biotinylated strands are immobilized on streptavidin-coated magnetic beads, which serve as a support for sequencing primer (Seq primer) hybridization (Ghemrawi et al., 2023).

The PSQ process consists of successive single-base extensions that progressively determine the template strand sequence. During each nucleotide incorporation event, PPi is released by DNA polymerase and detected through a chemiluminescent reaction (Ghemrawi et al., 2023).

The steps that follow the incorporation of a nucleotide in PSQ are shown in Figure 7. The four dNTPs are added to the reaction mixture one after the other in a predetermined order. When a complementary nucleotide is incorporated (1), the polymerase releases PPi (2), which is converted to ATP by the enzyme ATP sulfurylase in the presence of adenosine 5'-phosphosulfate (APS) (3). The ATP produced provides energy to luciferase, which catalyzes the oxidation of luciferin with emission of light (4) (Ghemrawi et al., 2023). The intensity of the generated light signal is proportional to the amount of ATP produced and is detected by a specialized camera. Since the order of nucleotide addition is known, the DNA sequence can be directly deduced from the observed signal. Subsequently, a degrading enzyme, apyrase, removes the unincorporated nucleotides and ATP, preparing the system for the next cycle (5).

The chemiluminescent signal is graphically represented as a series of peaks in relation to nucleotide dispensations, generating a trace called a pyrogram. These profiles are generally easy to interpret: the presence or absence of peaks, as well as their height, provide direct information about the DNA sequence (Ghemrawi et al., 2023). However, PSQ shows reduced accuracy in homopolymeric regions, with error rates increasing as the length of consecutive identical bases grows, which can make exact base calling challenging (Ivády et al., 2018).

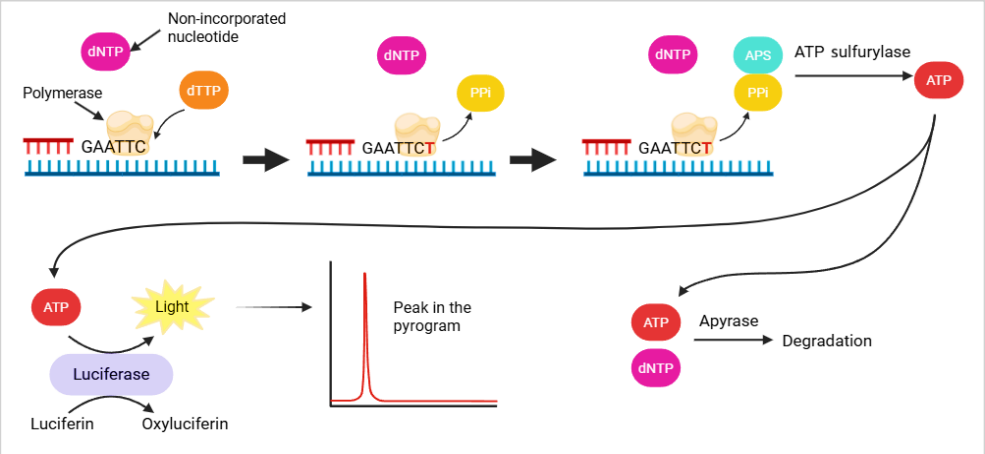

Figure 7

Schematic representation of the cascade of reactions following the incorporation of a nucleotide in PSQ, resulting in a peak in the pyrogram (created with BioRender.com)

Following nucleotide incorporation (1), pyrophosphate (PPi) is released (2) and converted into ATP by ATP sulfurylase in the presence of adenosine 5'-phosphosulfate (APS) (3). The ATP produced drives the luciferase reaction, resulting in light emission proportional to the number of incorporated nucleotides (4). Unused nucleotides and ATP are then degraded by apyrase, preparing the system for the next cycle (5).

In the current configuration of PSQ instruments, such as Qiagen's PyroMark series, one or more target sequences are initially identified and then amplified by PCR. The system requires the use of at least two PCR primers and one Seq primer. The amplification primers are designed in the regions flanking the target, while one of the two PCR primers is labeled with biotin at the 5' end. The Seq primer is generally designed in the opposite orientation to the biotinylated strand and is complementary to it. Although it is possible to amplify relatively long fragments, up to about 400 bp, the sequencing efficiency decreases significantly beyond 140 bases. This decline is attributed to a progressive dilution effect of the enzymes during nucleotide incorporation cycles, which reduces their catalytic activity (Ghemrawi et al., 2023).

To facilitate the development of reliable assays, design tools are available to assess the risk of nonspecific pairings and other issues, such as hairpin or dimer formation, taking thermodynamic aspects into account. From an operational standpoint, PSQ analysis requires attention to several key aspects. First, the instrument must undergo maintenance washes and pre-wash cycles to ensure cartridge cleanliness; diagnostic tests of the injectors can be performed regularly as a quality control measure. Second, streptavidin-coated magnetic beads must be thoroughly vortexed before use, as uneven bead distribution can compromise repeatability. Since the beads settle rapidly, using electronic pipettes and frequently agitating the container reduces pipetting errors. Finally, the enzymes and substrates used are sensitive to light and repeated freeze–thaw cycles and should not be vortexed; careful handling is therefore essential to ensure reaction efficiency and successful PSQ analysis (Ghemrawi et al., 2023).

4. EXPERIMENTAL PART

4.1. Honey and *A. mellifera* samples

A total of 141 honey samples and 45 *A. mellifera* individuals were analyzed in this study. Their geographic origin is summarized in Tables 1 and 2.

Table 1

Geographic origin of honey samples

Macro-area	Sub-area	Country	Federal state / region	n
Europe (n=113)	EU (n=108)	Austria (n=45)	Lower Austria	11
			Salzburg	5
			Styria	5
			Upper Austria	5
			Burgenland	4
			Carinthia	3
			Vienna	3
			Vorarlberg	3
			n. a.	6
		Italy (n=17)	Lazio	2
			Sicily	2
			Trentino	2
			Liguria	1
			Veneto	1
			n. a.	9
		Germany		10
		Bulgaria		7
		Greece		6
		Hungary		6
		France		3
		Romania		3
		Croatia		2
		Spain		2
		Czech Republic		1
		Estonia		1
		Latvia		1
		Slovakia		1
		Slovenia		1
		Mixed EU Honey		2
	Non-EU (n=5)	North Macedonia		3
		Bosnia and Herzegovina		1
		Russia		1
Non-Europe (n=7)		Turkey		2
		Australia		1
		Brazil		1
		New Zealand		1
		Nigeria		1
		Yemen		1
Mixed EU / non-EU Honey				13
n. a.				8
Total				141

Table 2

Geographic origin of A. mellifera samples

Area	Country	Federal state / region	n
EU (n=39)	Austria (n=29)	Lower Austria	13
		Carinthia	8
		Salzburg	5
		Upper Austria	2
		Styria	1
	Italy (n=9)	Trentino	4
		Lazio	3
		Liguria	2
	Croatia		1
Non-EU (n=6)	Bosnia and Herzegovina		4
	North Macedonia		2
Total			45

Section 9.4. includes two additional tables (Tables 26 and 27) providing further details on the samples, including the types of honey declared by the producer or beekeeper and the *A. mellifera* subspecies indicated by the beekeeper. As shown in these tables, a variety of honey types was collected to evaluate the performance of each method across slightly different matrices. *A. mellifera* individuals were obtained from beekeepers who identified them as *A. m. carnica*, *A. m. ligustica*, *A. m. macedonica*, or declared hybrids. Some beekeepers noted that colonies are periodically renewed, as hybridization can occur over time. Therefore, complete genetic purity at the subspecies level cannot be guaranteed.

The honey samples were distinguishable by sensory characteristics such as color (ranging from nearly transparent to dark brown), viscosity, and the rare presence of foreign material, likely of plant origin. The bees from different colonies were also distinguishable: drones were noticeably larger than workers from the same colony, and individuals varied in size, color patterns, and wing shape and length. However, morphological identification of the bees was not the focus of this study.

The honey samples were obtained from supermarkets, organic stores, online orders, or directly from beekeepers. In the latter case, beekeepers also provided deceased *A. mellifera* individuals from their own hives, which had contributed to producing the same honey. Details on the selection of honey and *A. mellifera* samples based on their geographic origin are reported in Section 5.1.

All samples were assigned identification codes. Honey samples were labeled with the prefix P or HP followed by a number in the order of collection. *A. mellifera* samples were labeled with PBF or HPBF followed by a number in the order of collection. The dual labeling reflects the fact that another honey study was conducted in parallel by our research group; although this distinction was not required for the present study, the same labeling was retained for consistency.

Once obtained and coded, honey samples were stored at room temperature, away from heat sources and direct sunlight, while the bees were stored at −20°C. DNA extracts obtained from the samples were also stored at −20°C.

4.2. Primer design

As described in Section 3.1, primer design is divided into three main phases: identification of the target sequence, *in silico* evaluation of primer properties, and experimental optimization and validation.

For the present study, sequences rich in SNPs within the mitochondrial ND4 gene were sought. An initial primer pair, designated BEE 3, was identified but proved suboptimal and was progressively modified, ultimately leading to the development of the BEE 3_2 primer pair, which demonstrated significantly improved performance. In addition to BEE 3_2, a complementary assay, BEE 6, was also developed. The decision-making process that guided these modifications, along with the results of *in silico* testing for the final assays (BEE 3_2 and BEE 6) and their experimental optimization, are described in detail in Section 5.2.

4.2.1. Identification of the target sequence

The initial steps, performed using NCBI BLAST (National Center for Biotechnology Information's Basic Local Alignment Search Tool), are illustrated in Figure 8. First, the sequence of interest (here, the BEE 3_2 Fw primer) is entered into the "Enter Query Sequence" field (1); alternatively, a genomic sequence accession number from a paper or article can be used. The species of interest (*A. mellifera*) can also be specified (2). In the "Program Selection" section, the tool is set to search for highly similar sequences (3), and the search is initiated by clicking "BLAST" (4). The NCBI results consist of a list with the best matches at the top (Figure 9), from which the sequence of interest can be selected—in this example, the one outlined in red.

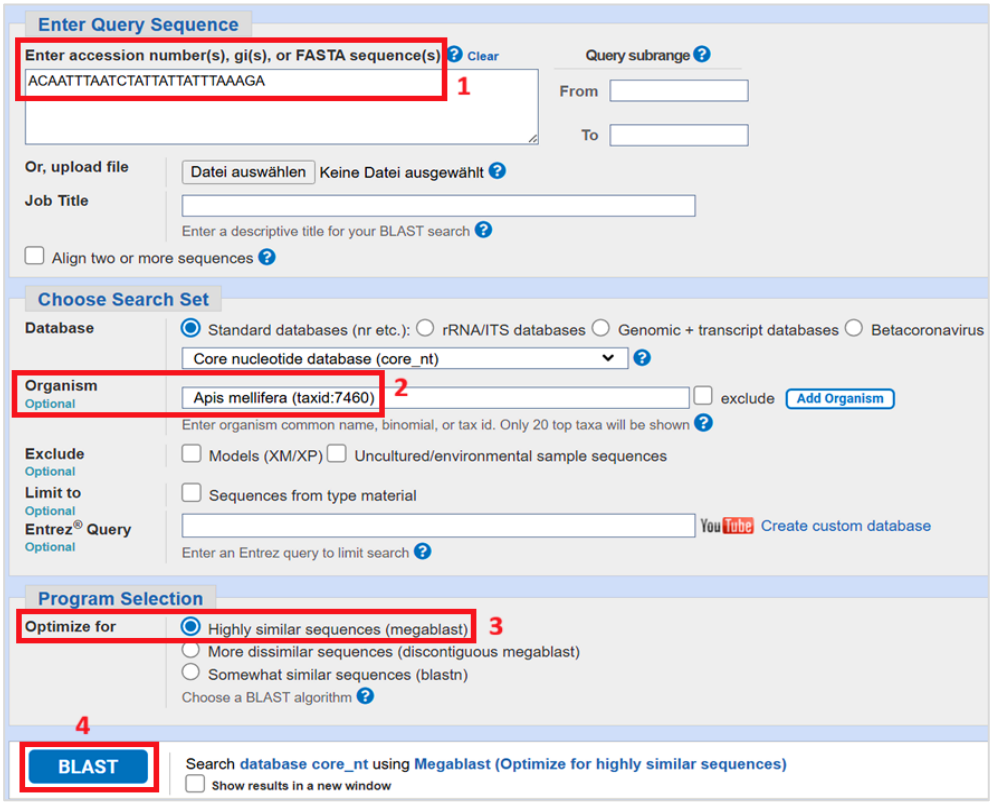

Figure 8

Initial BLAST query input for the BEE 3_2 Fw primer, including sequence entry and species selection (screenshot from the NCBI Nucleotide BLAST online tool - BLAST: Basic Local Alignment Search Tool)

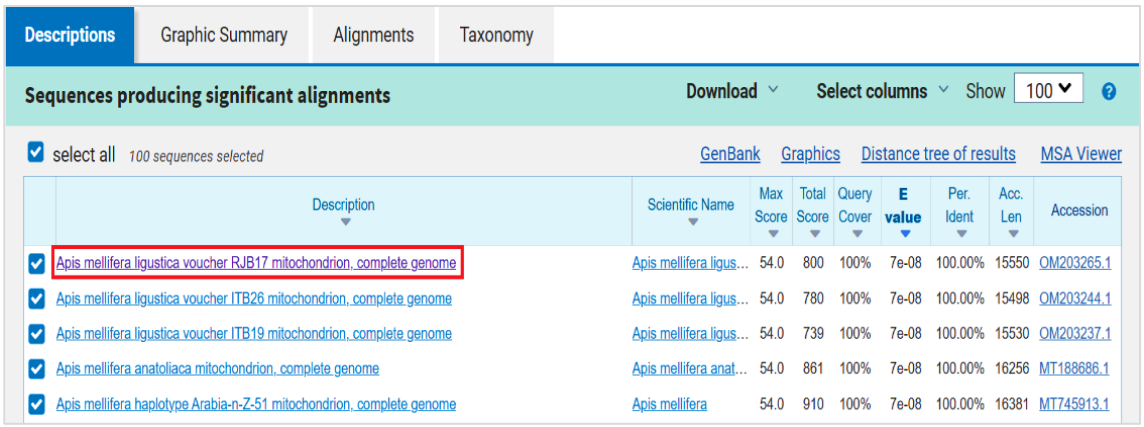

Figure 9

BLAST search results showing sequences with the highest similarity to the query at the top of the list (screenshot from the NCBI Nucleotide BLAST online tool - BLAST: Basic Local Alignment Search Tool)

At this stage, the Graphics function can be selected, as shown in Figure 10. This generates a graph like the one in Figure 11, representing the two DNA strands. Once the first and last nucleotides of the target sequence (in this case, the Fw primer of BEE 3_2) have been identified, a marker can be applied by right-clicking on the chosen nucleotide and selecting "Set New Marker At Position." The result is shown in Figure 12, with the first and last nucleotides of the Fw primer highlighted in blue and green, respectively.

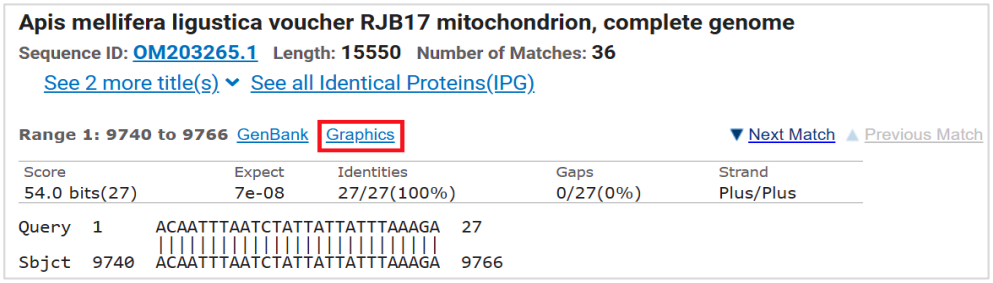

Figure 10

Selection of the Graphics function to visualize the BLAST alignment (screenshot from the NCBI Nucleotide BLAST online tool - BLAST: Basic Local Alignment Search Tool)

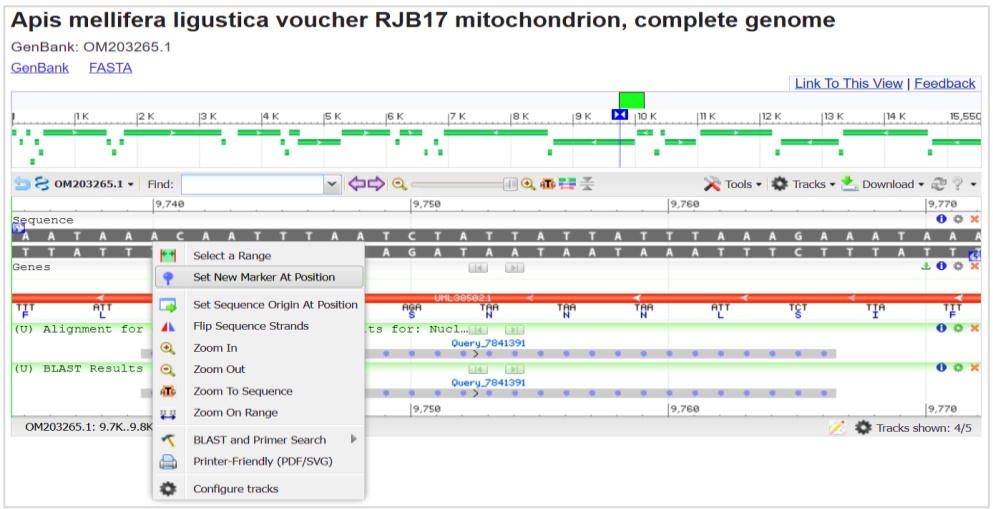

Figure 11

Representation of the two DNA strands generated by the Graphics function with marker being set (screenshot from the NCBI Nucleotide BLAST online tool - BLAST: Basic Local Alignment Search Tool)

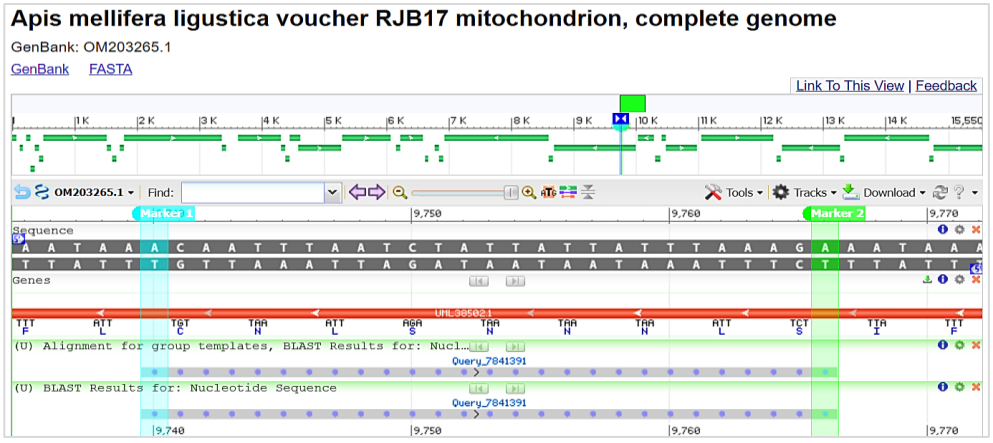

Figure 12

Marked positions of the first and last nucleotides of the Fw primer in the BEE 3_2 sequence, highlighted in blue and green (screenshot from the NCBI Nucleotide BLAST online tool - BLAST: Basic Local Alignment Search Tool)

Finally, once the sequence of interest is marked, the "Tools" drop-down menu is opened and the option "Sequence Text View" is selected, as shown in Figure 13. At this point, the Sequence View appears, where it is easy to find the nucleotides previously marked in blue and green, as shown in Figure 14. This procedure was applied to each subspecies of interest of *A. mellifera*, in search of SNPs within the amplicon.

Using this approach, it was possible to select the sequences to be amplified in the ND4 gene, ensuring that there were no SNPs within the primer binding sites and that the amplicons contained a sufficient number of SNPs. Additionally, it allowed the annotation of sequence differences among the various *A. mellifera* subspecies, enabling their genetic discrimination. Details on the selected primers, the amplicon, and the SNPs it contains are provided in Section 5.2, along with the full decision-making process that led to the development of the final BEE 3_2 assay and the complementary BEE 6 assay.

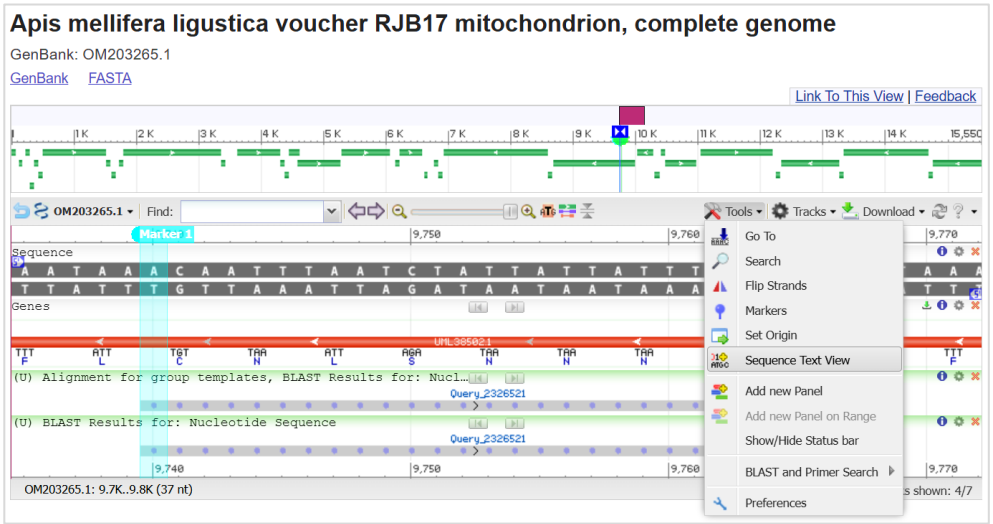

Figure 13

Selecting the "Sequence Text View" option from the Tools drop-down menu in Nucleotide BLAST (screenshot from the NCBI Nucleotide BLAST online tool - BLAST: Basic Local Alignment Search Tool)

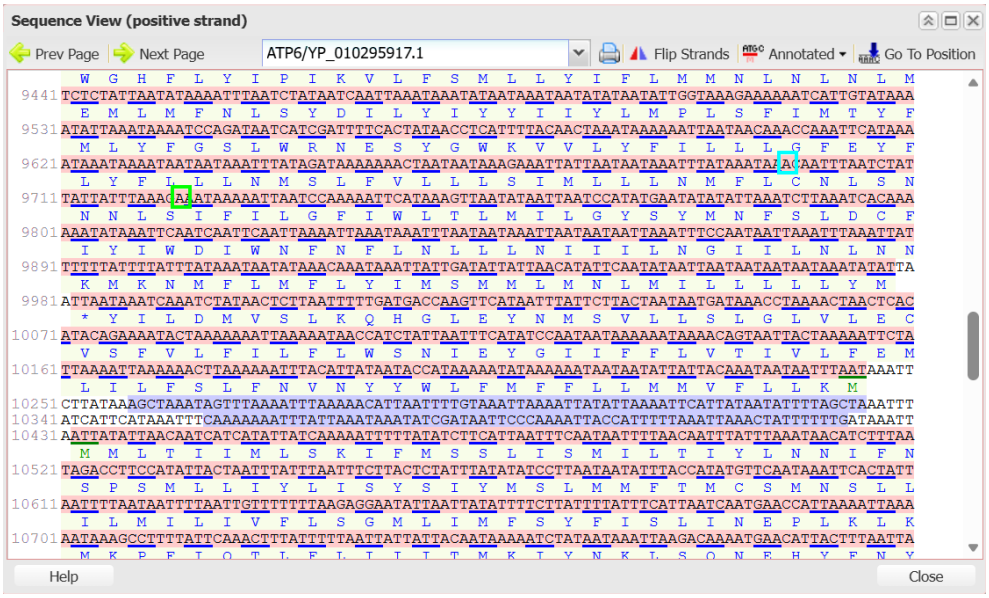

Figure 14

Sequence Text View displaying the previously marked nucleotides in blue and green (screenshot from the Nucleotide BLAST online tool - BLAST: Basic Local Alignment Search Tool)

4.2.2. *In silico* evaluation of primer properties

To verify the correct performance of the designed primers, several key parameters were defined and *in silico* tests were carried out using online tools. This approach made it possible to obtain theoretical predictions about how the primers are expected to behave during qPCR. However, it is important to note that these analyses provide only predictive insights and must be followed by experimental validation, as *in vitro* tests may yield results that differ from those obtained *in silico*.

First, it was verified that the Fw and Bio-Rev primers – where the Rev primer was biotinylated to enable subsequent PSQ – had Tm as similar as possible. For this purpose, the Oligonucleotide Properties Calculator, a general online tool for calculating oligonucleotide properties such as Tm and GC content, available at *oligocalc.eu*, was used. Figure 15 shows a screenshot of this online tool as used to calculate the parameters of the Fw primer for the BEE 3_2 assay. The primer sequence must be entered in the "Nucleotide base codes" field at the top (1) so that the calculator can perform the calculations. It is also important to select the correct type of molecule, in this case ssDNA (2). The parameters given particular attention include the primer length (3), its GC content (4), and the salt-adjusted Tm (5). The "salt-adjusted" option is selected because it allows the calculator to provide a value that better reflects actual experimental conditions of the PCR reaction, which occurs in a buffer containing salts rather than in pure water (von Ahsen et al., 2011).

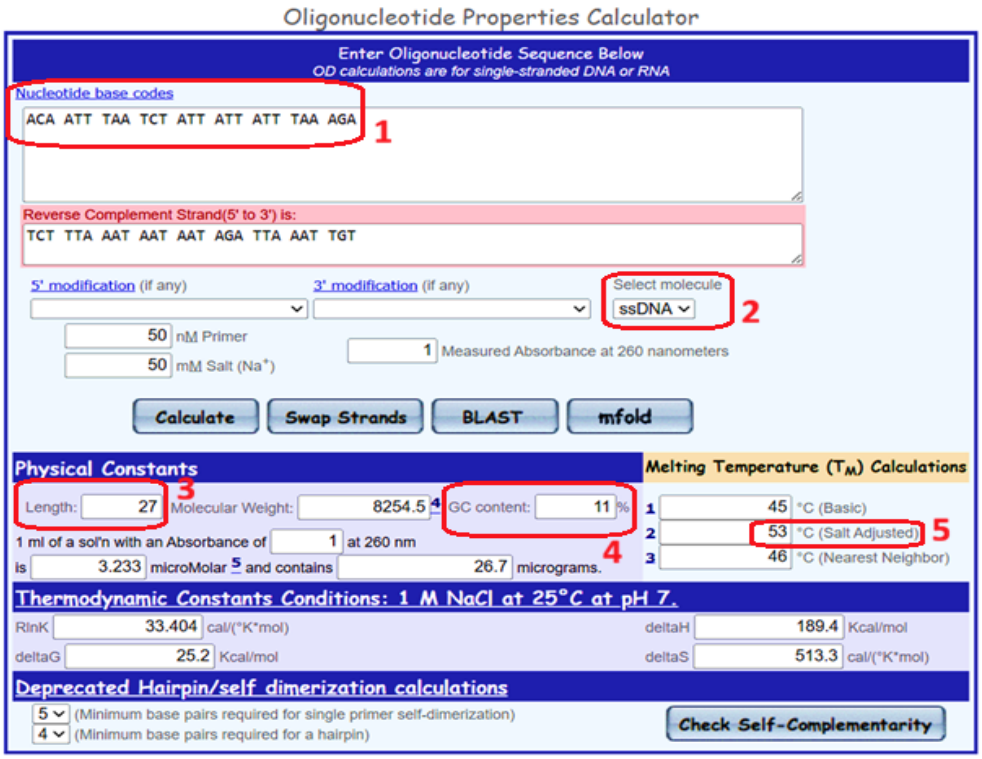

Figure 15

Screenshot of the Oligonucleotide Properties Calculator showing the BEE 3_2 Fw primer (https://oligocalc.eu/)

Highlighted numbers indicate: (1) nucleotide sequence input, (2) molecule type selection (ssDNA), (3) primer length, (4) GC content, and (5) salt-adjusted Tm. Adapted from Oligonucleotide Properties Calculator.

The same calculator was used to evaluate the Bio-Rev primer and, subsequently, the Seq primer, which is employed for PSQ but not for qPCR. The results obtained using the Oligonucleotide Properties Calculator for both the BEE 3_2 and BEE 6 assays are presented in Section 5.2.2.

Once it was verified that all the primers had appropriate Tm, GC content, and length, the next *in silico* test was performed using the RNAfold Webserver, an online bioinformatics tool that predicts the secondary structure of nucleic acid molecules from their nucleotide sequence. The user interface of the tool is shown in Figure 16, as used to calculate the parameters of the Fw primer for the BEE 3_2 assay. The primer sequence was first entered into the "Sequence Input" field (1). Subsequently, "DNA parameters" were selected under the "Energy Parameters" option to enable analysis of DNA molecules (2). The formation of secondary structures, such as hairpins, was then evaluated at 37°C and at a temperature 1°C below the previously calculated Tm (52°C in this case) (3).

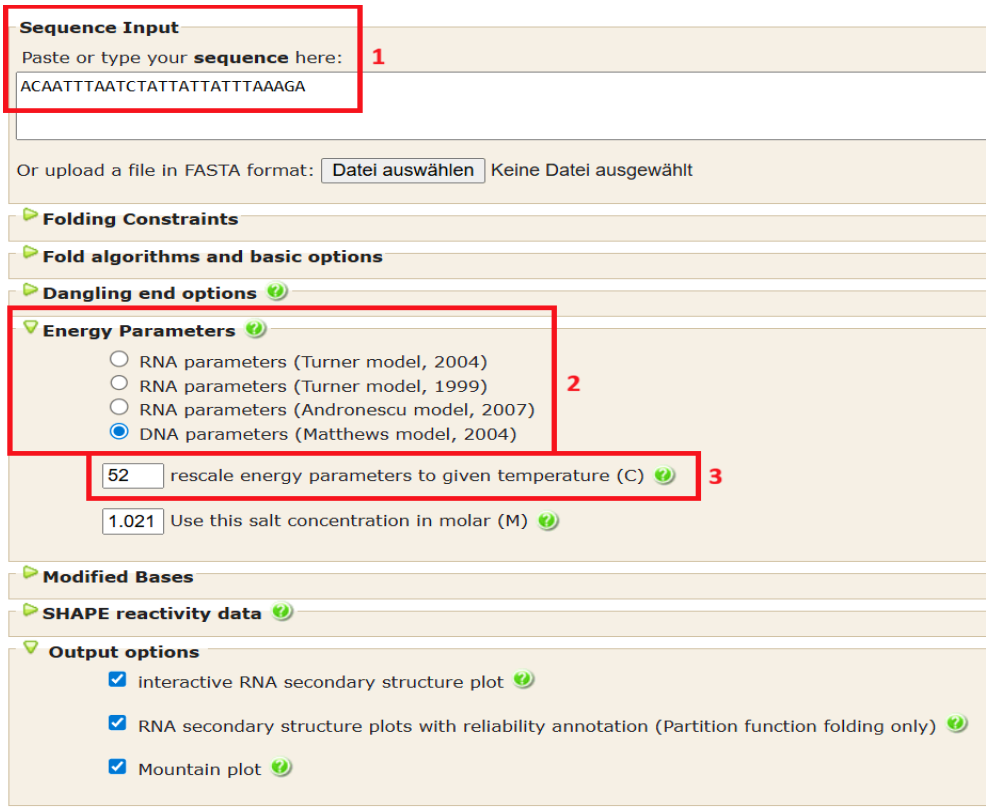

Figure 16

Screenshot of the RNAfold Webserver user interface for in silico analysis of the BEE 3_2 Fw primer (https://rna.tbi.univie.ac.at/cgi-bin/RNAWebSuite/RNAfold.cgi)

Highlighted areas indicate: (1) primer "Sequence Input" field, (2) selection of "DNA parameters" under the "Energy Parameters" option, and (3) temperature setting used to rescale energy parameters (52°C). Adapted from RNAfold Webserver.

The obtained RNAfold diagrams display the base-pairing probabilities of a primer at a given temperature. Red indicates a low probability of pairing, meaning that the nucleotide is unlikely to participate in forming a secondary structure, as such a structure would be unstable. In contrast, blue indicates a high probability of pairing, meaning that the nucleotide is likely to be involved in forming a secondary structure, as it would be more stable. The RNAfold diagrams obtained for the BEE 3_2 and BEE 6 primers are shown in Section 5.2.2.

Finally, the last *in silico* test was conducted using the online tool OligoAnalyzer. This tool allows the evaluation of potential homodimer formation of individual primers, as well as heterodimer formation between Fw and Rev primers. More negative ΔG (Gibbs free energy change) values indicate a higher probability of stable dimer formation. In general, primers showing no more than 6 contiguous complementary base pairs in predicted dimers and relatively weak interactions are considered suitable for PCR applications, as in this case (Owczarzy et al., 2008).

Figure 17 illustrates an example of the evaluation of potential homodimer formation of individual primers, as well as heterodimer formation, for the BEE 3_2 assay. In the OligoAnalyzer user interface, the sequence of interest (in this case, the Fw primer) is entered in the input field (1). The user can then select, on the right-hand side, whether to calculate self-dimer formation for this primer or heterodimer formation with the Bio-Rev primer (2). If "hetero-dimer" is selected, the tool prompts the user to enter the secondary sequence, as shown for the BEE 3_2 Bio-Rev primer marked in red in Figure 18.

Figure 17

Example of homodimer and heterodimer analysis performed with the OligoAnalyzer online tool (https://www.idtdna.com/calc/analyzer)

In this case, the BEE 3_2 Fw primer sequence is entered in the input field (1), and the user can select whether to evaluate self-dimer formation or heterodimer formation with the Bio-Rev primer (2).

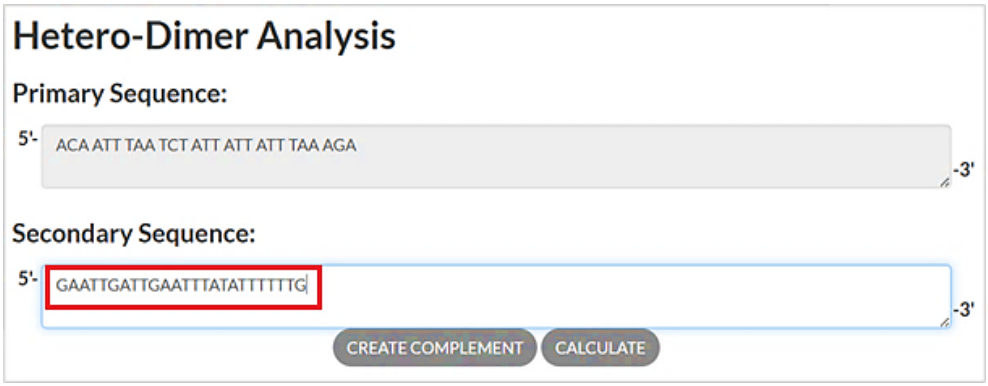

Figure 18

Evaluation of heterodimer formation for the BEE 3_2 assay using the OligoAnalyzer online tool (https://www.idtdna.com/calc/analyzer)

The BEE 3_2 Bio-Rev primer sequence (highlighted in red) is used as secondary sequence, while the Fw primer serves as the primary sequence for the calculation.

The OligoAnalyzer results for homodimer formation of the BEE 3_2 Fw, Bio-Rev, and Seq primers, as well as the heterodimer analysis between the BEE 3_2 Fw and Bio-Rev primers, are presented in Section 5.2.2, together with the results for the BEE 6 primers.

The primers that were deemed suitable following *in silico* evaluation were finally ordered from the chemical company Sigma-Aldrich and received in lyophilized form.

4.2.3. *In vitro* optimization and validation of the PCR assay

To determine the optimal experimental conditions for the developed assays, *in vitro* evaluation was performed following the *in silico* assessment. A preliminary qPCR was thus performed for all assays using the QuantStudio 5 Real-Time PCR System (Thermo Fisher Scientific). This instrument is equipped with VeriFlex temperature zone technology, which allows simultaneous testing of multiple annealing and elongation temperatures within a single qPCR run, facilitating rapid and efficient optimization of *in vitro* PCR conditions (Bustin & Huggett, 2017). All procedures were performed wearing nitrile gloves, and work surfaces were cleaned with DNA-ExitusPlus IF before and after handling.

Since the primers were delivered in lyophilized form, they first needed to be reconstituted. To do this, the pellets were collected at the bottom of their vials by a brief centrifugation. They were then diluted with RNase-free water and divided into aliquots under a sterile laminar flow hood. The specific volumes of RNase-free water required to achieve a final primer concentration of 100 µM are provided in the technical datasheets accompanying the Sigma-Aldrich primer pairs.

After adding the appropriate volume of RNase-free water to each vial, the solutions were vortexed three times for ten seconds at five-minute intervals, for a total of 20 min. Finally, each primer solution (Fw, Bio-Rev, and Seq) was aliquoted into 200 µL Eppendorf tubes, with each tube containing 10 µL of a 100 µM primer solution. The diluted primers were finally stored at −20°C.

For BEE 3_2, the following combinations of annealing (Ta) and elongation (Te) temperatures were evaluated:

- Ta 50°C / Te 56°C;
- Ta 50°C / Te 58°C;
- Ta 51.5°C / Te 56°C;
- Ta 51.5°C / Te 58°C.

The Ta were selected based on the calculated Tm of the BEE 3_2 primer pair (53°C), from which 1.5°C and 3°C were subtracted. The Te of 56°C and 58°C were selected to match the short length of the BEE 3_2 amplicon and to complement the tested Ta (50°C and 51.5°C). Testing these two closely spaced Te allowed empirical identification of the combination that provided efficient extension of the AT-rich BEE 3_2 amplicon while minimizing nonspecific amplification and primer–dimer formation, as previously observed for AT-rich templates (Bustin & Huggett, 2017; Dhatterwal et al., 2017). The cycling conditions and temperature profile used for BEE 3_2 qPCR optimization and subsequent HRM analysis are displayed in Table 3.

Table 3

Cycling conditions and temperature profile used for BEE 3_2 qPCR optimization and subsequent HRM analysis

Step		Time	Temperature	Repeat
Hold 1	Denaturation, activation of polymerase	5 min	95°C	
Cycling 1	Denaturation	15 s	94°C	Number of cycles: 50
	Annealing	30 s	50-51.5°C	
	Elongation	30 s	56-58°C	
Hold 2	Final elongation	10 min	56-58°C	
Hold 3	Denaturation	1 min	95°C	
Hold 4	Strand pairing	1 min	40°C	
HRM	HRM	-	60-95°C	0.025°C/s; 90s; gain opt 70

In the event of insufficient amplification, higher primer concentrations could have been tested; however, increased primer concentrations often promote primer–dimer formation. Therefore, a single primer concentration of 0.2 µM was used throughout this optimization step. To monitor primer–dimer formation and to exclude contamination, no-template control (NTC) wells were included. These wells contained the same master mix and primers, but 2 µL of RNase-free water instead of DNA extract.

The reagents used for this optimization experiment were prepared as shown in Table 4, resulting in a final primer concentration of 0.2 µM. The total volume of prepared reagents was sufficient for all 24 wells (including NTC) used in this preliminary test, with a 10% excess. Each well contained a final reaction volume of 20 µL, consisting of 18 µL of master mix (including primers and RNase-free water for dilution) and 2 µL of DNA extract, or 2 µL of RNase-free water in the case of NTCs.

Table 4

Composition of the BEE 3_2 qPCR Master Mix for a 24-well QuantStudio optimization experiment

Reagent	Volume (µL)
Rnase-free water	190.08
2x TypeIt HRM PCR master mix	264.00
Primer 10 µM Fw	10.56
Primer 10 µM Bio-Rev	10.56
Total	475.2

The two DNA extracts used for this test were obtained from known *A. mellifera* individuals. Each extract, along with the NTC, was tested in duplicate under the four Ta and Te combinations described above, resulting in 24 wells.

The same QuantStudio optimization assay was conducted for the BEE 6 primer pair as well. Different combinations of Ta and Te were tested using three *A. mellifera* DNA extracts and a NTC. The following conditions were evaluated:

- Ta 51°C / Te 58°C;
- Ta 51°C / Te 60°C;
- Ta 51°C / Te 62°C;
- Ta 53°C / Te 58°C;
- Ta 53°C / Te 60°C;
- Ta 53°C / Te 62°C.

The cycling conditions and temperature profile used for BEE 6 qPCR optimization and subsequent HRM analysis are displayed in Table 5.

Table 5

Cycling conditions and temperature profile used for BEE 6 qPCR optimization and subsequent HRM analysis

Step		Time	Temperature	Repeat
Hold 1	Denaturation, activation of polymerase	5 min	95°C	
Cycling 1	Denaturation	15 s	94°C	Number of cycles: 50
	Annealing	30 s	51-53°C	
	Elongation	30 s	58-60-62°C	
Hold 2	Final elongation	10 min	58-60-62°C	
Hold 3	Denaturation	1 min	95°C	
Hold 4	Strand pairing	1 min	40°C	
HRM	HRM	-	60-95°C	0.025°C/s; 90s; gain opt 70

The reagents used for this optimization experiment were prepared as shown in Table 6, resulting in a final primer concentration of 0.2 µM. The total volume of prepared reagents was sufficient for all 48 wells (including NTC) used in this preliminary test, with a 10% excess. Each well contained a final reaction volume of 20 µL, consisting of 18 µL of master mix (including primers and RNase-free water for dilution) and 2 µL of DNA extract, or 2 µL of RNase-free water in the case of NTCs.

Table 6
Composition of the BEE 6 qPCR Master Mix for a 48-well QuantStudio optimization experiment

Reagent	Volume (µL)
Rnase-free water	380.16
2x TypeIt HRM PCR master mix	528.00
Primer 10 µM Fw	21.12
Primer 10 µM Bio-Rev	21.12
Total	950.4

The three DNA extracts used for this test were obtained from known *A. mellifera* individuals. Each extract, along with the NTC, was tested in duplicate under the six Ta and Te combinations described above, resulting in 48 wells.

Among the tested combinations, the lowest Ct values were identified in order to determine the optimal Ta and Te combinations for each assay. Under these conditions, the absence of primer–dimer formation in the NTC wells was also verified and confirmed by HRM analysis. The results of these preliminary qPCR assays for the optimization of both BEE 3_2 and BEE 6 assays are presented in Section 5.2.3.

4.3. DNA extraction

To extract DNA from honey samples and from various individuals of *A. mellifera* belonging to different subspecies, two different extraction methods were used, namely DNeasy mericon Food Kit (Qiagen, Hilden, Germany) and BioSPE PureGenNucleo cfDNA kit (Affinisep, Petit-Couronne, France). All procedures were performed wearing nitrile gloves, and work surfaces were cleaned with DNA-ExitusPlus IF before and after handling.

The DNeasy mericon Food Kit was used for DNA extraction of both honey samples and bee specimens, whereas the BioSPE PureGenNucleo cfDNA kit was tested exclusively on honey samples. The reasons for this choice are explained in detail in Section 5.3.

4.3.1. Extraction with DNeasy mericon Food Kit (Qiagen)

The DNeasy mericon Food Kit is specifically designed for the isolation of high-quality nucleic acids from a wide range of raw and processed food matrices, while effectively limiting the co-extraction of PCR inhibitors. DNA extraction was performed according to the manufacturer's optimized protocol, which involves CTAB-based lysis, removal of inhibitory compounds by precipitation, and a chloroform extraction step prior to column-based purification. Before DNA isolation, samples underwent a preliminary preparation step, which differed depending on whether the material consisted of honey or *A. mellifera* specimens.

Preliminary sample preparation of honey samples

For honey samples, a preliminary sample preparation step was performed prior to DNA extraction using the DNeasy mericon Food Kit. Briefly, 15.0 g of honey were weighed into a 50 mL centrifuge tube and diluted to volume with RNase-free water. Samples were incubated in a thermomixer at 50°C for 10 min with agitation at 800 rpm. After incubation, tubes were shaken by hand and then centrifuged for 10 min at 4500 ×g at 20°C, resulting in the formation of visible pellets.

The supernatant was carefully discarded, and the pellet was resuspended in 0.5 mL of RNase-free water by gentle pipetting. The resuspended pellet was then transferred into a bead-beating tube containing two beads and subjected to mechanical disruption using the FastPrep bead-beating device with a pre-saved program (details are shown in Table 7). Following bead-beating, the beads were removed, and DNA extraction was completed according to the DNeasy mericon Food Kit protocol.

Table 7

Pre-saved homogenization program for the FastPrep-24 5G bead-beating device

Speed (m/s)	Adapter	Time (s)	Lysing Matrix	Quantity (mg)	Cycles
6	QuickPrep	40	M	150	3

Note: M = Lysing Matrix type M (as described in the FastPrep-24 5G manual).

Preliminary sample preparation of *A. mellifera* specimens

Bee samples (whole bee) were cut into small pieces and weighed into bead-beating tubes. Two beads and 1 mL of lysis buffer were added to each tube, and the samples were subjected to mechanical disruption using the FastPrep instrument. Following bead-beating, the beads were removed, and DNA extraction was completed according to the DNeasy mericon Food Kit protocol.

DNeasy mericon Food Kit (Qiagen) extraction from honey and *A. mellifera* samples

Following preliminary sample preparation and bead-beating, the treatment of honey and bee samples diverged slightly.

Honey: After bead-beating and beads removal, 200 mg of the processed honey sample were transferred into a new 2.0 mL microcentrifuge tube. For cell lysis, 1 mL of lysis buffer and 2.5 µL of Proteinase K solution were added, and the mixture was vortexed for 15 s. Samples were incubated at 60°C for 30 min with agitation at 1000 rpm.

Bees: After bead-beating and beads removal, 2.5 µL of Proteinase K solution were added directly to the disrupted bee samples. Samples were incubated at 60°C for 30 min with agitation at 1000 rpm.

After these lysis steps, DNA extraction was performed identically for both honey and *A. mellifera* samples using the DNeasy mericon Food Kit, following the manufacturer's protocol. Note: a suitable aliquot of the elution buffer was also placed in an microcentrifuge tube in the thermomixer from these initial steps, so that it remained heated until its subsequent use.

After the lysis incubation, samples were placed on ice for 5 min. The lysates were then centrifuged for 5 min at 2500 ×g at room temperature. Meanwhile, 500 µL of chloroform was added to a new 2.0 mL microcentrifuge tube. After centrifugation, 700 µL of the supernatant from each sample was transferred into the tube containing chloroform and vortexed for 15 s. Samples were centrifuged again for 15 min at 14000 ×g. During this centrifugation, 1 mL of PB buffer (binding buffer) was added to a fresh 2.0 mL microcentrifuge tube.

Following centrifugation, 250 µL of the upper aqueous phase was transferred into the tube containing PB buffer and mixed by vortexing. The mixture was then applied to the purple DNeasy mericon spin column. First, 650 µL of the sample was added to the column and centrifuged at 17900 ×g for 1 min; the flow-through was discarded. The step was repeated with an additional 600 µL of the sample, and the flow-through was again discarded.

The columns were washed with 500 µL of AW2 buffer (wash buffer) and centrifuged at 17900 ×g for 1 min, discarding the flow-through. A second centrifugation was performed to dry the column. Finally, columns were placed into 1.5 mL microcentrifuge tubes, and 50 µL of elution buffer was applied. After incubation at 60°C for 5 min, DNA was eluted by centrifugation at 17900 ×g for 1 min.

4.3.2. Extraction with BioSPE PureGenNucleo cfDNA kit (Affinisep)

The BioSPE PureGenNucleo cfDNA kit provides a convenient, all-in-one method for isolating, purifying, and concentrating circulating cell-free DNA and RNA from biological fluids such as human plasma or urine. For this study, the kit's protocol designed for urine samples was modified to allow extraction of DNA from honey.

Before use, some reagents had to be diluted according to the instructions provided with the kit. Carrier RNA was mixed with 1550 µL of Elution Buffer and used immediately, while the portion not used right away was divided into aliquots and stored at −20°C for later use. The Binding Buffer was prepared by adding the volume of isopropanol indicated on the original container, whereas Wash Buffer 1 and Wash Buffer 2 were prepared by adding the volumes of ethanol specified on their respective containers. All buffers were mixed thoroughly after the addition of alcohol to ensure homogeneity before proceeding with cfDNA extraction.

15.0 g of honey were weighed into a 50 mL tube and brought to volume with RNase-free water up to the mark. Samples were incubated in a thermomixer at 50°C and 800 rpm for 10 min, then briefly shaken by hand to ensure thorough mixing. The mixture was centrifuged at 4500 ×g for 10 min at 20°C, producing visible pellets. The supernatant was discarded, and the pellet was resuspended in 0.5 mL of RNase-free water, mixing thoroughly to recover all material from the tube walls. The resuspended pellet was transferred to a bead-beating tube containing two beads and 1 mL of lysis buffer, then processed using the bead-beating device with the pre-saved program shown in Table 7. After disruption, the tube was vortexed and flipped over several times.

1 mL of the disrupted honey was then transferred to a 5 mL microcentrifuge tube and combined with 125 µL of Proteinase K and 5 µL of carrier RNA (0.2 µg/µL). The mixture was vortexed for 30 s and incubated at 60°C for 30 min. Following incubation, 3600 µL of binding buffer was added, the sample was vortexed, and the mixture was placed on ice for 5 min. The lysate was applied to the spin column in six consecutive 800 µL aliquots, centrifuging at 16000 ×g for 1 min and discarding the flow-through after each spin.

Columns were washed sequentially with 600 µL of Wash Buffer 1, 750 µL of Wash Buffer 2, and 750 µL of ethanol, centrifuging at 16000 ×g for 1 min and discarding the flow-through after each wash. To dry the columns, they were centrifuged at 16000 ×g for 3 min and then incubated at 56°C for 10 min. Columns were transferred to 1.5 mL microcentrifuge tubes, and 60 µL of elution buffer was added. After 3 min incubation at room temperature, DNA was eluted by centrifugation at 16000 ×g for 1 min. The elution step was repeated once to maximize DNA recovery.

Following completion of the extraction, DNA concentrations of the extracts were determined by fluorimetry, and the extracts were subsequently stored at −20°C.

4.3.3. Concentration determination with Invitrogen Qubit 4 Fluorimeter

DNA concentration was measured using the Qubit dsDNA HS Assay Kit (Invitrogen). Prior to use, the Qubit Buffer and dye solution were vortexed to ensure homogeneity. The required volumes of Buffer and dye were calculated using the fluorimeter's Reagent Calculator based on the number of DNA extracts, plus the two standards provided with the kit for the calibration curve.

For assay preparation, Buffer and dye were combined in a 2.0 mL microcentrifuge tube and vortexed. For each DNA extract and standard, 190 µL of the prepared Buffer-dye solution was added to a Qubit assay tube, followed by 10 µL of DNA extract or standard. The tubes were briefly vortexed and incubated at room temperature for 2 min.

Finally, fluorescence measurements were performed on the Qubit 4 using the dsDNA HS Assay protocol. Sample DNA concentrations were determined from the calibration curve generated with the two standards. A detailed comparison of DNA yield from honey using the Affinisep and Qiagen extraction kits is presented in Section 5.3.

4.4. Real-time PCR (qPCR)

PCR preparations were carried out in three physically separated laboratories to minimize the risk of contamination; a dedicated laboratory coat was used in each laboratory. All procedures were performed wearing nitrile gloves, and work surfaces were cleaned with DNA-ExitusPlus IF before and after handling. DNA extracts, primer pairs, PCR master mix, and a metal cooling plate were stored at −20°C in our laboratory. The metal cooling plate comprised 72 tube positions and was used during PCR setup.

For transportation to the other laboratories, the primer pair, RNase-free water, 2× Type-it HRM PCR Master Mix, a cooling bag, and the metal cooling plate were placed in a polystyrene container. Preparation of the PCR master mix was performed in a separate laboratory. Prior to preparation, the required volumes of all components were calculated.

DNA extracts were almost always analyzed in duplicate, and a NTC was always included in duplicate. Accordingly, a full PCR assay using a single primer pair consisted of 35 DNA extracts analyzed in duplicate plus one NTC in duplicate, resulting in the use of all 72 tube positions. An Excel spreadsheet routinely used within the research group was employed to calculate the required volumes of reagents based on the number of DNA extracts included in each assay.

The amount of Fw and Bio-Rev primer depended on the target primer concentration selected for the assay. However, all assays applied in this study – namely BEE 3_2, BEE 6, and the previously developed BEE 2_1 assay already established in the research group – were performed using an optimized primer concentration of 0.2 µM. All assays were conducted using a final reaction volume of 20 µL, including reagents and either DNA extract or NTC.

Table 8 illustrates an example of a full PCR setup with all 72 tube positions occupied and the corresponding volumes of reagents, primers, and DNA extracts or NTC.

Table 8

Example of a full PCR setup and corresponding reagent volumes

Primer concentration in the master mix solution	0.2 µM
Scale (used wells)	72 (+10%)
Components of the master mix solution	
Rnase-free water	570.24 µL
2x TypeIt HRM PCR master mix	792.00 µL
Primer 10 µM Fw	31.68 µL
Primer 10 µM Bio-Rev	31.68 µL
Total	1425.6 µL
Mastermix solution per well	18 µL
DNA-extract 2.5 ng/µL	2 µL

Two considerations apply to Table 8. The calculated volumes correspond to a full PCR setup using 72 tube positions, with an additional 10% included, as indicated by the “Scale” value. Furthermore, DNA extracts were required to have a maximum concentration of 2.5 ng/µL. Extracts exceeding this concentration were diluted to 2.5 ng/µL using RNase-free water prior to pipetting for the PCR assay. In addition to this adjustment, honeybee DNA extracts were further diluted 1:10 to minimize potential matrix effects and to ensure that the fluorescence signal during the early PCR cycles remained low. All of these steps were performed in our laboratory.

First, the reagents (master mix and RNase-free water), primers, and samples, all stored at −20°C, were thawed. The primers had previously been reconstituted and aliquoted into 10 µL portions at a concentration of 100 µM, as described in Section 4.2.3. As indicated in Table 8, the calculations were based on a working primer concentration of 10 µM; therefore, the primers were diluted 1:10 with 90 µL of RNase-free water to reach the desired concentration, followed by brief vortexing. All of these steps were also performed in our laboratory.

The subsequent steps were carried out in a second laboratory under a sterile laminar flow hood. The master mix solution was prepared in a 2 mL microcentrifuge tube by pipetting the volumes specified in Table 8. The preparation began with the addition of RNase-free water, followed by the master mix (briefly vortexed prior to pipetting), and finally the Fw and Bio-Rev primers (also briefly vortexed before addition). Once all components were combined, the entire master mix solution in the 2 mL tube was briefly vortexed to ensure thorough mixing. At this stage, at least 4 µL of RNase-free water was also pipetted into a small, dedicated microcentrifuge tube, which would later serve as NTC.

The strip tubes specifically designed for the Rotor-Gene Q thermocycler were labeled according to their intended positions in the rotor and then placed in the 72-position metal cooling plate. 18 µL of the master mix solution were pipetted into each strip tube, and the tubes were subsequently closed with strip caps.

The master mix, RNase-free water, and diluted primers were returned to the freezer, while the DNA extracts from honeybee or honey samples were placed in a polystyrene box along with the metal plate containing the prepared strip tubes and the ice bag. The entire setup was then transported to a third laboratory, where the following steps were performed under a sterile laminar flow hood. At this stage, 2 µL of each DNA extract or 2 µL of RNase-free water (for NTC) were pipetted into the corresponding strip tubes already containing the master mix solution. Finally, the strip tubes were closed again with the strip caps.

The metal plate containing the strip tubes, now ready for PCR, was returned to the polystyrene box with the ice bag, together with the DNA extracts. The DNA extracts were then returned to the freezer in our laboratory. The final step took place in a separate room of the second laboratory mentioned earlier, where the Rotor-Gene Q thermocycler is located. The strip tubes were loaded into the rotor of the thermocycler in the order corresponding to their previously assigned labels and secured with the device's dedicated rotor ring, and the thermocycler lid was then closed.

At this stage, the PCR run was set up using the Rotor-Gene Q Series software. This software allows the user to define the optimal Ta and Te for each specific primer pair and assay, creating a custom temperature program. These settings can be adjusted in the "Edit Profile" window, as illustrated in Figure 19, which shows the selection of the Ta within the Cycling section. Tables 9–11 report the optimized temperature programs for qPCR and HRM corresponding to the BEE 3_2 and BEE 6 assays, and for the BEE 2_1 assay, which was already in use within our research group; the design and optimization of the latter are therefore not presented in this thesis.

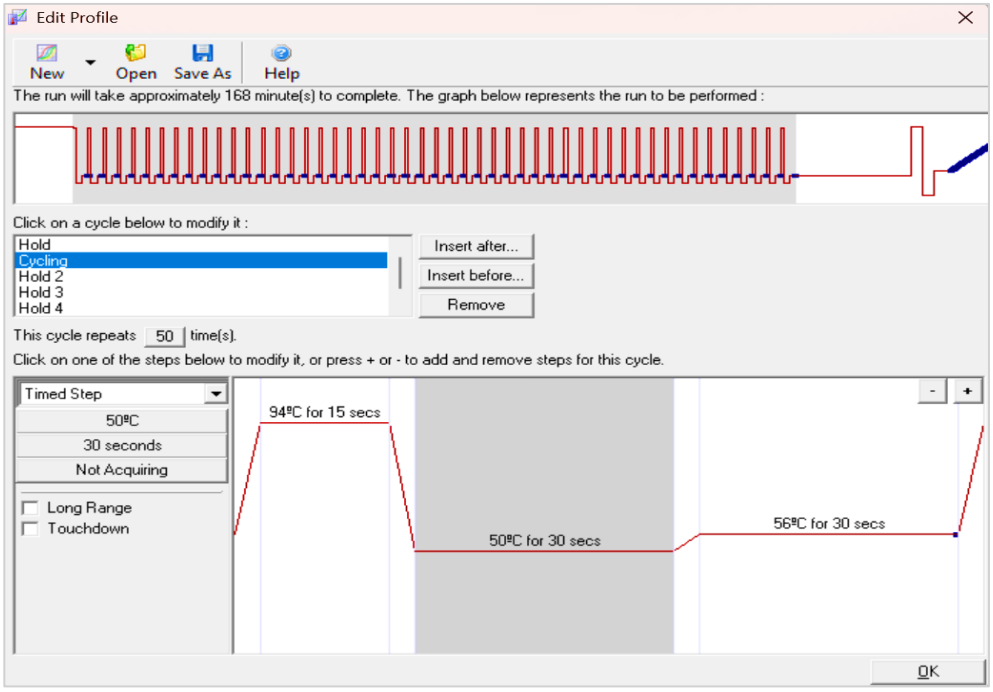

Figure 19
"Edit Profile" window in the Rotor-Gene Q Series software

Table 9

Optimized temperature program for qPCR and HRM applied to the BEE 3_2 assay

Step		Time	Temperature	Repeat
Hold 1	Denaturation, activation of polymerase	5 min	95°C	
Cycling 1	Denaturation	15 s	94°C	Number of cycles: 50
	Annealing	30 s	50°C	
	Elongation	30 s	56°C	
Hold 2	Final elongation	10 min	56°C	
Hold 3	Denaturation	1 min	95°C	
Hold 4	Strand pairing	1 min	40°C	
HRM	HRM	-	60-80°C	0.1°C/s; 90s; gain opt 70

Table 10

Optimized temperature program for qPCR and HRM applied to the BEE 6 assay

Step		Time	Temperature	Repeat
Hold 1	Denaturation, activation of polymerase	5 min	95°C	
Cycling 1	Denaturation	15 s	94°C	Number of cycles: 50
	Annealing	30 s	51°C	
	Elongation	30 s	58°C	
Hold 2	Final elongation	10 min	58°C	
Hold 3	Denaturation	1 min	95°C	
Hold 4	Strand pairing	1 min	40°C	
HRM	HRM	-	60-80°C	0.1°C/s; 90s; gain opt 70

Table 11

Optimized temperature program for qPCR and HRM applied to the BEE 2_1 assay

Step		Time	Temperature	Repeat
Hold 1	Denaturation, activation of polymerase	5 min	95°C	
Cycling 1	Denaturation	15 s	94°C	Number of cycles: 50
	Annealing	30 s	55.6°C	
	Elongation	30 s	65°C	
Hold 2	Final elongation	10 min	65°C	
Hold 3	Denaturation	1 min	95°C	
Hold 4	Strand pairing	1 min	40°C	
HRM	HRM	-	65-80°C	0.1°C/s; 90s; gain opt 70

In the software's "Edit Samples" window, the name of the DNA extract in each strip tube must be assigned to its corresponding rotor position (Figure 20). For all positions, "Unknown" should be selected in the "Type" column and "Yes" in the "Selected" column to ensure inclusion in the analysis; otherwise, the detector will exclude the signal. The color assigned to each position can also be manually changed and defines the color of the corresponding curve in the final plot.

Once all parameters have been verified, the PCR run can be initiated, and the ice bag and metal block returned to the freezer. At the end of the PCR run and subsequent HRM analysis, results are automatically saved by the software. When the run file is opened, the amplification plot is displayed automatically but can also be accessed through the Analysis window (Figure 21). The strip tubes containing the amplicons can then be removed from the thermocycler and stored at −20°C (in a separate room to prevent contamination) for subsequent analyses, such as PSQ.

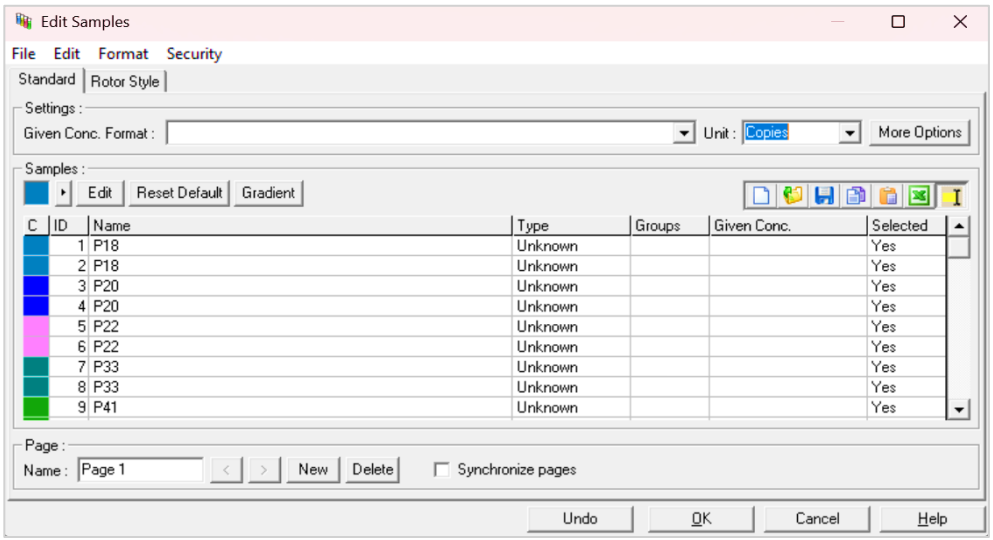

Figure 20

"Edit Samples" window in the Rotor-Gene Q Series software

4.5. High resolution melting (HRM) analysis

The Rotor-Gene Q thermocycler allows assays to be performed either as qPCR alone or as qPCR followed by HRM analysis. Moreover, although HRM requires a preceding PCR amplification step, it can be carried out without quantitative evaluation, depending on the assay design. In the vast majority of our experiments, qPCR was automatically followed by HRM analysis, with the thermocycler detecting fluorescence signals during both steps and providing the corresponding results.

In addition, some HRM analyses were performed on amplicons generated in previous qPCR runs. This approach was used to compare the clarity of melting plots obtained at different temperature ramp rates and to identify the conditions that produced the most distinct melting profiles. The temperature ramp rate during HRM analysis can be adjusted in the *Edit Profile* window (already shown in Figure 19). In this window, it is also possible to define the temperature range over which fluorescence monitoring is performed. During assay optimization, a wide temperature range is typically monitored, as the Tm of the amplicons is not yet known. Once the melting behavior has been characterized, the temperature range can be narrowed to reduce analysis time.

The temperature increments applied during HRM analysis and tested in this study are:

- +0.025°C/s
- +0.1°C/s
- +0.2°C/s
- +0.3°C/s

During HRM analysis, the thermocycler gradually increased the temperature at the selected ramp rate within the defined temperature range. At the end of the run, the results were automatically saved by the software, and the strip tubes containing the amplicons could be retrieved and stored at −20°C for subsequent analyses.

The Rotor-Gene Q Series Software was used to evaluate the results of both qPCR and HRM analysis. Figure 21 shows the "Analysis" window, which allows to select what plot should be visualized: amplification plot from qPCR (under Quantitation → Cycling A Green) (A), derivative melting plot displayed by plotting the negative first derivative of fluorescence as a function of temperature (Melt → HRM A. HRM) (B), or melting plot displayed by plotting fluorescence intensity as a function of temperature (Other → High Resolution Melt Analysis) (C).

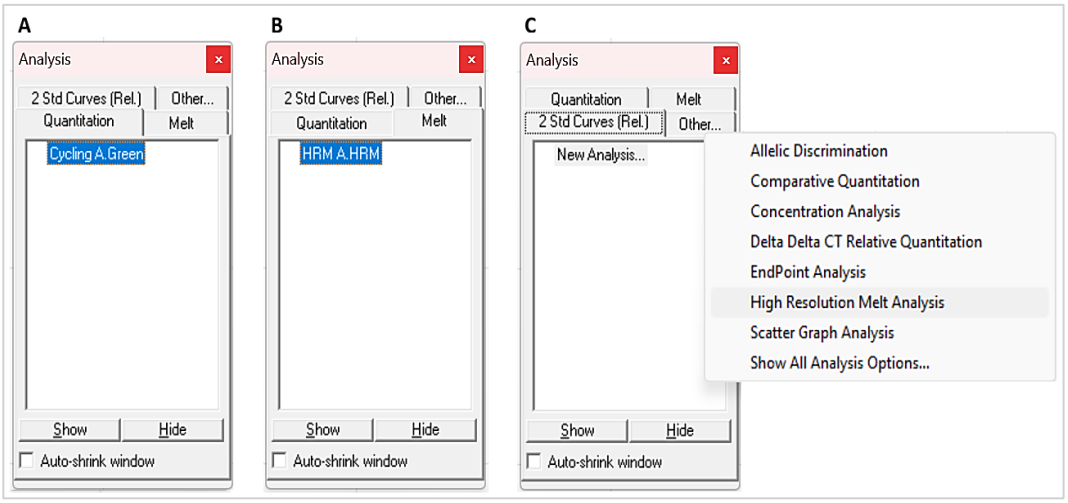

Figure 21

Analysis window in the Rotor-Gene Q Series software

Available plot types: (A) amplification plot from qPCR, (B) derivative melting plot, and (C) fluorescence melting plot for HRM analysis.

To ensure correct visualization of HRM curves, an initial normalization step is required. Figure 22 shows an example of the normalization process, which was performed using the instrument software by manually defining the pre-melt and post-melt normalization regions. The boundaries of the normalized temperature range were determined by selecting the lower temperature region preceding DNA melting and the higher temperature region following complete strand dissociation, which were set to 100% and 0% fluorescence, respectively. The software then normalized all curves to these regions, allowing direct comparison of melting profiles across samples. The final result of the normalization process in this example is shown in Figure 23. After normalization, all HRM curves start from the same fluorescence level at the lower temperature limit and converge to a common baseline at the higher temperature limit. This alignment removes differences in absolute fluorescence intensity among samples, allowing the melting behavior of each amplicon to be directly compared based on curve shape and transition profile.

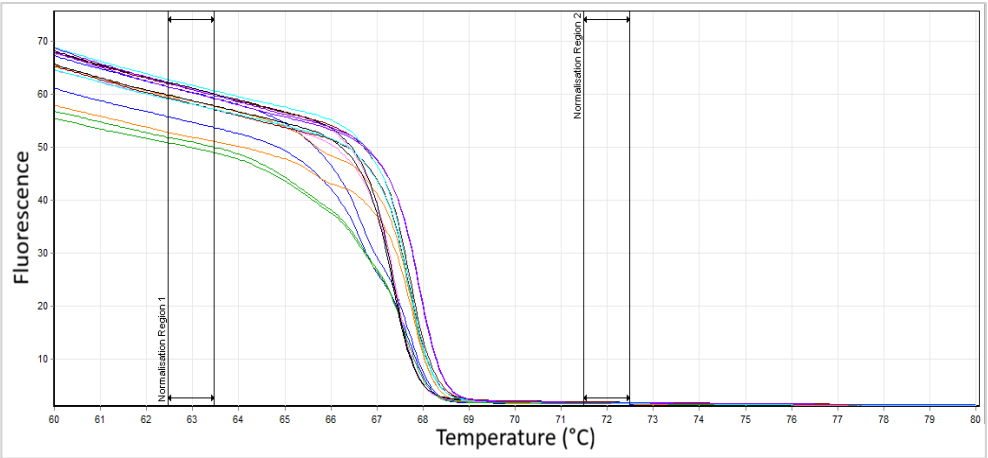

Figure 22

Example of a HRM curve normalization procedure (screenshot from the Rotor-Gene Q software)

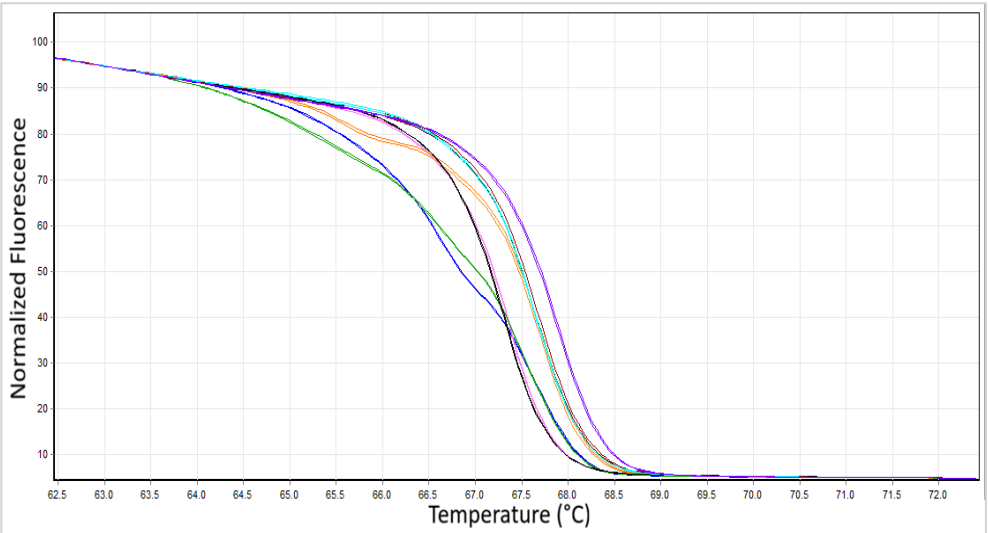

Figure 23

Normalized versions of the HRM curves presented in Figure 22 (screenshot from Rotor-Gene Q)

At this point, the results can be correctly visualized, allowing clear comparison of the melting curves and enabling the identification of differences in the genomic sequence of the amplicons.

4.6. Pyrosequencing (PSQ)

To perform PSQ of qPCR products, a dedicated sequencing assay must first be designed for each BEE assay, as each primer pair (Fw and Bio-Rev) amplifies a different sequence and may contain distinct SNPs. Sequencing assays are created using the PyroMark Q48 Autoprep software. As shown in Figure 24, the “File” menu is selected, followed by “New Assay.” Multiple options are available, but in this study only the SNP Assay and Seq Assay options were used.

The SNP assay analyzes one or more known nucleotide variations by targeting a specified SNP position, where the corresponding peak in the pyrogram is used for genotyping. The Seq Assay performs *de novo* sequencing of a DNA fragment without prior knowledge of the expected sequence. The four nucleotides are dispensed sequentially at each position, and the resulting pyrogram enables reconstruction of the full sequence and detection of multiple variations.

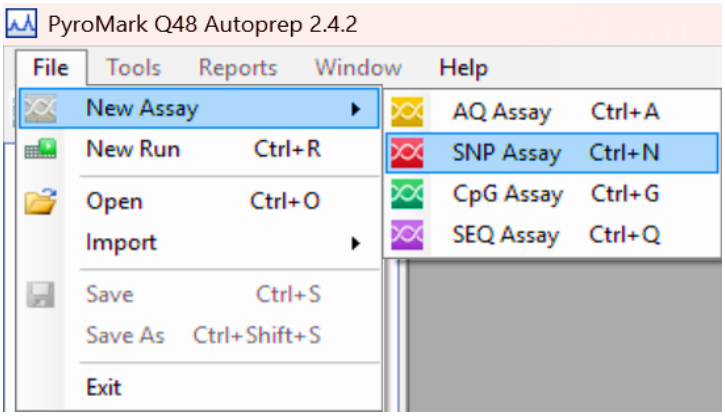

Figure 24

Creation of a new sequencing assay in PyroMark Q48 Autoprep software (screenshot from the PyroMark Q48 Autoprep software)

Figure 25 shows an example of SNP Assay creation for the BEE 3_2 assay. The target sequence is entered starting from the first nucleotide immediately downstream of the Seq primer (1). At positions where an SNP is expected (highlighted in red under "Sequence to Analyze"), the possible nucleotides for that SNP are entered, separated by a slash; more than two alternatives can be specified. The "Generate Dispensation Order" button is then selected (2), and the software automatically generates the dispensation order (3). A histogram is displayed showing the expected relative peak heights (4). For each SNP position, the histogram indicates the expected peak heights for the alternative nucleotides, depending on which nucleotide is incorporated. The software also includes control nucleotides (highlighted in red in the histogram) to verify correct nucleotide delivery. The new SNP Assay file is then saved.

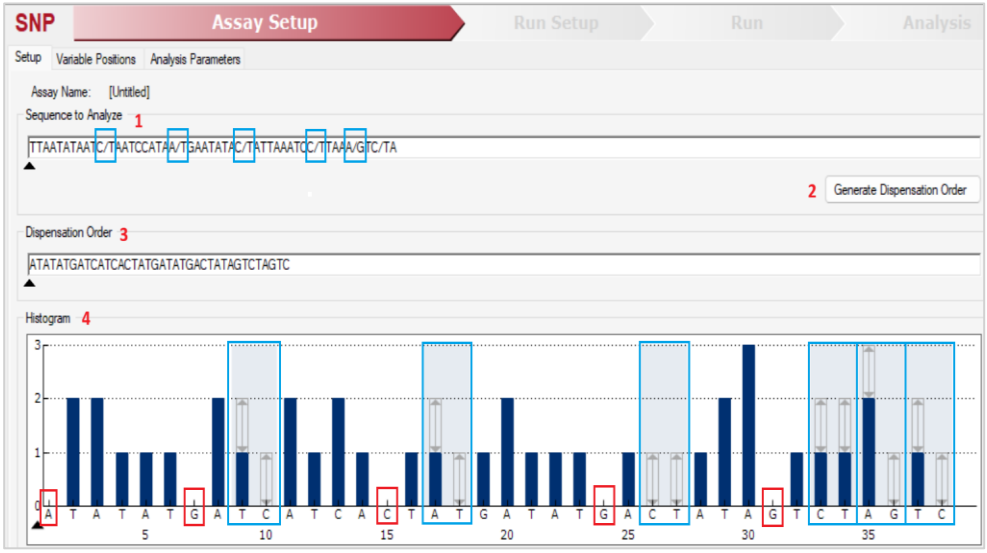

Figure 25

Example of SNP Assay creation for the BEE 3_2 assay in the PyroMark Q48 Autoprep software
(1) Entry of the amplicon sequence; expected SNP positions are highlighted in blue and alternative nucleotides are specified using a slash. (2) "Generate Dispensation Order" command. (3) Generated dispensation order. (4) Histogram showing the expected relative peak heights, including alternative peaks at SNP positions (highlighted in blue) and control nucleotides (highlighted in red).

A new run is initiated by selecting "File → New Run" in the PyroMark Q48 Autoprep software, which displays the interface shown in Figure 26. In the "Disc Setup" section (1), data for each well are entered. For well A1 (out of 48 wells), the assay (BEE 3_2) is loaded by right-clicking, selecting "Load Assay," and choosing the saved assay file; the sample name and the qPCR date and well of the template are also entered. The information for A1 is displayed in the "Well Information" field (2). Primer Loading is set to "Automatic" (3), so the Seq primer can be pipetted into its designated injector and automatically dispensed into the wells. The "Manual" option is used only when testing more than four Seq primers in a single run, in which case the primers are pipetted manually into each well. Once data for all wells are entered, the new run file is saved.

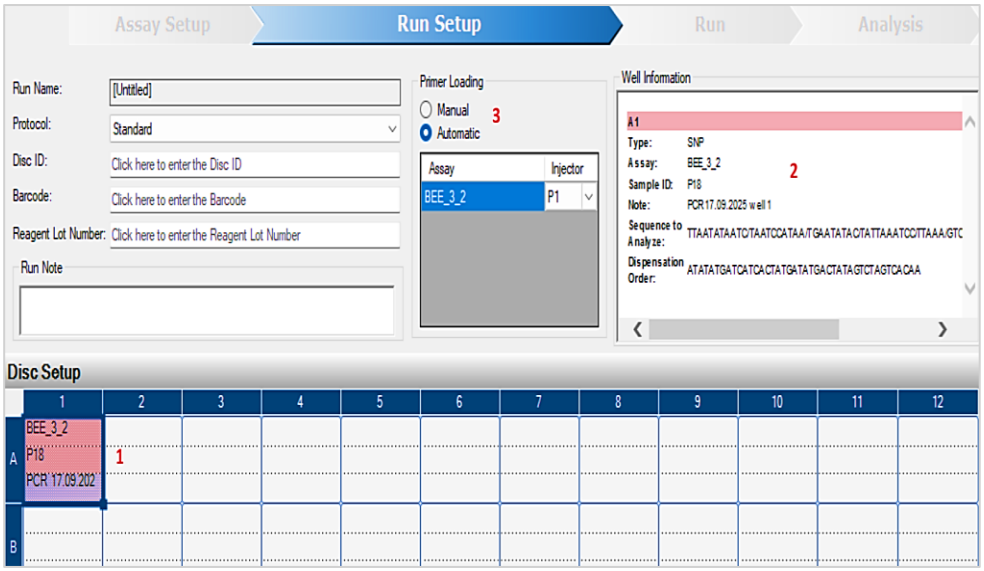

Figure 26

Setup of a new PSQ run in the PyroMark Q48 Autoprep software

(The "New Run" interface is shown with the Disc Setup section highlighted. For each well, chosen assay, sample name, and corresponding qPCR information are entered (1). Selected well information is displayed in the "Well Information" field (2). Primer Loading is set to "Automatic" (3), allowing Seq primers to be pipetted into their designated injectors and dispensed automatically into the wells.

Before the run, the PSQ run file is loaded onto a USB drive. All required reagents are removed from storage and allowed to thaw. The Seq primer, previously aliquoted at 100 µM, is diluted first to 10 µM and then to 4 µM using deionized water. The PyroMark PSQ kit containing dNTPs, denaturation solution, enzyme mix (DNA polymerase, ATP sulfurylase, luciferase, and apyrase), substrate mix (luciferin and APS), and annealing buffer, is prepared; enzyme and substrate mixes are supplied in lyophilized form. Magnetic beads and qPCR products generated with the same assay as the Seq primer are also prepared. All reagents are kept in a dedicated polystyrene box during setup.

The PyroMark Q48 instrument is switched on, and the "Cleaning" function is selected from the home screen. The injectors to be used are selected (droplet symbol), ensuring that an absorber strip is inserted with both ends meeting at 9 o'clock. Cleaning is performed following the instructions, pipetting 200 µL of deionized water into the injectors and avoiding tip contact with the injectors, or changing tips if contact occurs. Cleaning is repeated twice.

After cleaning, the USB drive is inserted, and “Sequence” is selected. The appropriate run is chosen and started. On the “Set Up Injectors” screen, “Last Run of the Day” is selected if applicable. The instrument calculates the reagent volumes required for each injector based on the number of wells. The indicated volumes are pipetted into the corresponding injectors following the on-screen instructions. Newly opened enzyme and substrate mixes are each reconstituted with 660 µL of annealing buffer, mixed gently to avoid foaming, and care is taken to avoid cross-contamination. After use, diluted enzyme and substrate mixes are stored at -20°C.

Once all reagents are pipetted, clicking Start triggers two automatic checks: (1) Primer Test, verifying the correct availability and placement of Seq primers in the injectors, and (2) Injector Test, confirming that each injector can aspirate and dispense the planned volumes (denaturation solution, enzyme mix, substrate mix, annealing buffer).

After these tests, the instrument prompts loading of 3 µL of magnetic beads and 10 µL of template into each well. The sample disc is inserted correctly when a small metal pin fits into a corresponding hole, and the absorber strip is replaced. Magnetic beads are vortexed immediately before use and pipetted into a maximum of three wells at a time, re-vortexing between batches due to rapid sedimentation. Subsequently, 10 µL of template DNA is added to each well. The PSQ run is then started.

After the run, the USB drive with the saved data is removed, the disc is removed, the absorber strip is changed, and two cleaning cycles are performed if it is the last run of the day. The injector lids are opened to prevent condensation, the absorber strip is removed, and the instrument is switched off.

The sequencing results saved on the USB drive are visualized on a PC using the PyroMark Q48 Autoprep software. Details on result interpretation are provided in Section 4.6.1., while Section 4.6.2. describes the creation of an Excel table to determine the percentage frequency of a nucleotide at a given SNP based on the relative peak heights in the pyrogram.

4.6.1. Approach for PSQ data evaluation

At this stage, it is necessary to verify whether the PSQ results match the expected outcomes. While mtDNA, which is maternally inherited, is expected to be homozygous in individual bees, honey samples may contain DNA from one or multiple subspecies in varying proportions. This situation mimics heterozygosity but actually represents a mixture of homozygotes.

The PyroMark Q48 Autoprep Software indicates the outcome of PSQ analyses using color codes, as shown in Figure 27: blue (valid result / passed), yellow (check / attention required), and red (failed analysis / error). Some reported errors may reflect real technical issues (listed under “Warnings” in Figure 27), such as a suspicious drop during nucleotide dispensation caused by faulty injectors. However, in honey samples, biologically valid results are often flagged in red. This occurs because the system was designed to analyze DNA from organisms that are either homozygous – showing 100% of one allele – or heterozygous – showing a 50%-50% allele distribution – and not mixtures of homozygotes. Consequently, the software does not recognize intermediate situations typical of honey samples, where a nucleotide at a given SNP may, for example, be present at 75%.

Figure 28 shows the pyrogram with the observed peaks and corresponding software calls, indicating which nucleotides are detected at each SNP in a given sample. Right-clicking also allows displaying histograms of the expected peak heights (shown in the figure). In this example, the second SNP is flagged in red because peaks for both C and T are present, but their heights do not match the expected histogram. Consequently, this pattern does not correspond to either perfect heterozygosity (50% C / 50% T) or perfect homozygosity (100% C / 0% T, or vice versa), the only situations recognized as valid by the software.

Figure 29 shows the histogram of expected relative peak heights predicted by the PyroMark Q48 Autoprep software for the BEE 3_2 assay. For each SNP, two alternative scenarios are shown, corresponding to the incorporation of either one of the two possible nucleotides at that position. For example, at SNP1, if nucleotide A is incorporated, the A peak has a relative height of 2 because an A immediately precedes the SNP; its signal adds to the SNP A signal, producing a double-height peak, while the G peak is absent. If G is incorporated at the SNP, both A and G peaks have a relative height of 1.

To calculate the actual nucleotide percentages at each SNP, a dedicated Excel spreadsheet was developed, as described in the following sections.

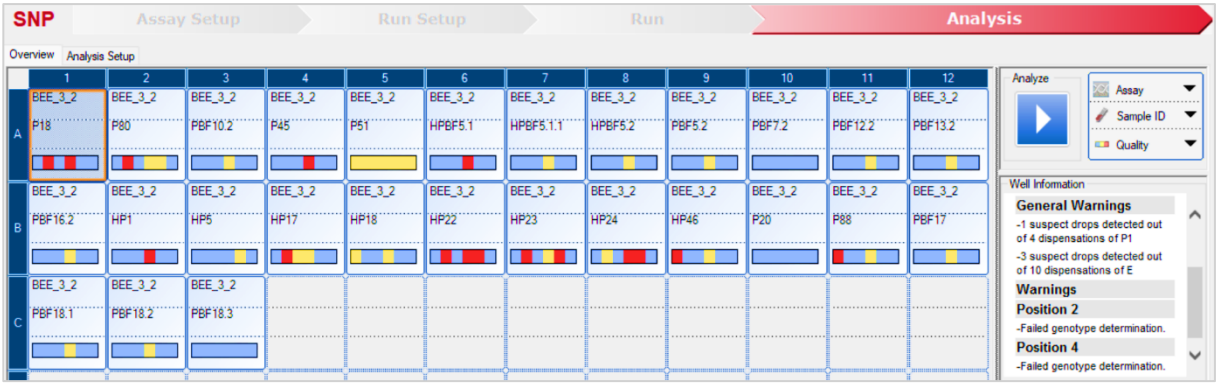

Figure 27
PyroMark Q48 Autoprep analysis overview showing SNP assay results with color-coded quality calls (blue, yellow, red) and associated software warnings (BEE 3_2 assay, sample P18) (screenshot from the PyroMark Q48 Autoprep software)

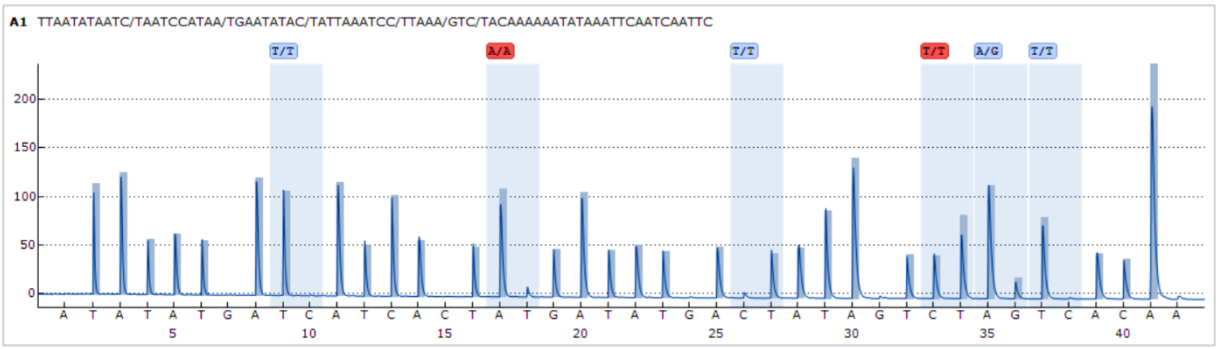

Figure 28
Pyrogram and corresponding expected peak-height histogram illustrating software SNP calls and quality flagging in a honey sample (BEE 3_2 assay, sample P18) (screenshot from the PyroMark Q48 Autoprep software)

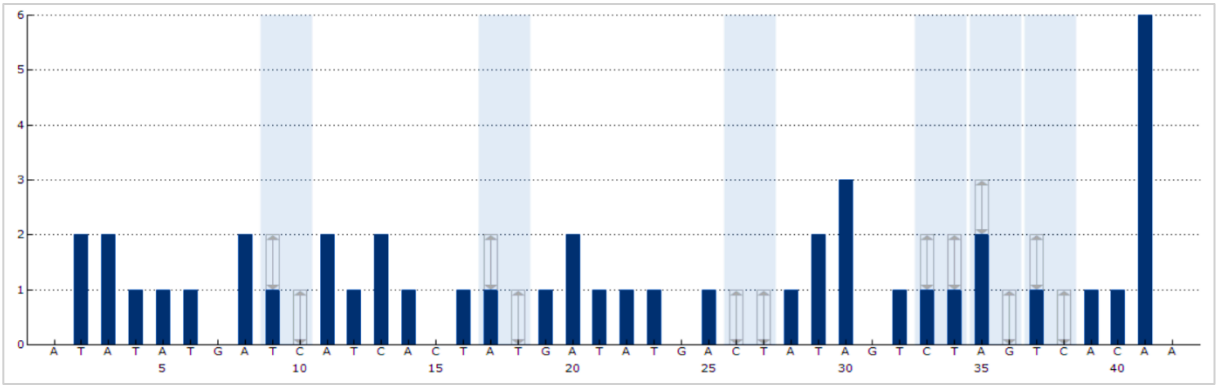

Figure 29

Expected relative peak heights for alternative nucleotide incorporation at SNP positions (BEE 3_2) (predicted by the PyroMark Q48 Autoprep software)

4.6.2. Quantification of nucleotide proportions at each SNP based on pyrogram peak heights

To quantify the proportion of each nucleotide at every SNP for each assay, an Excel spreadsheet was developed to calculate percentages based on observed pyrogram peak heights. Peak height reports were first exported and entered into the spreadsheet. The SNP positions and the corresponding nucleotide dispensation order used for the BEE 3_2 assay are shown in Table 12. Formulas at each SNP automatically calculate nucleotide percentages. These formulas implement a set of correction rules that were applied systematically to all SNP positions in all PSQ assays when required by the pyrogram context (e.g., adenine signal correction or consecutive incorporation of the same nucleotide). The example shown in Figures 30–32 (sample P18, BEE 3_2) illustrates how these corrections were implemented in practice, including the following cases:

1) Higher signal for adenine (A): In PSQ, A peaks are often slightly higher than other nucleotides due to the use of the modified nucleotide dATPαS (deoxyadenosine α-thiotriphosphate). dATPαS is incorporated by DNA polymerase but is not a substrate for luciferase, preventing background luminescence from normal dATP. Light is thus produced only upon nucleotide incorporation, and the system is calibrated to enhance A detection (Ronaghi et al., 1996). This constant effect can be corrected; for example, in Figure 30, the A peak at Dispensation 17 is multiplied by 0.9 to normalize it relative to other nucleotides.
2) Consecutive incorporation of the same nucleotide: When the same nucleotide is incorporated consecutively, the resulting peak is proportionally higher. In Figure 30, Dispensations 17 and 18 correspond to an A and a T, respectively (see Table 12). The SNP being analyzed (A or T) is preceded by an A. If an A is incorporated at the SNP, its signal adds to the preceding A, producing a roughly double-height peak. To focus only on the SNP signal, the peak is normalized by subtracting the height of the nearest single-nucleotide peak (other than A, as A peaks are higher and require correction). In Figure 30, this corresponds to subtracting the height of Dispensation 16, where a single T is incorporated.
3) After subtraction, the ratio between nucleotides at the SNP can occasionally be negative or exceed 100%, which is meaningless. To correct this, values below 0% were set to 0%, and values above 100% are set to 100%, as illustrated in Figures 31–32.

Table 34 in Section 9.4. summarizes the corrections applied to each SNP for all PSQ assays, including the reference peaks used and the corresponding calculation formulas.

Table 12

Sequence context, SNP positions, and nucleotide dispensation order for the BEE 3_2 PSQ assay

Analyzed sequence with SNPs marked in blue
1 2 3 4 5 6 TTAATATAATC/TAATCCATAA/TGAATATAC/TATTAAATCC/TTAAA/GTC/TACAAAAAATATAAATTCAATCAATTC

Dispensation order with SNPs marked in blue and control dispensations marked in red																																						
							SNP1								SNP2											SNP3								SNP4		SNP5		SNP6			
1	2	3	4	5	6	7	8	9	10	11	12	13	14	15	16	17	18	19	20	21	22	23	24	25	26	27	28	29	30	31	32	33	34	35	36	37	38	39	40	41	42
A	T	A	T	A	T	G	A	T	C	A	T	C	A	C	T	A	T	G	A	T	A	T	G	A	C	T	A	T	A	G	T	C	T	A	G	T	C	A	C	A	A

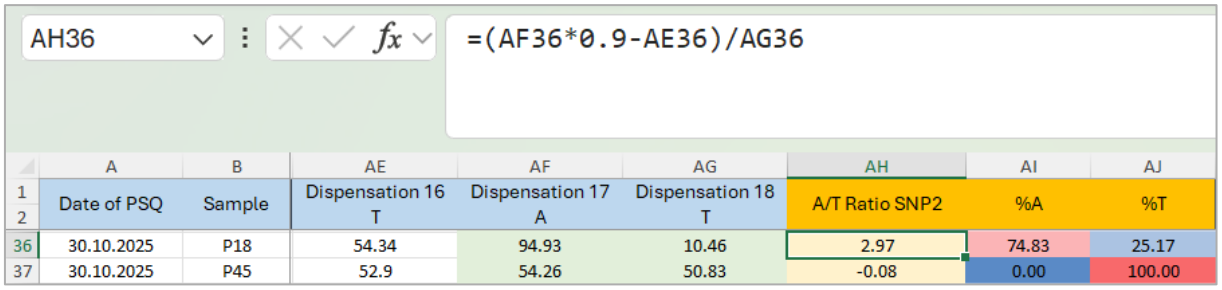

	A	B	AE	AF	AG	AH	AI	AJ
1	Date of PSQ	Sample	Dispensation 16	Dispensation 17	Dispensation 18	A/T Ratio SNP2	%A	%T
2			T	A	T			
36	30.10.2025	P18	54.34	94.93	10.46	2.97	74.83	25.17
37	30.10.2025	P45	52.9	54.26	50.83	-0.08	0.00	100.00

Figure 30

Example calculation of nucleotide ratios at SNP2 based on pyrogram peak heights (sample P18, BEE 3_2 assay) (Excel spreadsheet)

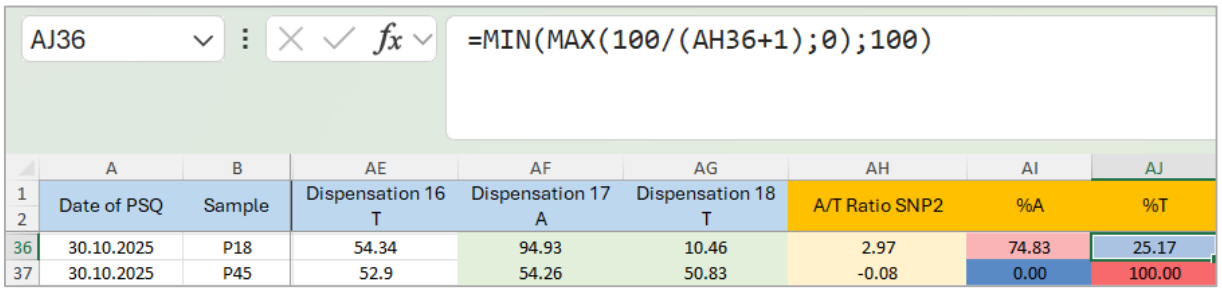

	A	B	AE	AF	AG	AH	AI	AJ
1	Date of PSQ	Sample	Dispensation 16	Dispensation 17	Dispensation 18	A/T Ratio SNP2	%A	%T
2			T	A	T			
36	30.10.2025	P18	54.34	94.93	10.46	2.97	74.83	25.17
37	30.10.2025	P45	52.9	54.26	50.83	-0.08	0.00	100.00

Figure 31

Example calculation of the percentage of the second possible nucleotide (T) at SNP2 from the ratio (sample P18, BEE 3_2 assay) (Excel spreadsheet)

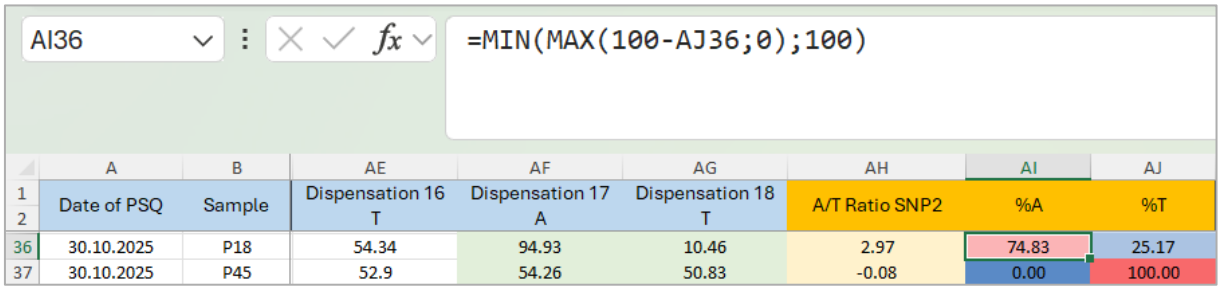

	A	B	AE	AF	AG	AH	AI	AJ
1	Date of PSQ	Sample	Dispensation 16	Dispensation 17	Dispensation 18	A/T Ratio SNP2	%A	%T
2			T	A	T			
36	30.10.2025	P18	54.34	94.93	10.46	2.97	74.83	25.17
37	30.10.2025	P45	52.9	54.26	50.83	-0.08	0.00	100.00

Figure 32

Example calculation of the percentage of the first possible nucleotide (A) at SNP2, obtained by subtracting the percentage of the second possible nucleotide from 100% (sample P18, BEE 3_2) (Excel spreadsheet)

5. RESULTS AND DISCUSSION

5.1. Selection of honey and *A. mellifera* samples

As mentioned in the previous sections, the aim of this study was to identify the DNA of different *A. mellifera* subspecies in honey, with a focus on the legally protected *A. m. carnica* from Austria. Detecting subspecies-specific DNA provides indirect information on geographic origin of honey, relevant for labeling verification and regulatory compliance, as well as subspecies protection.

Honey samples were selected to represent a wide range of geographic origins and subspecies distributions. The sampling strategy aimed to include all nine Austrian federal states; however, samples from Tyrol were received at a late stage of the study and could not be processed in time for DNA extraction, qPCR, and PSQ, and were therefore not included in the present analysis. Future studies addressing the genetic characterization of honey of Austrian origin are recommended to include samples from Tyrol to ensure complete geographic coverage.

The analyzed samples included honey from the remaining Austrian federal states, neighboring countries such as Hungary and Slovakia, regions traditionally associated with *A. m. mellifera* (France, Germany, Latvia, Estonia, and Russia) or other European subspecies (Italy, North Macedonia, Spain), non-European countries with endemic subspecies (Turkey, Nigeria, Yemen), and countries where European subspecies were historically introduced (Brazil, Australia, and New Zealand). Mixtures of EU and non-EU honey were also analyzed to assess whether blended products could be genetically distinguished from Austrian honey. Details are provided in Section 4.1. (Table 1) and in Section 9.4. (Table 26).

DNA from individual bees was also analyzed to complement honey data. These samples consisted mostly of workers, with a smaller number of drones included to verify mtDNA consistency within colonies. Analysis of bee DNA allowed comparison with honey DNA, assessing whether the same subspecies could be identified in honey produced by those colonies. Bees were obtained from Austrian beekeepers, including those from federal states legally protecting *A. m. carnica*, as well as from Italy (Trentino, Liguria, Lazio) and North Macedonia. Details are shown in Section 4.1. (Table 2) and in Section 9.4. (Table 27).

Some beekeepers provided information on the subspecies present in their colonies (*A. m. carnica*, *A. m. ligustica*, *A. m. macedonica*, or declared hybrids), but they also noted that colonies are periodically renewed, as hybridization can occur over time. Therefore, while a predominant subspecies can generally be expected in managed colonies, absolute genetic purity cannot be guaranteed. In some Austrian bees, even the specific variant of *A. m. carnica* (Alpine or Pannonian) was known, highlighting the importance of considering intra-subspecies variation.

This sampling strategy, including honey samples from diverse geographic origins and various *A. mellifera* subspecies, allowed us to assess differences in genetic patterns in honey according to provenance and to compare these patterns with those observed in the corresponding bee populations. The approach was chosen to identify specific genetic patterns in Austrian honeys, facilitating their distinction from samples originating in other countries, while capturing genetically meaningful variation among subspecies.

5.2. Primer design

High haplotype diversity is particularly desirable in our study, as it enhances the ability to distinguish among honeybee subspecies. In this context, Henriques et al. (2019) reported that the mitochondrial genes showing the highest haplotype diversity in *A. mellifera* were CYTB (cytochrome b), ND4 (NADH dehydrogenase subunit 4), and COX1 (cytochrome c oxidase subunit 1). Haplotypes are defined as sets of linked genetic variants that are typically inherited together, as recombination rarely disrupts these associations (Scott et al., 2021). Since a primer pair (BEE 2_1) targeting a region of COX1 was already in use within our research group, subsequent assay development focused on the CYTB and ND4 genes.

For the ND4 gene, Veisi et al. (2020) described the amplification of a mtDNA segment in *A. mellifera* for sequencing. The reported amplicon was approximately 1,790 bp in length and therefore unsuitable for our purpose. Using Nucleotide BLAST, a shorter 160 bp region within this sequence was identified that contained 13 SNPs and was considered suitable for downstream analyses. New Fw and Rev primers were designed to flank this region, enabling efficient amplification; this primer pair and assay configuration were assigned the name BEE 3. This assay involved only the use of a Fw primer and a Bio-Rev primer, with the Fw primer also serving as the sequencing (Seq) primer.

Following primer design, *in silico* evaluation, and optimization of reaction conditions, the BEE 3 assay was tested on DNA from *A. mellifera* specimens and honey samples. Amplification was robust when using bee extracts, whereas amplification from honey extracts was often weak, likely due to the lower concentration of bee DNA in honey. To improve amplification efficiency in honey samples, the Te was modified, and primer concentration was increased. However, increasing primer concentration also promoted primer-dimer formation, necessitating a compromise between amplification efficiency and dimer suppression.

Although qPCR amplification performance was acceptable under optimized conditions, subsequent HRM analysis generated highly complex melting plots that were difficult to interpret. This effect was most likely attributable to the high number of SNPs present within the amplified region. When multiple SNPs are included within a single amplicon, their combined effects on duplex stability can produce overlapping or ambiguous melting profiles, thereby limiting the ability to discriminate among genotypes and accurately group samples.

To address this limitation, the target sequence was shortened to the first 8 SNPs, considered sufficient to discriminate most *A. mellifera* subspecies of interest. A new primer pair (Fw and Bio-Rev) was designed and named BEE 3_1. In this configuration, the Fw primer from the original BEE 3 assay was repurposed as the Seq primer. Although BEE 3_1 passed *in silico* evaluation, its *in vitro* application produced insufficient amplification and weak sequencing signals, indicating suboptimal performance.

Subsequently, the target region was further reduced to include only the first four SNPs, leading to the development of a new assay, named BEE 3_2, which ultimately proved to be effective. In this assay, a new Bio-Rev primer for qPCR was designed to anneal further upstream, while the Fw and Seq primers were modified based on the BEE 3_1 design. In the next sections, only the primer design and optimization of the successful BEE 3_2 assay are described, whereas the BEE 3 and BEE 3_1 assays are not discussed further, as they did not meet the required performance criteria.

5.2.1. Identification of the target sequence

According to the principles outlined in Section 3.1., the primers (Fw, Bio-Rev and Seq) of the BEE 3_2 assay were designed based on Tm, GC content, and appropriate length, then evaluated *in silico* to minimize the formation of secondary structures and primer dimers. Short amplicons were preferred for qPCR, whereas for SNP genotyping by HRM and PSQ, amplicons were designed to include the polymorphic sites while avoiding SNPs within primer-binding regions for efficient amplification and accurate genotype assignment. Following initial sequence design and *in silico* evaluation, an *in vitro* optimization phase was performed to identify the most suitable experimental conditions for the assay.

To develop the primers (Fw, Bio-Rev and Seq) for the BEE 3 assay, we first identified the primer binding sites reported by Veisi et al. (2020). As the assay targets a barcode region, conserved flanking sites were selected to ensure universal primer annealing, while the intervening sequence contains variable positions enabling discrimination among *A. mellifera* subspecies. These sites were verified using Nucleotide BLAST against sequences from all relevant *A. mellifera* subspecies (e.g., *A. m. carnica*, *A. m. ligustica*, *A. m. mellifera*) to ensure broad applicability. Analysis of the long amplicon described by Veisi revealed multiple SNPs. Candidate regions without SNPs were then selected as primer binding sites to generate a shorter, more suitable amplicon. Figure 33 shows the very long amplicon described by Veisi and containing the BEE 3 amplicon (1). The BEE 3 assay was subsequently refined into BEE 3_1 (2) and finally to the successful BEE 3_2 (3).

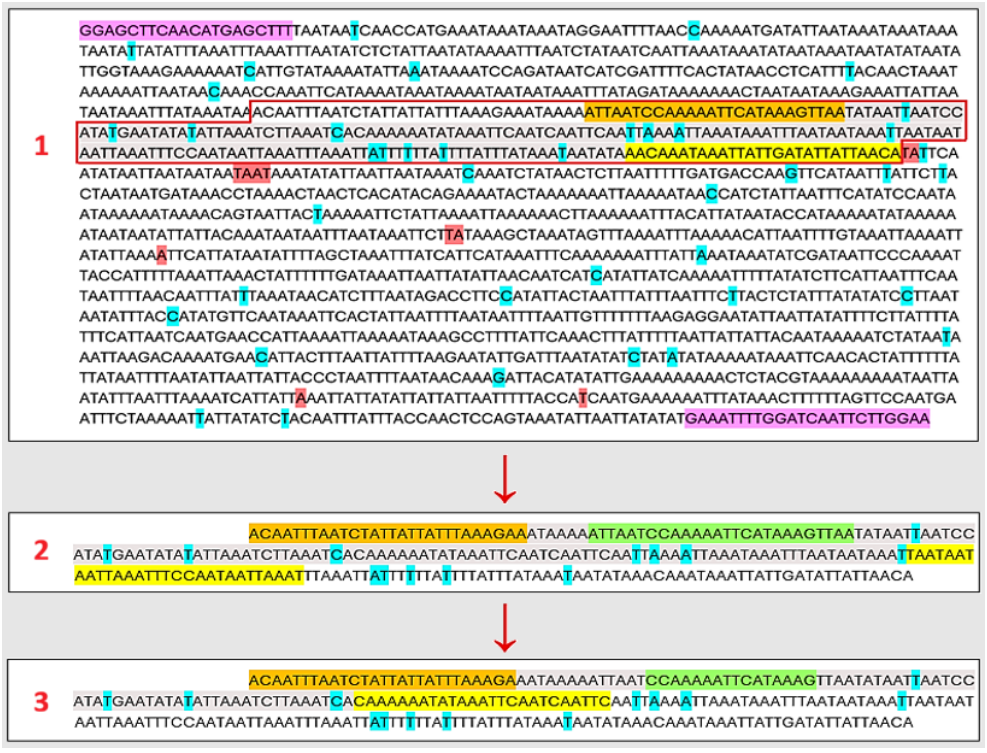

Figure 33

Refinement of the ND4 target region from the Veisi et al. (2020) amplicon to BEE 3_2

The long ND4 amplicon described by Veisi et al. (2020) is shown in panel (1), with the region selected for the BEE 3 assay marked in red. This region was shortened to BEE 3_1 (2) and further refined to the final BEE 3_2 (3). The genomic sequence corresponds *to A. m. carnica* (NCBI reference NC_061380.1). Highlighted regions indicate Veisi et al. (2020) primer binding sites (pink), newly designed Fw (orange), Bio-Rev (yellow), and Seq (green) primer binding sites, as well as SNPs (blue) and insertions (red).

Table 13 shows the six *A. mellifera* subspecies initially considered, as reported in Momeni et al. (2021). Regarding *A. m. carpatica*, it is cited in quotation marks in that dataset, reflecting its status as a local population of *A. m. carnica* rather than a formally recognized subspecies. Although not always listed as a separate subspecies in modern taxonomic databases, *A. m. carpatica* was included in this study for geographic completeness. The table also illustrates that, based on sequencing, the 13 SNPs included in the BEE 3 amplicon would ideally allow these six subspecies to be distinguished from each other.

Table 13

A. mellifera subspecies initially included in this study and their SNP profiles in the BEE 3 amplicon

A. mellifera subspecies	Accession number	SNP number												
		1	2	3	4	5	6	7	8	9	10	11	12	13
A. m. mellifera	AP018403.1	C	T	C	T	T	T	A	T	A	T	T	T	T
A. m. carnica	OM203241.1	C	T	T	T	T	T	A	T	A	T	T	T	T
A. m. iberiensis	MN585110.1	T	A	T	T	C	T	A	A	T	A	A	T	T
A. m. ligustica	KJ396182.1	T	A	T	T	C	T	G	A	A	T	T	T	T
A. m. anatoliaca	NC_061380.1	T	T	T	C	T	A	A	T	A	T	T	T	T
A. m. carpatica	MT188686.1	T	T	T	T	T	T	A	T	A	T	T	C	C

Note. Accession numbers refer to GenBank entries for the corresponding mitochondrial sequences. The 13 SNPs included in the BEE 3 amplicon would ideally allow these subspecies to be distinguished from each other based on sequence variation.

From Table 13, it is evident that even an amplicon including only the first 8 SNPs (as in the BEE 3_1 assay) allows these six subspecies to be distinguished through sequencing. On the other hand, if limited to the first four SNPs (as in the BEE 3_2 assay), discrimination between *A. m. iberiensis* and *A. m. ligustica* would not be possible.

However, during the course of the study, new and highly relevant information was encountered. First, the existence of two variants of the subspecies *A. m. carnica* – the Pannonian and Alpine variants – was noted; these variants are distinguishable both morphologically and genetically (Balazs et al., 2025).

BLAST accession numbers for these two variants were then searched, leading to a study by Moškrič et al. (2022), in which accession numbers for all subspecies included in their analysis were provided. These were adopted, and the number of subspecies considered in the present study was also expanded. This led to the identification of further important findings.

Specifically, the sequence for *A. m. mellifera* reported by Moškrič differed from the previously used sequence and contained an additional SNP, which corresponded to a variant observed during sequencing of a bee extract that had previously been unidentifiable. Furthermore, by including additional subspecies belonging to the A lineage, such as *A. m. capensis*, *A. m. intermissa*, and *A. m. ruttneri* (Ilyasov et al., 2020), an additional SNP was revealed. These two additional SNPs increased the number of SNPs in the BEE 3_2 amplicon from 4 to 6.

Finally, the study by Moškrič et al. (2022) included multiple BLAST accession numbers for both *A. m. ligustica* and *A. m. intermissa*, each corresponding to different sequences within the respective subspecies. All of these sequences were also considered in the present study.

Table 14 presents the *A. mellifera* subspecies ultimately selected for analysis, based on all the information gradually uncovered during the study. The six SNPs within the BEE 3_2 amplicon are indicated, together with the BLAST accession numbers of the corresponding subspecies sequences.

Table 14

A. mellifera subspecies ultimately selected for the study and their SNP profiles in the BEE 3_2 amplicon

A. mellifera subspecies	Accession number	SNP number					
		1	2	3	4*	5*	6
A. m. carpatica	AP018403	C	T	C	T	A	T
A. m. carnica (Pannonian)	MN_250878.1	C	T	T	T	A	T
A. m. ligustica	NC_001566	C	T	T	T	A	T
A. m. carnica (Alpine)	NC_061380.1	T	T	T	T	A	C
A. m. ligustica	MH341408	T	T	T	T	A	T
A. m. anatoliaca	MT188686	T	T	T	T	A	T
A. m. caucasica	AP018404	T	T	T	T	A	T
A. m. mellifera	KY926884	T	T	T	C	A	T
A. m. iberiensis	MN585110	T	A	T	T	A	T
A. m. siciliana	MZ981768	T	A	T	T	A	T
A. m. scutellata	KY614238	T	A	T	T	A	T
A. m. intermissa	KY926883	T	A	T	T	A	T
A. m. ruttneri	MN714162.1	T	A	T	T	G	T
A. m. intermissa	KM458618	T	A	T	T	G	T
A. m. capensis	KX870183	T	A	T	T	G	T

Note. The two additional SNPs, which were initially unknown, are indicated with an asterisk (*).

Table 14 shows that the BEE 3_2 assay would allow the Alpine variant of *A. m. carnica* to be distinguished from all other subspecies through sequencing. However, the distinction of the Pannonian variant of *A. m. carnica* from *A. m. ligustica* would remain unresolved, which is crucial given that this study aimed to develop a method for identifying *A. mellifera* subspecies in honey, with particular focus on *A. m. carnica*, a subspecies native to Austria.

To address this limitation, the BEE 6 assay was also developed, based on amplification, HRM analysis, and PSQ of a short mtDNA fragment containing a single SNP (position 8924 of the mitochondrial genome) enabling discrimination between the Pannonian variant of *A. m. carnica* and *A. m. ligustica*. or this SNP, an A was expected for both variants of *A. m. carnica* (Alpine and Pannonian), whereas a G was expected for all *A. m. ligustica* sequences listed in Table 14, based on BLAST data. These expected differences were subsequently verified through experimental analyses, the results of which will be presented in the following sections.

5.2.2. *In silico* evaluation of primer properties

Using the Oligonucleotide Properties Calculator, the key parameters of the primers for the BEE 3_2 and BEE 6 assays were calculated and are presented below in Tables 15 and 16.

Table 15

In silico primer properties for the BEE 3_2 assay calculated using the Oligonucleotide Properties Calculator

Primer	Sequence (5' → 3')	Length	GC content	Tm
Fw	ACAATTTAATCTATTATTATTTAAAGA	27 bp	11%	53°C
Bio-Rev	GAATTGATTGAATTTATATTTTTTG	25 bp	16%	53°C
Seq	CCAAAAATTCATAAAG	16 bp	25%	38°C

Table 16

In silico primer properties for the BEE 6 assay calculated using the Oligonucleotide Properties Calculator

Primer	Sequence (5' → 3')	Length	GC content	Tm
Fw	AACCACGAAATTATCCCAATTA	22 bp	32%	55°C
Bio-Rev	AATATAGGATCTCCAGTTTCTT	22 bp	32%	55°C
Seq	CCCAATTAATAATATAACC	19 bp	26%	46°C

As shown in Tables 15 and 16, the salt-adjusted Tm calculated for the Fw and Bio-Rev primers were identical – as intended – for both assays and fell within an acceptable range, although slightly low. Primer lengths were also appropriate. However, the low GC content of the primers used in the BEE 3_2 assay is noteworthy. This is attributable to the extremely AT-rich nature of the target genomic region, for which no alternative primer designs with higher GC content could be identified. Nevertheless, these primers were retained for further testing.

With regard to the Seq primers, both length and calculated Tm are relatively low, particularly in the BEE 3_2 assay. However, Buck et al. (1999) demonstrated that Seq primers can vary widely in length while still supporting effective sequencing, consistent with the primers designed in this study. In addition, Alexander et al. (2005) discussed practical considerations for PSQ primer design, emphasizing that primer performance depends on overall sequence characteristics rather than strictly on high Tm. Accordingly, the Seq primers were considered suitable.

At this stage, the potential formation of secondary structures was evaluated using the RNAfold Webserver. Figure 34 shows the RNAfold diagrams obtained for the BEE 3_2 Fw primer at 37°C (A) and 52°C (1°C below the Tm) (B). Since no hairpins were formed at 52°C, the primer was considered suitable, although the presence of green and blue colors indicates a certain risk of secondary structure formation. The same test was performed for the BEE 3_2 Bio-Rev primer, and the obtained diagrams are shown in Figure 35. For the BEE 3_2 Seq primer, this *in silico* test was performed only at a temperature of 37°C, and the result is shown in Figure 36. The RNAfold diagrams for the BEE 6 assay are shown in Figures 37–39.

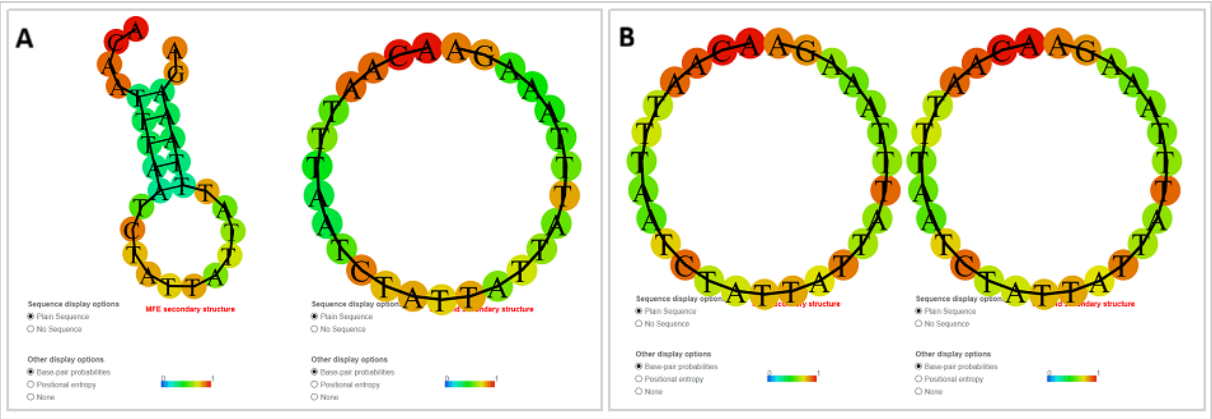

Figure 34

RNAfold diagrams of the BEE 3_2 Fw primer at 37°C (A) and 52°C (B). Generated using the RNAfold Webserver (https://rna.tbi.univie.ac.at/cgi-bin/RNAWebSuite/RNAfold.cgi)

No hairpins were observed at 52°C, indicating that the primer is suitable, although the green and blue colors suggest a minor risk of secondary structure formation.

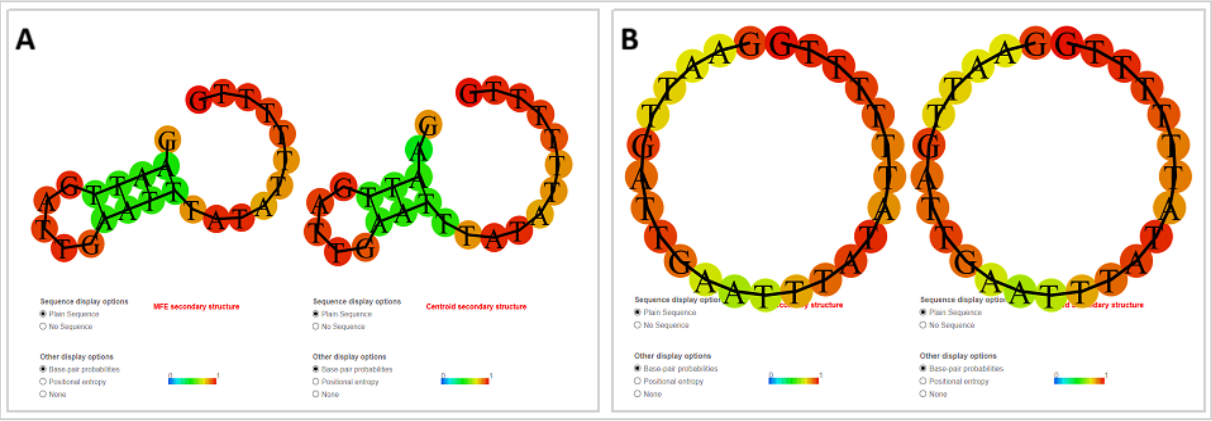

Figure 35

RNAfold diagrams of the BEE 3_2 Bio-Rev primer at 37°C (A) and 52°C (B). Generated using the RNAfold Webserver (https://rna.tbi.univie.ac.at/cgi-bin/RNAWebSuite/RNAfold.cgi)

No hairpins were observed at 52°C, indicating that the primer is suitable.

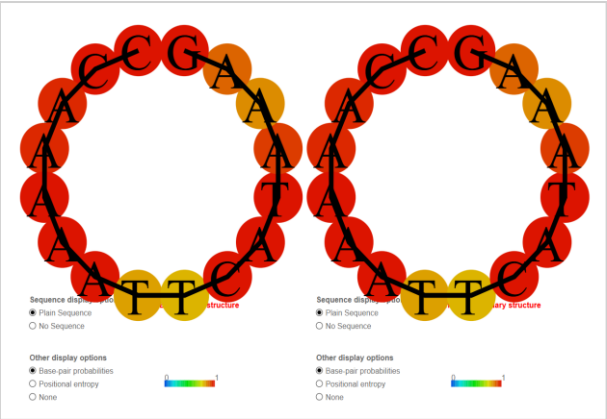

Figure 36

RNAfold diagrams of the BEE 3_2 Seq primer at 37°C. Generated using the RNAfold Webserver (https://rna.tbi.univie.ac.at/cgi-bin/RNAWebSuite/RNAfold.cgi)

No hairpins were observed, indicating that the primer is suitable.

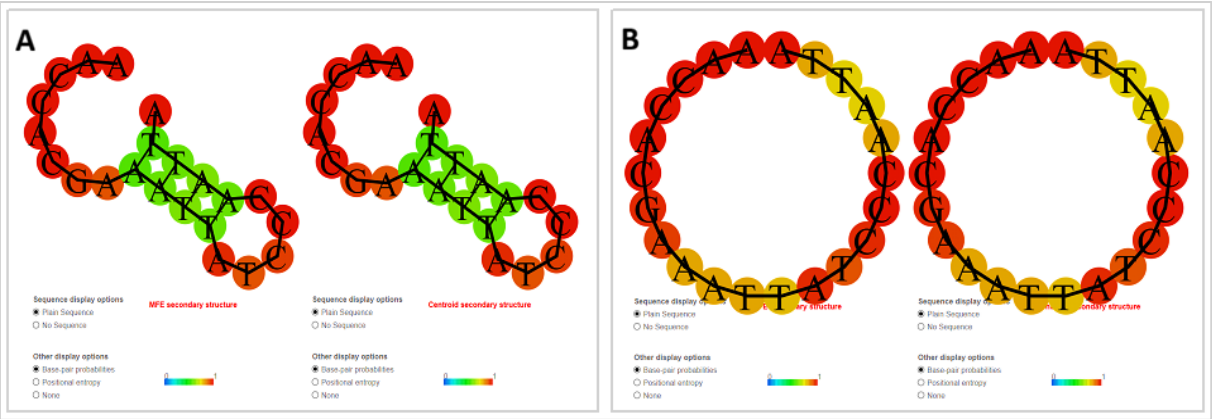

Figure 37

RNAfold diagrams of the BEE 6 Fw primer at 37°C (A) and 54°C (B). Generated using the RNAfold Webserver (https://rna.tbi.univie.ac.at/cgi-bin/RNAWebSuite/RNAfold.cgi)

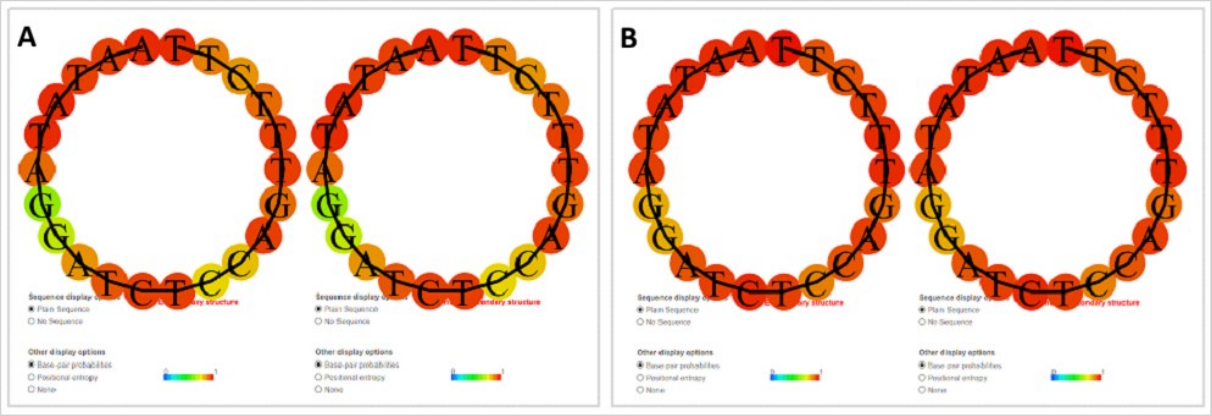

Figure 38

RNAfold diagrams of the BEE 6 Bio-Rev primer at 37°C (A) and 54°C (B). Generated using the RNAfold Webserver (https://rna.tbi.univie.ac.at/cgi-bin/RNAWebSuite/RNAfold.cgi)

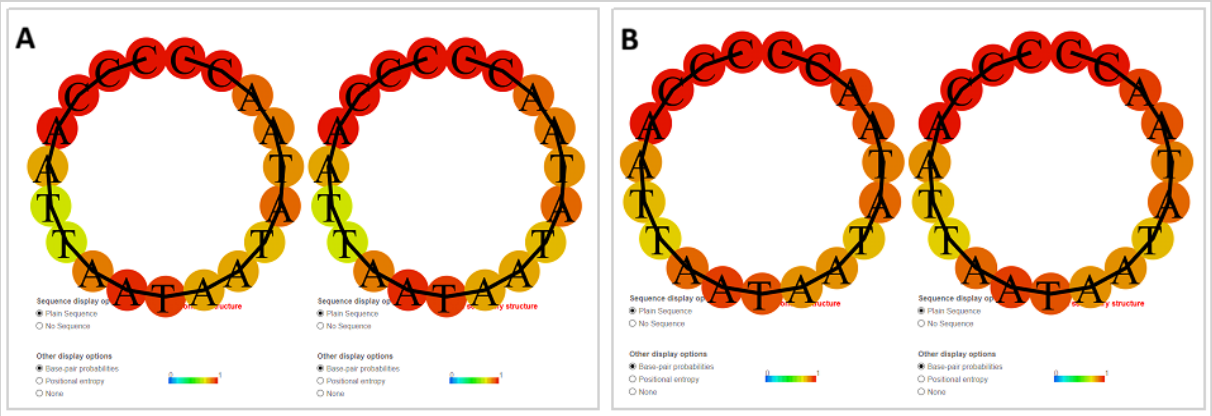

Figure 39

RNAfold diagrams of the BEE 6 Seq primer at 37°C (A) and 45°C (B). Generated using the RNAfold Webserver (https://rna.tbi.univie.ac.at/cgi-bin/RNAWebSuite/RNAfold.cgi)

Finally, the last *in silico* test was conducted using the online tool OligoAnalyzer. Figure 40 shows the OligoAnalyzer results for homodimer formation of the BEE 3_2 Fw primer, with predicted dimers ranked by decreasing probability of formation; only the top three are displayed. The ΔG and the number of matching base pairs are highlighted in red, and the results are acceptable, with a maximum of six matching base pairs. The same test was conducted for the BEE 3_2 Bio-Rev and the BEE 3_2 Seq primer (results are shown in Figure 41–42), also with acceptable results. Figure 43 presents the corresponding heterodimer analysis between the BEE 3_2 Fw and Bio-Rev primers, again showing only the top three ranked dimers and yielding acceptable results. The ΔG and the number of matching base pairs are highlighted in red.

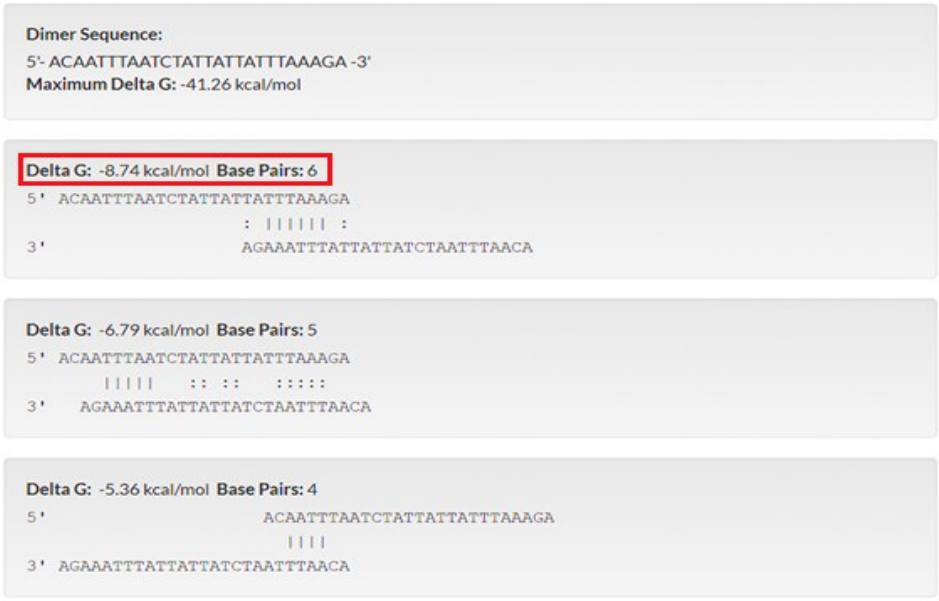

Figure 40

Results for homodimer formation of the BEE 3_2 Fw primer using OligoAnalyzer (*https://www.idtdna.com/calc/analyzer*).

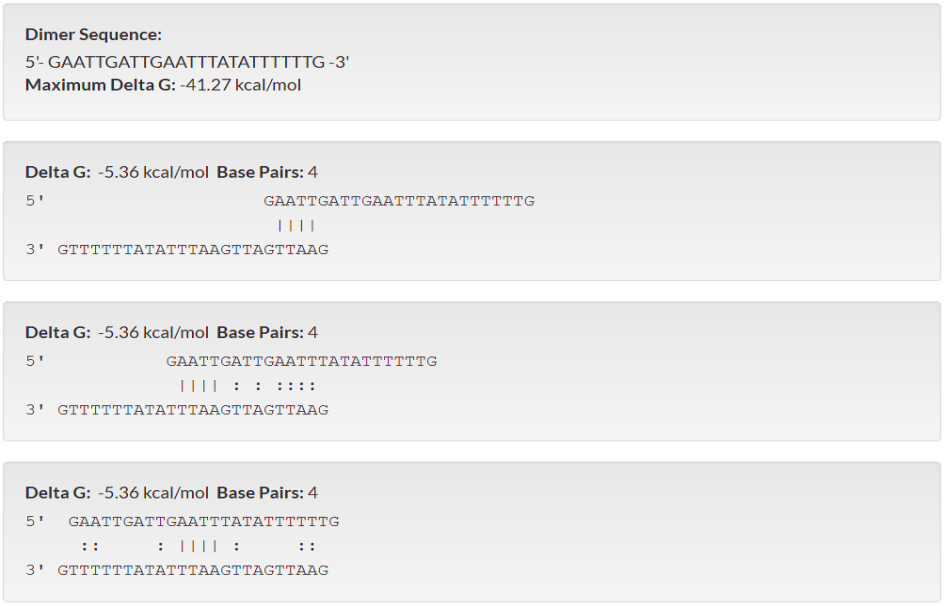

Figure 41

Results for homodimer formation of the BEE 3_2 Bio-Rev primer using OligoAnalyzer (*https://www.idtdna.com/calc/analyzer*).

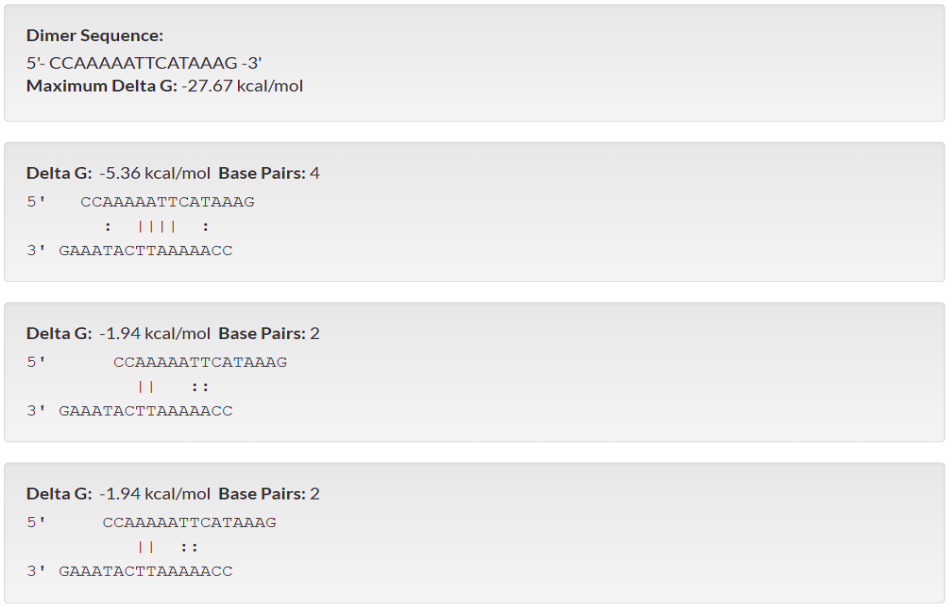

Figure 42

Results for homodimer formation of the BEE 3_2 Seq primer using OligoAnalyzer (https://www.idtdna.com/calc/analyzer).

Figure 43

Results for heterodimer formation between the BEE 3_2 Fw and Bio-Rev primers using OligoAnalyzer (https://www.idtdna.com/calc/analyzer)

Figures 61–63 in Section 9.4. show the OligoAnalyzer results for homodimer formation of the BEE 6 Fw, Bio-Rev, and Seq primers, with predicted dimers ranked by decreasing probability; only the top three are displayed. Figure 64 presents the corresponding heterodimer analysis between the BEE 6 Fw and Bio-Rev primers, again showing only the top three ranked dimers. All of these tests yielded acceptable results.

5.2.3. *In vitro* optimization and validation of the PCR assay

The final step of primer design consisted of a preliminary qPCR assay to evaluate *in vitro* the performance of primers that had been successfully validated *in silico* and to determine the optimal operating conditions of the assay. This test was conducted using a QuantStudio 5 thermocycler. In particular, the optimal Ta and Te were identified, and primer-dimer formation was excluded.

Figure 44 shows the amplification of a single bee DNA extract using the BEE 3_2 assay under different Ta and Te combinations. Although each condition was run in duplicate, only one replicate per Ta/Te combination is shown to avoid visual clutter. The fluorescence signal increases exponentially before reaching a plateau. The amplification curve crossed the predefined threshold at cycle Ct; lower Ct values were associated with improved assay performance.

In this optimization test, the lowest Ct value was obtained at Ta 50°C and Te 56°C (green curve). For all other combinations, the curves were shifted to the right, reaching the threshold later and yielding higher Ct values. Therefore, Ta 50°C and Te 56°C were selected as the optimal conditions for the BEE 3_2 assay.

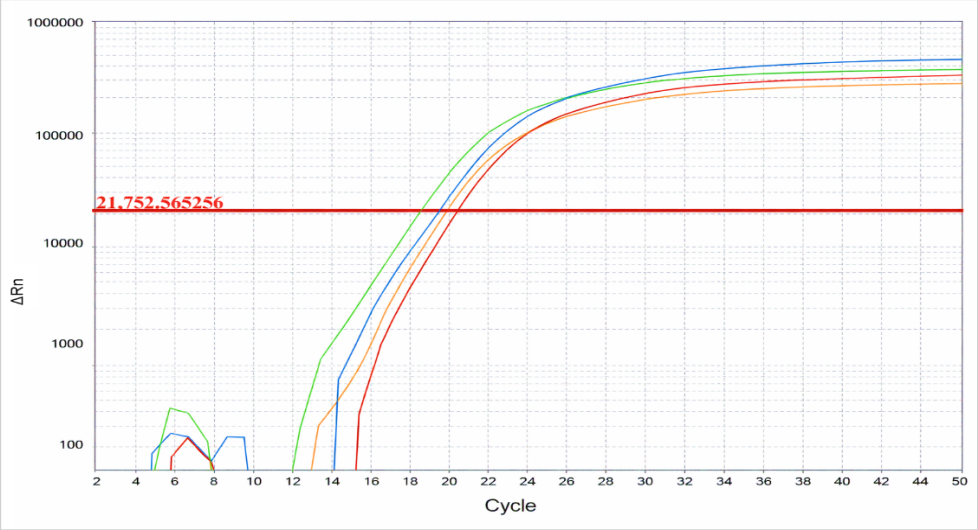

Figure 44

QuantStudio amplification plot for a honeybee DNA extract (single replicate) using BEE 3_2

Fluorescence signal is plotted against cycle number, and the point where the curve crosses the horizontal threshold line indicates the Ct. Temperature combinations: Ta 50°C and Te 56°C (green), Ta 50°C and Te 58°C (blue), Ta 51.5°C and Te 56°C (orange), Ta 51.5°C and Te 58°C (red).

No primer–dimer formation was observed in the NTC wells under these conditions, as confirmed by the HRM analysis shown in Figure 45. The curves are shown in duplicate. As illustrated, the target sequences within the DNA extracts (green) were successfully amplified at Ta 50°C and Te 56°C, and the PCR products displayed a distinct melting peak. In contrast, the NTCs (black), which contained primers but no template, showed no melting peaks, confirming the absence of primer–dimer formation under the same Ta and Te conditions.

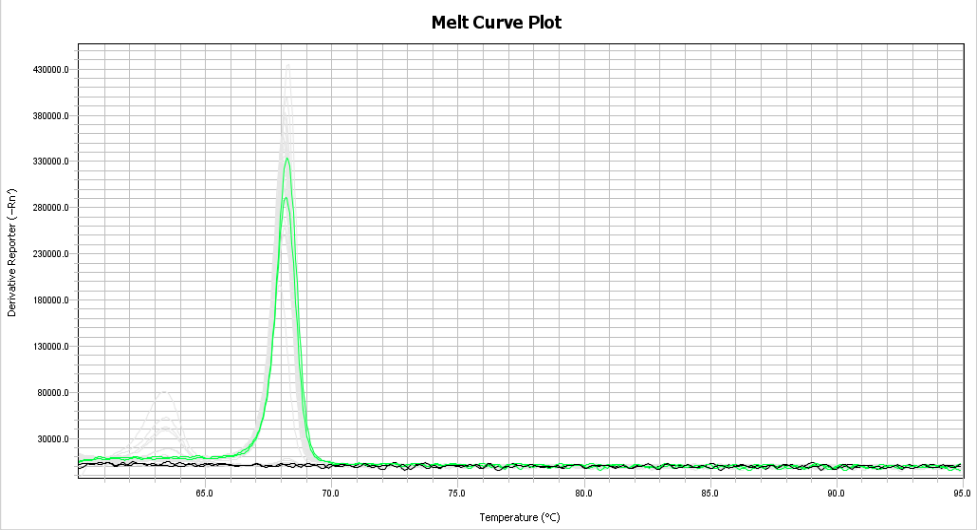

Figure 45

QuantStudio derivative melting plot for a bee DNA extract and NTC (in duplicate) using BEE 3_2

The negative derivative of fluorescence (-dF/dT) is plotted against increasing temperature, and the peak (in green) maximum corresponds to the Tm of the amplicons. No peak is observed for the NTC (in black), indicating the absence of amplification and primer–dimer formation.

The same evaluation was performed for the BEE 6 assay to determine its optimal amplification conditions. Figure 46 shows the amplification curves from a single bee DNA extract using the BEE 6 assay under different Ta and Te combinations. Although each condition was run in duplicate, only one replicate per Ta/Te combination is shown to avoid confusion. Among the tested combinations, the lowest Ct values across all samples were obtained at Ta 51°C and Te 58°C (green curve), which were therefore selected as the optimal conditions for the BEE 6 assay. No primer–dimer formation was observed in the NTC wells under these conditions, as further confirmed by HRM analysis.

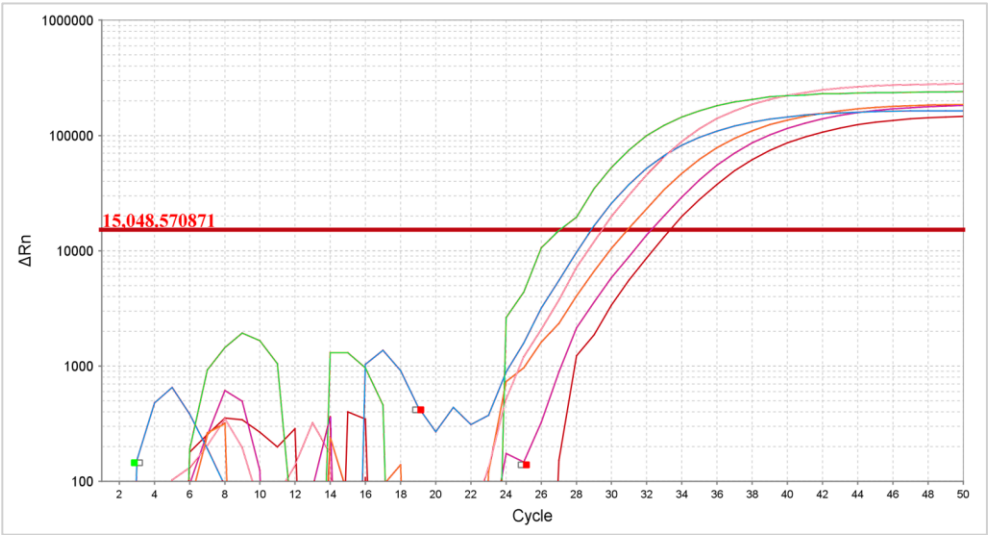

Figure 46

QuantStudio amplification plot for a honeybee DNA extract (single replicate) using BEE 6

Fluorescence signal is plotted against cycle number, and the point where the curve crosses the horizontal threshold line indicates the Ct. Temperature combinations: Ta 51°C and Te 58°C (green), Ta 53°C and Te 58°C (blue), Ta 51°C and Te 60°C (pink), Ta 53°C and Te 60°C (orange), Ta 51°C and Te 62°C (purple), Ta 53°C and Te 62°C (red).

5.2.4. Development and evaluation of nDNA analysis methods and the csd gene

To assess whether differences in nDNA could support the patterns observed in mtDNA among *A. mellifera* subspecies, regions of the nDNA with high variability were also sought. For this purpose, an Excel file provided as supplementary material in a paper published by Bovo et al. (2022) was used. One table in this file lists genetic variants identified by the authors through genotyping by sequencing (GBS) across honey and bee DNA samples, including nDNA SNPs. From this list, two regions of suitable length for qPCR amplification and subsequent PSQ were selected. Primer pairs, named BEE 4 and BEE 5, were designed to amplify these nDNA regions, and both assays were tested and optimized *in silico* as described above.

Although the primers performed reasonably well, it quickly became apparent that this approach was not suitable for assigning honey or bee samples to specific geographic origins. In both HRM analysis and sequencing, all worker bees were heterozygous at least at one SNP, while drones were consistently homozygous at every SNP, even when workers and drones originated from the same population and were likely offspring of the same queen.

This pattern was explained by the fact that both amplified sequences were located within the complementary sex determiner (csd) gene, which controls sex determination in *A. mellifera* larvae, as illustrated in Figure 47.

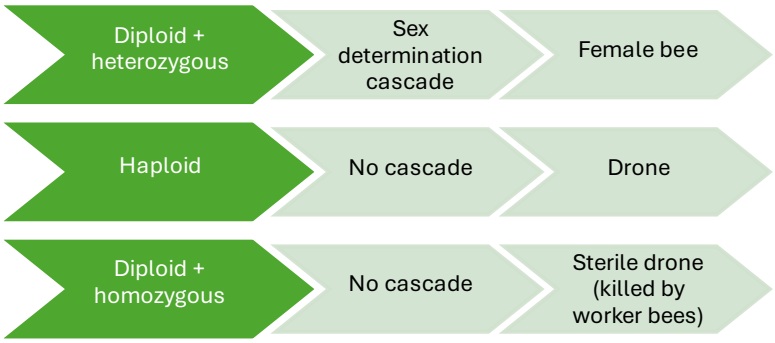

Figure 47
Influence of the csd gene in the determination of the sex of A. mellifera larvae

Since only homozygous diploid larvae are sterile, there is a genetic advantage in maintaining high csd diversity in bee populations. The queen's natural polyandrous mating behavior, along with mating flights far from the hive, reduces the likelihood of identical csd alleles co-occurring. However, the frequency of identical alleles can increase in populations with higher inbreeding, such as those under selective breeding programs (Hyink et al., 2013).

Although the csd gene is highly variable (Hyink et al., 2013), its variation is not phylogenetic and therefore cannot be used to distinguish *A. mellifera* subspecies in honey samples. Based on our observations, it can, however, serve as a species marker and provide information on allelic diversity within colonies, which reflects the genetic health of the colony. Analyses require intact DNA, so the method works more reliably on bees than on honey.

5.3. DNA extraction

Initially, DNA extraction from both honey and bees was performed exclusively using the DNeasy mericon Food Kit (Qiagen). DNA yields from *A. mellifera* samples were consistently high, providing more than enough material for successful downstream analyses, including qPCR, HRM, and PSQ. In contrast, DNA extracted from honey was sometimes of insufficient quantity, leading to poor qPCR amplification and, consequently, suboptimal results in HRM and PSQ. Notably, acacia honey samples were frequently associated with these difficulties, which can be plausibly explained as follows.

Extracting DNA from honey is generally challenging because its complex composition – including high sugar content, organic acids, and other compounds – can interfere with DNA recovery and subsequent molecular analyses (Kek et al., 2018). Most recoverable DNA in honey is associated with particulate material such as pollen and cellular debris, and DNA yield and amplifiability are strongly influenced by the choice of extraction method and sample preparation (Guertler et al., 2014; Soares et al., 2015). Consequently, the removal of solid particles, including cells, during honey processing can substantially reduce the amount of DNA available for molecular analysis.

Acacia honey, valued for its light color and clarity, is among the white or light honeys that are commonly processed commercially to meet consumer preferences for visually clear products. Filtration is a documented step in commercial honey processing, removing the majority of pollen grains, cellular debris, and other particulate matter (Wilczyńska, 2014). Techniques such as microfiltration and ultrafiltration are also employed to clarify honey and remove suspended solids of cellular size (Barhate et al., 2003). From these observations, it can be inferred that the frequent processing of acacia honey to achieve a clear, visually appealing product may contribute to its comparatively low DNA content, including bee DNA, due to the reduction of pollen, cells, and other particulate-associated material.

To improve satisfactory DNA yields from all honey types, the BioSPE PureGenNucleo cfDNA kit (Affinisep) was also tested and, after successful evaluation, became the kit of choice for DNA extraction from honey samples. This kit was never tested on bees, which continued to be processed exclusively with the DNeasy mericon Food Kit (Qiagen).

5.3.1. Comparison of DNA yield from honey using Affinisep and Qiagen extraction kits

To determine the most suitable method for DNA extraction from honey, a comparison was performed between the DNA yield obtained using the BioSPE PureGenNucleo cfDNA Kit (Affinisep) and the DNeasy mericon Food Kit (Qiagen), following extraction and fluorimetric quantification of the DNA concentration. It is important to note that the Qiagen kit produced a final DNA extract volume of 50 µL, whereas the Affinisep kit yielded 120 µL of extract, representing a 2.4-fold higher volume.

Table 17 shows the results of DNA extractions from 13 honey samples using the Qiagen and Affinisep kits. The second-to-last column reports the ratio between the DNA concentration of the extract obtained with the Affinisep kit and that obtained with the Qiagen kit, indicating how much higher the DNA concentration was when using the Affinisep kit. For example, for sample P41, the DNA concentration of the extract obtained with the Affinisep kit was 11.45 times higher than that obtained with the Qiagen kit.

However, it should be noted that the Affinisep kit produces a final extract volume 2.4 times larger than the Qiagen kit. Therefore, in the last column, the values in the second-to-last column were multiplied by 2.4 to account for the difference in extract volume. This allows an estimation of the total DNA yield, showing that for sample P41, the total DNA obtained with the Affinisep kit was 27.48 times greater than that obtained with the Qiagen kit.

Table 17

DNA concentration ratios and corresponding total DNA yield ratios obtained from honey samples using Qiagen and Affinisep extraction kits

Sample ID	Honey type	DNA (ng/µL) Qiagen	DNA (ng/µL) Affinisep	Affinisep / Qiagen concentration ratio	Affinisep / Qiagen total DNA ratio
P41	Acacia	0.03	0.30	11.45	27.48
P47	Sweet pea	0.45	1.52	3.38	8.11
P70	Blossom	0.23	0.75	3.26	7.83
P75	Blossom	0.07	1.31	19.55	46.93
P79	Sunflower	0.59	5.00	8.50	20.41
P81	Sweet chestnut	0.70	3.22	4.60	11.04
P82	Chestnut, blossom, honeydew	0.77	3.18	4.11	9.86
P83	Linden	0.75	3.90	5.20	12.48
P84	Linden	0.32	2.04	6.38	15.30
P85	Acacia with blossom	2.20	5.18	2.35	5.65
P86	Acacia	0.05	0.58	12.62	30.29
P88	Acacia	0.07	0.61	8.94	21.47
P89	Chestnut	0.52	2.00	3.86	9.27

Note. Concentration ratios indicate the fold difference in DNA concentration between Affinisep and Qiagen extracts. Given that the Affinisep kit produces a final elution volume 2.4 times larger than the Qiagen kit, multiplication of the concentration ratio by this factor results in the corresponding total DNA yield ratio.

A paired Wilcoxon signed-rank test confirmed that the Affinisep kit yielded significantly higher DNA concentrations than the Qiagen kit across all honey samples. This difference remained significant after accounting for the larger final elution volume, indicating a higher total DNA yield for the Affinisep kit ($W = 0$, $n = 13$, $p < 0.001$). Figure 48 presents the comparison of DNA yield between the two kits as a boxplot, illustrating the distribution across the 13 samples. Based on DNA yield and cost per sample, the Affinisep kit was selected as the preferred method for honey extraction, whereas Qiagen remained the method of choice for bee samples.

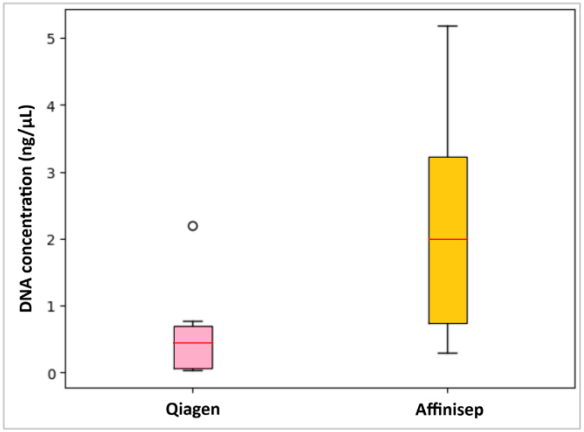

Figure 48

Comparison of DNA yield between Affinisep and Qiagen extraction kits

5.4. Real-time PCR (qPCR)

After DNA extraction from *A. mellifera* individuals and honey samples, the extracts were amplified by qPCR as described in Section 4.4., using the primer pairs BEE 2_1, BEE 3_2, and BEE 6.

Some methodological considerations should be noted. As described in the theoretical section, qPCR protocols typically involve a maximum of 40 amplification cycles, as the reaction usually reaches a plateau phase beyond this point, with no further meaningful amplification. Increasing the number of cycles can also increase the risk of nonspecific amplification, background noise, and primer-dimer formation. However, due to the complex nature of honey as a biological matrix and the reduced concentration of extractable DNA, an extended amplification protocol of 50 cycles was adopted to ensure reliable target detection. Honey is a challenging matrix because DNA is often fragmented, degraded and present at low concentrations.

This approach was further justified by the fact that the analysis was not primarily focused on quantitative assessment, and subsequent HRM and PSQ analyses provided independent confirmation that late amplification signals represented genuine target amplification rather than artifacts.

Extending the number of amplification cycles was particularly important for the BEE 3_2 assay applied to honey samples, as BEE 3_2 showed lower amplification efficiency compared to BEE 2_1 and BEE 6. DNA extracted from individual bee specimens was generally sufficient for efficient amplification, with curves reaching the plateau phase well before the 50th cycle in all three assays. For BEE 2_1 and BEE 6, the plateau was reached earlier than the 50th cycle in the majority of honey samples. By contrast, BEE 3_2 exhibited lower amplification efficiency in honey-derived DNA, making the extended cycle protocol necessary to achieve detectable amplification.

Figures 49 and 50 show representative amplification plots obtained using BEE 2_1 and BEE 3_2, respectively, including three bee-derived and one honey-derived DNA extracts. Figure 49 illustrates that DNA from individual bees reached the plateau phase earlier than honey-derived DNA, consistent with higher DNA concentration and quality, and the fact that bee-derived DNA consists only of bee DNA, whereas honey-derived DNA also contains plant and other organism DNA.

Figure 50 shows amplification curves for the same samples using BEE 3_2. Bee-derived DNA again reached the plateau earlier than honey-derived DNA. However, amplification curves were consistently shifted to higher cycle numbers compared to BEE 2_1, reflecting lower amplification efficiency. In a few cases (not shown here), amplification was insufficient to produce products suitable for HRM and PSQ.

As no fluorescence threshold was defined, amplification curves were evaluated qualitatively based on signal progression, plateau attainment, and relative positioning. Overall, these results highlight the greater difficulty of amplifying DNA from honey and the comparatively lower efficiency of BEE 3_2.

The BEE 6 assay exhibited amplification performance comparable to BEE 2_1 for both bee- and honey-derived DNA; no substantial differences were observed, and representative plots are not shown.

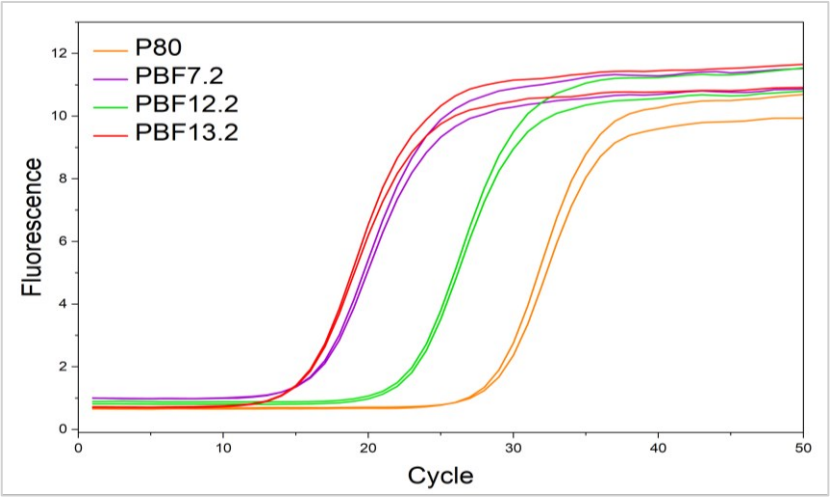

Figure 49
Representative qPCR amplification curves (in duplicate) from bee and honey DNA samples (BEE 2_1) (exported from Rotor-Gene Q to Origin)

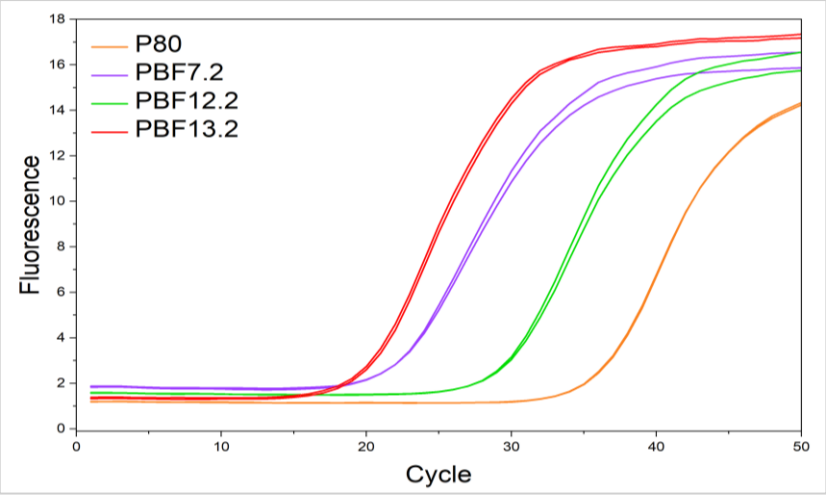

Figure 50
Representative qPCR amplification curves (in duplicate) from bee and honey DNA samples (BEE 3_2) (exported from Rotor-Gene Q to Origin)

BEE 2_1 and BEE 6 provided sufficient amplification in 98% and 100% of honey-derived DNA samples, respectively, while BEE 3_2 was slightly less efficient. Sufficient amplification was defined as the absence of the warning "genotype determination was not possible due to low peak height" in subsequent PSQ. Using this criterion, 91% of BEE 3_2 samples achieved sufficient amplification for HRM and PSQ. In the remaining 9%, genotype determination was not possible due to low peak height caused by insufficient qPCR amplification (see Section 5.6.). Considering the challenging honey matrix and typically low DNA yield, this performance is satisfactory.

One run showed consistently weak amplification across several samples and was excluded from the evaluation, as altered HRM profiles likely reflected suboptimal amplification rather than intrinsic assay behavior, although PCR products were still sufficient for PSQ.

Overall, qPCR provided a reliable basis for HRM and PSQ analyses despite some variability between primer sets and sample types. Amplification curves and HRM plots from the Rotor-Gene Q instrument were exported to Origin for direct run-to-run comparison.

5.5. High resolution melting (HRM) analysis

HRM analysis was used to detect sequence variation in the amplicons generated with the BEE 2_1, BEE 3_2, and BEE 6 assays. Sequence variants reported for *A. mellifera* subspecies differ at several SNP positions within these amplicons, which may influence the GC content and therefore the melting behavior of the PCR products. Table 18 summarizes the SNP patterns of the sequence variants reported in NCBI reference sequences for the BEE 2_1, BEE 3_2, and BEE 6 amplicons. These sequence differences form the basis for interpreting HRM melting profiles and are also used later for PSQ analysis (see Section 5.6.).

Table 18

Expected PSQ results for BEE 2_1, BEE 3_2, and BEE 6 assays across A. mellifera subspecies

A. mellifera subspecies	Accession number	SNP number BEE 2_1						SNP number BEE 3_2						SNP nr. BEE 6
		1	2	3*	4	5*	6	1	2	3	4*	5*	6	1
Pannonian carnica	MN_250878.1	G	C	T	T	T	C	C	T	T	T	A	T	A
Reference ligustica	NC_001566	G	C	T	T	T	C	C	T	T	T	A	T	G
Alpine carnica	NC_061380.1	A	C	T	T	T	C	T	T	T	T	A	C	A
Alternative ligustica	MH341408	A	C	T	T	T	C	T	T	T	T	A	T	G
A. m. carpatica	AP018403	G	C	T	T	T	C	C	T	C	T	A	T	G
A. m. anatoliaca	MT188686	A	C	T	T	T	C	T	T	T	T	A	T	A
A. m. caucasica	AP018404	A	C	T	T	T	C	T	T	T	T	A	T	A
A. m. mellifera **/***	KY926884	A	T	C	C	C	T	T	T	T	C	A	T	A
A. m. iberiensis	MN585110	A	T	T	C	T	T	T	A	T	T	A	T	A
A. m. siciliana	MZ981768	A	T	T	C	T	T	T	A	T	T	A	T	A
A. m. scutellata **/***	KY614238	A	T	T	C	T	T	T	A	T	T	A	T	A
A. m. intermissa	KY926883	A	T	T	T	T	T	T	A	T	T	A	T	A
A. m. ruttneri	MN714162.1	A	T	T	C	T	T	T	A	T	T	G	T	A
A. m. intermissa	KM458618	A	T	T	C	T	T	T	A	T	T	G	T	A
A. m. capensis ***	KX870183	A	T	T	C	T	T	T	A	T	T	G	T	A

Note. *The table shows the expected SNP patterns for each subspecies. The additional SNPs, which were initially unknown in assays BEE 2_1 and BEE 3_2, are indicated with a single asterisk (*). Subspecies marked with two asterisks (**) carry SNPs within the primer binding sites of the BEE 2_1 assay, while those marked with three asterisks (***) carry SNPs within the primer binding sites of the BEE 6 assay. Amplification of BEE 2_1 was successfully tested in an A. m. mellifera individual (sample PBF18.3) carrying such mismatches, indicating that they do not necessarily prevent PCR. For BEE 6, and for subspecies for which no individuals were available (e.g., A. m. capensis and A. m. scutellata), the effect of these mismatches on amplification remains unknown.*

As shown in Table 18, both BEE 2_1 and BEE 3_2 amplicons contain six informative SNPs. At the beginning of this study, however, only four SNPs per assay were known, which explains why some PSQ datasets report only four SNPs, whereas more recent runs include all six. The additional SNPs were identified following Moškrič et al. (2022) based on BLAST analysis of reference sequences (see Section 5.2.1.).

Analysis of these sequences revealed two variants of *A. m. ligustica* (“Reference ligustica” and “Alternative ligustica”) and two variants of *A. m. carnica* (“Pannonian carnica” and “Alpine carnica”). Based on these reference sequences, the two *A. m. carnica* variants can theoretically be distinguished using PSQ with either BEE 2_1 or BEE 3_2, while Alpine carnica and Alternative ligustica can be distinguished using BEE 3_2.

The only distinction not theoretically achievable with BEE 2_1 or BEE 3_2 is between Pannonian carnica and Reference ligustica. To address this limitation, the BEE 6 assay was developed to target a single SNP enabling this differentiation.

To evaluate the shape of melting plots at different temperature ramp rates and identify conditions producing the most distinct profiles, HRM analyses were performed on amplicons from previous qPCR runs using the BEE 2_1 primer pair. The selected temperature increment of +0.1°C/s was subsequently applied to all primer sets in later HRM analyses. Figure 51 shows derivative melting plots from two DNA extracts (pink: DNA extracted from honey of mixed EU/non-EU origin; blue: bee-derived DNA), tested at various temperature increments. The bee-derived ND4 amplicon, originating from a single individual and therefore representing a single mitochondrial haplotype, yielded a narrow and regular peak, largely unaffected by the temperature increment.

In contrast, the honey-derived mtDNA extract represents a mixture of homozygotes, as expected from the mixed honey origin. This mixture produced an irregular peak shape with a subtle shoulder, indicative of different sequence variants melting at slightly different temperatures, simulating heterozygosity. This irregularity is most apparent at increments of +0.025°C/s and +0.1°C/s. At higher increments (+0.2°C/s and +0.3°C/s), the peak irregularities are smoothed, making heterozygosity harder to discern, while the slowest increment (+0.025°C/s) produces increased noise, particularly on the ascending slope of the peak. Li et al. (2017) reported similar effects of ramp rate on HRM peak shape. Based on these observations, a temperature increment of +0.1°C/s was chosen for subsequent HRM analyses as an optimal compromise between a clean, low-noise signal and preservation of informative features. Non-derivative sigmoidal HRM curves were minimally affected by ramp rate and are therefore not shown.

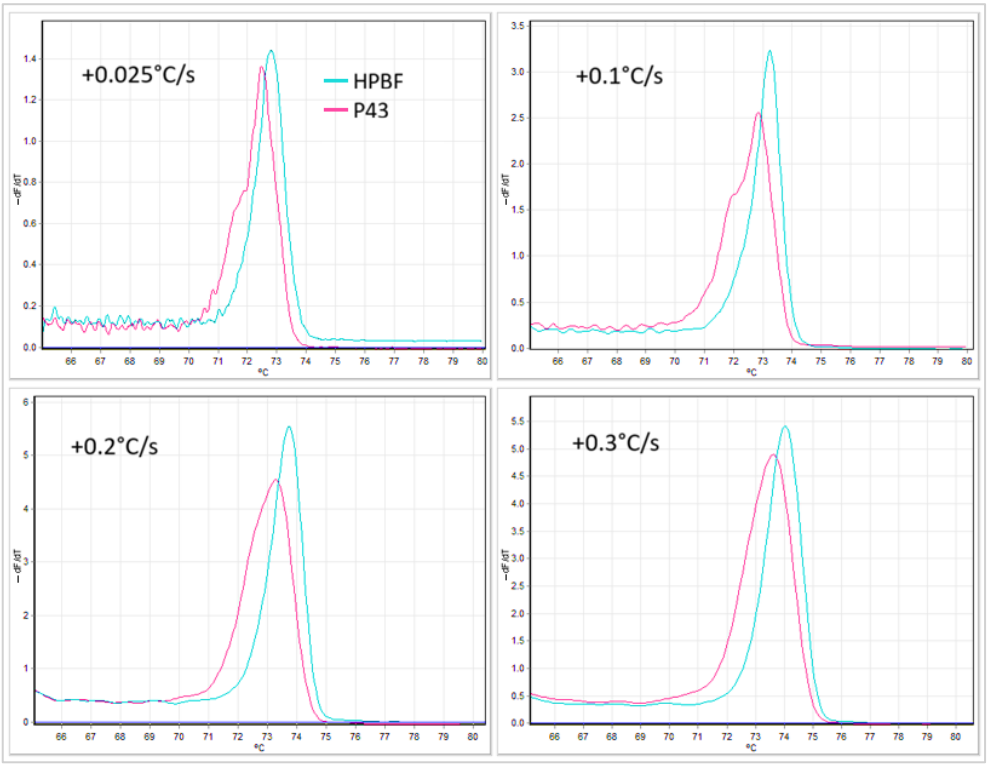

Figure 51
Derivative melting plots of bee- (HPBF) and honey (P43) DNA (single replicate) at varied temperature increments (screenshot from the Rotor-Gene Q software)

For the purpose of this study, samples were considered distinguishable by HRM when at least one of the following criteria was met:

- a repeatable shift in Tm observed consistently across independent runs.
- a consistent difference in peak shape (e.g., presence of shoulders or multiple peaks) observed across independent runs.

Minor variations in peak height or fluorescence intensity were not considered discriminatory, as these were attributable to inter-run variability.

Based on peak morphology, HRM profiles were categorized into distinct categories to facilitate comparison among bee subspecies and honey samples from different geographic origins:

- Single peak – A single, well-defined melting maximum without additional shoulders or secondary peaks.
- Shouldered peak – A primary melting maximum with a visible shoulder but no clearly separated second maximum.
- Double peak – Two distinct melting maxima separated by a visible minimum in the derivative curve (major peak + minor lower Tm peak).
- Symmetrical double peak – A double peak pattern in which the two melting maxima are of comparable height, forming a nearly symmetrical profile.

Ambiguous profiles were assigned to a peak category based on the dominant pattern across runs. In Section 9.4. tables, Tm values show the average across runs (single and shouldered peaks), the major peak average (double peaks), or a range (encompassing symmetrical double peaks).

5.5.1. HRM results for the BEE 2_1 assay

Tables 28–29 in Section 9.4. summarize the results, with representative samples shown in this section to illustrate HRM patterns. “No proper amplification” means that sequence assignment in later PSQ was impossible due to low peak height; otherwise, amplification was sufficient.

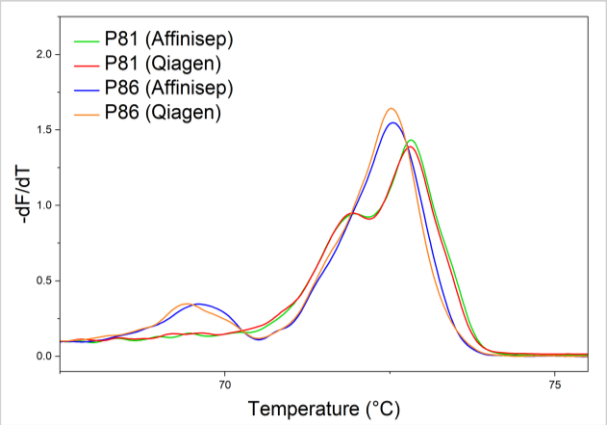

Figure 52
Derivative melting plots of honey-derived DNA extracted using Qiagen and Affinisep kits (BEE 2_1) (single replicate; exported from Rotor-Gene Q to Origin)

First, the consistency of HRM results from DNA extracted with the Qiagen and Affinisep kits was evaluated in a single run using the BEE 2_1 assay. Figure 52 shows melt peaks from two honey samples, with Qiagen- and Affinisep-derived extracts in different colors. HRM profiles were nearly identical, and the same pattern was observed across all 13 samples, indicating that both kits are suitable for HRM and do not introduce artifacts.

In total, 122 honey-derived and 42 bee-derived DNA extracts were analyzed using the BEE 2_1 assay. HRM results were repeatable across independent runs, with consistent Tm values and peak shapes. Bee-derived DNA consistently produced single peaks. *A. m. carnica* samples showed an overall Tm of approximately 72.8°C, with the Alpine variant averaging 72.6°C and the Pannonian 73.0°C. *A. m. macedonica* displayed an average Tm of 72.4°C.

The small difference between Alpine *A. m. carnica* and *A. m. macedonica* (~0.2°C) indicates that they cannot be reliably distinguished based on Tm alone; however, *A. m. macedonica* can be clearly differentiated from Pannonian *A. m. carnica*, with a Tm difference of about 0.6°C. Similarly, the Alpine and Pannonian *A. m. carnica* variants differ by about 0.4°C, making them distinguishable using this assay. On the other hand, DNA from *A. m. ligustica* samples fell within a broader Tm range of 73.0–73.7°C, suggesting that some of our samples may include bees belonging to other subspecies rather than only to *A. m. ligustica*.

To support these observations, Figure 53 shows representative samples PBF7.2 (*A. m. macedonica*) and PBF12.2 (Alpine *A. m. carnica*), which display the same Tm, while both are clearly distinguishable from PBF13.2 (Pannonian *A. m. carnica*). According to BLAST, the two *A. m. carnica* variants differ by a single SNP among the six in the amplicon, with the Pannonian variant carrying a G at a position where the Alpine variant has an A (Table 18). This nucleotide substitution corresponds to the slightly higher Tm observed for Pannonian carnica. No sequence for *A. m. macedonica* was available in BLAST; however, based on the HRM results, its GC content within the BEE 2_1 amplicon is expected to be the same as that of the Alpine *A. m. carnica* variant.

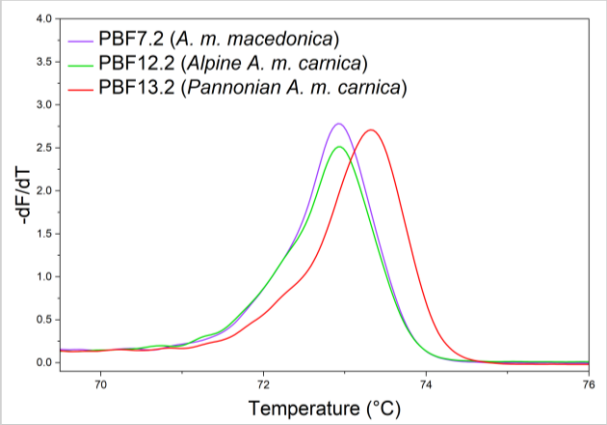

Figure 53
Derivative melting plots from three bee-derived DNA extracts obtained with the BEE 2_1 assay, highlighting differences in CG content (single replicate; exported from Rotor-Gene Q to Origin)

Overall, honey-derived DNA samples showed a mix of single, shouldered, and double peak profiles, reflecting the heterogeneous origin of DNA in honey. The Tm range largely overlapped with that of bee-derived samples. Among Austrian honey samples (n=36), 19 had single peaks, 14 shouldered peaks, and 3 double peaks, so 92% showed single or shouldered profiles. Observed Tm values ranged from 72.3 to 73.2°C, mostly clustering between 72.6 and 73.0°C. In contrast, 6 of 7 EU/non-EU honey samples displayed shouldered peaks, with Tm overlapping Austrian samples. HRM thus highlighted trends in DNA heterogeneity and could distinguish some patterns, but geographic discrimination was unclear. Results were subsequently validated by PSQ, which confirmed HRM-inferred profiles and further assessed honey origin (see Section 5.6.).

Figure 54 shows representative shouldered peaks observed in three EU/non-EU honey samples.

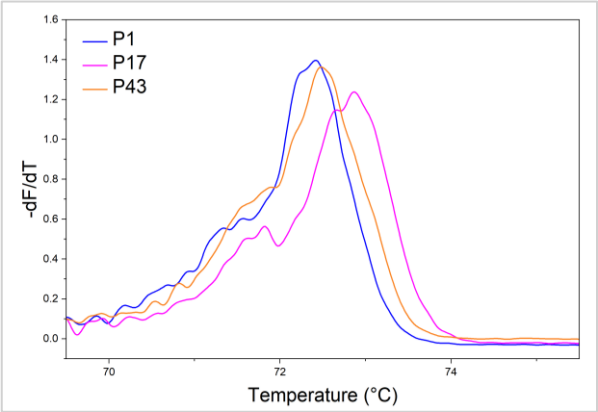

Figure 54
Representative shouldered derivative melting plots from three EU/non-EU honey samples (BEE 2_1) (single replicate; exported from Rotor-Gene Q to Origin)

5.5.2. HRM results for the BEE 3_2 assay

Complete results are shown in Tables 30–31 (Section 9.4.), while HRM patterns of selected samples are shown in this section. Samples from the poorly performing run described in Section 5.4. and excluded from BEE 3_2 evaluation are marked with an asterisk (*) in the tables.

In total, 107 honey-derived and 14 bee-derived extracts were analyzed. The assay proved repeatable, with consistent Tm values and peak shapes across runs; slight inter-run differences in curve position or signal intensity were not attributable to intrinsic melting behavior. Honey-derived DNA produced more complex HRM profiles, reflecting the heterogeneous origin of DNA in honey, whereas bee-derived DNA consistently produced single peaks. CG content primarily drove Tm differences between subspecies: *A. m. macedonica* had a lower Tm (67.3°C), *A. m. carnica* ranged 67.7–68.0°C, whereas *A. m. ligustica* showed a broader range (67.3–67.9°C), warranting PSQ verification (see Section 5.6.). Distinguishing Alpine and Pannonian *A. m. carnica* variants was more difficult because both amplicons contain the same number of C despite differing positions (see Table 18); nevertheless, slight CG-driven Tm differences were detectable (Figure 55).

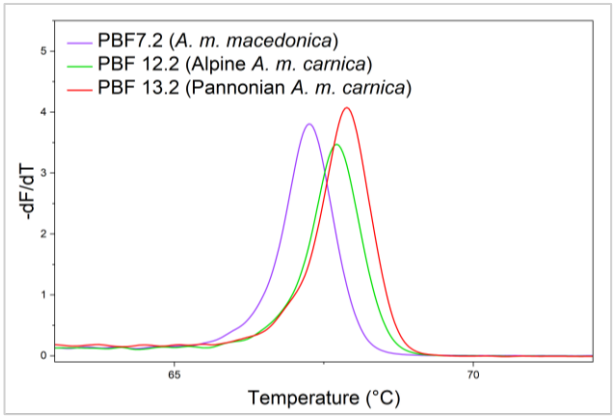

Figure 55
Derivative melting plots from three bee-derived DNA extracts obtained with the BEE 3_2 assay, highlighting differences in CG content (single replicate; exported from Rotor-Gene Q to Origin)

Among Austrian honey (n=35), 30 samples (85%) exhibited single (n=12) or double peaks (n=18), with 27 of these falling within 67.5–68.0°C. The typical peak patterns from Austrian honey samples are shown in Figure 56. All EU/non-EU honey samples analyzed (n=6) displayed shouldered peaks (with 5 in the same Tm range of Austrian honey) indicating the presence of multiple sequence variants. Representative examples are shown in Figure 57. HRM profiles were thus indicative of honey origin and were subsequently confirmed by PSQ (see Section 5.6.).

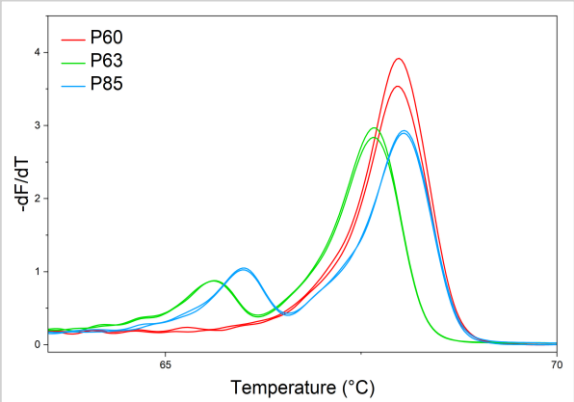

Figure 56
Derivative melting plots for Austrian honey samples (shown in duplicate) analyzed with BEE 3_2, illustrating two typical peak patterns: double peaks (P63, P85) and single peak (P60) (exported from Rotor-Gene Q to Origin).

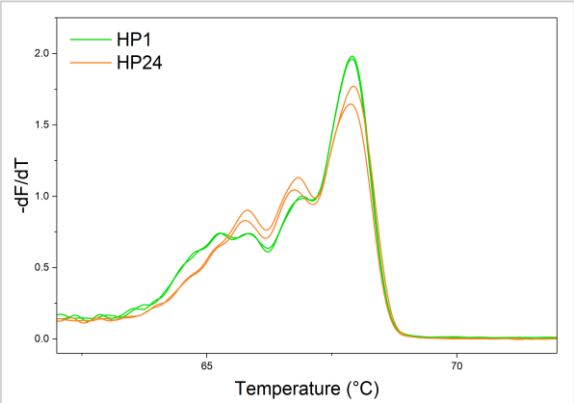

Figure 57
Derivative melting plots for two mixed EU/non-EU honey samples (shown in duplicate) analyzed with BEE 3_2, showing the characteristic shouldered pattern on the left slope (exported from Rotor-Gene Q to Origin)

5.5.3. HRM results for the BEE 6 assay

The complete results are presented in Tables 32-33 in the Section 9.4. 14 honey-derived and 10 bee-derived DNA extracts were analyzed. Only a single run was performed, so repeatability could not be assessed. The BEE 6 primers were, in fact, received at a very late stage of this study, limiting opportunities for additional replicates.

BEE 6 targets a very short sequence with a single SNP that strongly influences Tm. Bee samples produced single peaks, clearly divided into two Tm groups (69.5°C and 70.3°C), reflecting the nucleotide in the SNP. Representative peaks are shown in Figure 58. However, the observed Tm clusters did not fully match predictions based on BLAST sequences or beekeeper-reported subspecies; this discrepancy was also visible in PSQ, as summarized in Table 25 (Section 5.6.3.).

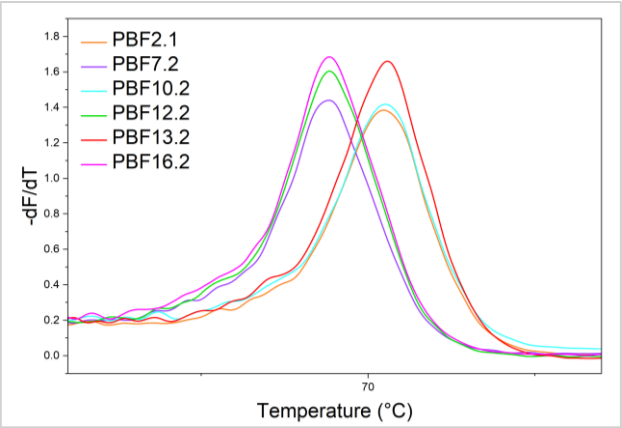

Figure 58
Derivative melting plots from six bee-derived DNA extracts obtained with the BEE 6 assay, highlighting differences in the single SNP in the amplicon (single replicate; exported from Rotor-Gene Q to Origin)

Only three samples exhibited the higher Tm (70.3°C): PBF2.1 (reported as *A. m. carnica* and assignable to the Pannonian variant via BEE 2_1 HRM), PBF10.2 (*A. m. carnica / A. m. ligustica* hybrid), and PBF13.2 (Pannonian carnica). In contrast, Alpine carnica (PBF12.2) showed the lower Tm (69.5°C), unexpectedly differing from the Pannonian variant, although all *A. m. carnica* samples were expected to cluster together. These results demonstrate that BEE 6 can distinguish two groups based on the single SNP in the amplicon, but the Tm-based clustering did not match BLAST sequences (Table 18) or beekeeper-reported subspecies, prompting PSQ analysis for further information. Interpretation was also limited by the small sample size.

Regarding the honey samples (7 Austrian and 7 non-Austrian), BEE 6 HRM analysis revealed two Tm clusters (~69.3–69.6 °C and ~70.0–70.2 °C). However, these were not clearly separated, as most samples had Tm values within the range defined by the two bee populations (69.5–70.3 °C), making confident cluster assignment uncertain. In addition, 10 of the 14 samples (71%) exhibited shouldered peaks, and both single and shouldered patterns were observed across multiple countries of origin. Overall, HRM results alone did not allow a clear distinction of samples by geographic origin. Therefore, PSQ analysis was performed to obtain more detailed information.

5.5.4. Summary of HRM analysis

HRM analysis was used as a screening approach for detecting sequence variation across the three assays, although its discriminatory power varied depending on the assay:

BEE 2_1
Strengths: BEE 2_1 reliably separated *A. m. macedonica* from Pannonian *A. m. carnica*, based on small but consistent Tm differences. HRM profiles also revealed characteristic features in honey samples, such as the frequent occurrence of shouldered peaks in EU/non-EU honey, which may aid interpretation. Differences in Tm were also observed between Alpine and Pannonian carnica.
Limitations: The assay could not reliably differentiate Alpine *A. m. carnica* from *A. m. macedonica*, nor fully determine the geographic origin of honey, as Austrian and EU/non-EU samples showed overlapping Tm ranges and peak shapes.

BEE 3_2

Strengths: BEE 3_2 reliably distinguished *A. m. macedonica* from both *A. m. carnica* variants. HRM profiles also reflected honey origin: EU/non-EU samples consistently showed typical shouldered peaks, while Austrian honey mainly produced characteristic single or double peaks.
Limitations: Some honey-derived samples with overlapping Tm ranges could not be fully assigned to a geographic origin based on HRM alone. In addition, the distinction between the Alpine and Pannonian variants of *A. m. carnica* was less pronounced with this assay.

BEE 6

Strengths: BEE 6 clearly separated bee extracts into two groups based on the single SNP in its short amplicon, producing distinct Tm clusters. This made it useful for detecting genotype variants in bee samples.
Limitations: Bee samples did not cluster as expected from BLAST, prompting PSQ confirmation; clustering was much more challenging in honey samples, and HRM profiles did not reliably indicate honey origin; the single-run, limited sample set prevented repeatability assessment.

Overall, HRM proved to be a fast, low-cost screening approach for detecting sequence variation, allowing rapid identification of Tm shifts and peak shape differences that reflect nucleotide polymorphisms. However, HRM infers variation indirectly from melting behavior and cannot always resolve closely related variants, SNPs with minimal Tm effects, or variants with identical CG content. To validate HRM patterns and precisely define the nucleotide differences, results were subsequently analyzed by PSQ (see Section 5.6.).

5.6. Pyrosequencing (PSQ)

To identify which *A. mellifera* subspecies contributed to a given honey sample, qPCR amplicons were sequenced using PSQ. Analyses were performed with the BEE 2_1 assay, already in use in our laboratory, and the newly developed BEE 3_2 and BEE 6 assays (see Section 4.6. for assay design and run preparation).

The only distinction not theoretically achievable with BEE 2_1 or BEE 3_2 is between Pannonian carnica and Reference ligustica. To address this limitation, the BEE 6 assay was developed to target a single SNP expected to enable this differentiation (see Section 5.2.1.).

The SNP patterns of the sequence variants used for interpretation are summarized in Table 18. Details on SNP positions and primer mismatches are indicated in the table notes. These considerations provide the framework for interpreting the empirical PSQ results presented in the next sections.

5.6.1. PSQ results for the BEE 2_1 assay

The PSQ analysis using the BEE 2_1 assay was performed on 188 amplicons from DNA extracted from bee and honey samples (153 honey-derived and 35 bee-derived), analyzed across multiple PSQ runs. The full dataset, presented as tabular heatmap showing the percentage of each nucleotide at every SNP position, is available in Table 35 (Section 9.4.), with percentages calculated from pyrogram peak heights as described in Section 4.6. To assess repeatability, 67 DNA extracts were sequenced in multiple runs, each providing independent confirmation of HRM-inferred polymorphisms. Results were considered repeatable if all measurements fell within ±5 percentage points of the mean value.

Within this subset, 55% of the samples (n=37) showed consistent results across all SNPs, while 30% (n=20) were repeatable for all positions except SNP6, which is known to show reduced sequencing efficiency toward the end of the run. Finally, 15% of the samples (n=10) displayed discrepancies at SNPs other than SNP6. These observations indicate that, while the assay is generally robust, some variability is expected, mostly in honey and at later sequencing positions.

Results for bee specimens

With regard to the *A. mellifera* samples analyzed with BEE 2_1, all bees reported by the beekeepers as pure *A. m. carnica* (n=16) yielded sequences consistent with the BLAST reference sequences summarized in Table 18. Two sets of bees were explicitly provided as belonging to the Alpine (PBF12.1 and PBF12.2) and Pannonian (PBF13.1 and PBF13.2) variants. The sequences obtained for these individuals matched the expected profiles and were therefore used as reference bees in this study.

The bees originating from North Macedonia and reported as *A. m. macedonica* (PBF7.1 and PBF7.2) yielded the same sequence as the Alpine variant of *A. m. carnica*. Since no corresponding BLAST sequences were available for *A. m. macedonica*, a direct comparison was not possible. Based on these results, the assay can distinguish between the Alpine and Pannonian variants of *A. m. carnica* but cannot differentiate the Alpine variant from *A. m. macedonica*.

The interpretation of bees reported as *A. m. ligustica* is more complex. One bee from the Italian region of Liguria (PBF8.1) yielded a sequence compatible only with *A. m. intermissa* (accession number KY926883), suggesting that hybridization may have occurred. For sample PBF9.1 from the Italian region of Trentino, the obtained sequence did not match any available BLAST reference. The beekeeper had reported that the colonies were hybrids of *A. m. carnic*a and *A. m. ligustica*. The unexpected sequence suggests additional hybridization events involving other subspecies beyond those declared. Other bees from the same beekeeper showed sequences typical of Pannonian carnica, consistent with the declared hybrid origin. However, this sequence is also identical to that expected for Reference ligustica according to BLAST. Sample PBF18.3 from Lazio (Italy) yielded a sequence compatible with *A. m. mellifera*. The beekeeper reported keeping *A. m. ligustica* queens but noted that colonies are renewed approximately every two years, making hybridization unavoidable. Since this bee was sampled shortly before colony renewal, the presence of an *A. m. mellifera* genotype is plausible. Although the bee appears phenotypically as *A. m. ligustica*, its mtDNA – encoding genes involved in cellular respiration – likely originated from an *A. m. mellifera* queen. For the BEE 2_1 assay in PBF18.3, nucleotide percentages at SNPs 4 and 5 were lower than for other SNPs and bees, likely due to primer site mismatches in *A. m. mellifera* mtDNA. Confirmation of this assignment is expected from the BEE 3_2 results. The beekeeper's other bees (PBF18.1 and PBF18.2) showed sequences compatible with Alternative ligustica, indistinguishable from Alpine carnica using BEE 2_1.

Based on these results, samples PBF12.1 and PBF12.2 were selected as reference individuals for the Alpine carnica variant, while PBF13.1 and PBF13.2 were selected as references for the Pannonian variant. Samples PBF7.1 and PBF7.2 were used as representatives of *A. m. macedonica*. For *A. m. ligustica*, samples PBF18.1 and PBF18.2 appeared promising as references for the Alternative ligustica variant, pending confirmation from the other assays. Finally, sample PBF18.3 may serve as a reference for *A. m. mellifera*, pending confirmation by the additional assays.

Representative nucleotide percentages for selected bee samples are shown in Table 19. The corresponding SNP profiles and their assigned subspecies or variants are summarized in Table 20, which provides a compact overview of the bee samples that can serve as reference individuals based on PSQ results obtained with the BEE 2_1 assay.

Table 19

Nucleotide percentages at each SNP for selected bee samples (BEE 2_1)

Sample ID	Origin	SNP1		SNP2		SNP3		SNP4		SNP5		SNP6	
		% A	% G	% C	% T	%C	%T	% C	% T	%C	%T	% C	% T
PBF7.2	North Macedonia	98.8	1.2	98.2	1.8	7.4	92.6	0.0	100	2.6	97.4	89.1	10.9
PBF12.2	Austria (Carinthia)	98.3	1.7	98.1	1.9	7.4	92.6	0.0	100	3.1	96.9	89.4	10.6
PBF13.2	Austria (Salzburg)	3.8	96.2	97.6	2.4	2.2	97.8	0.0	100	2.4	97.6	99.0	1.0
PBF18.2	Italy (Lazio)	98.5	1.5	98.2	1.8	4.7	95.3	0.0	100	3.4	96.6	91.6	8.4
PBF18.3	Italy (Lazio)	99.0	1.0	2.6	97.4	94.6	5.4	81.6	18.4	75.3	24.7	0.0	100

Table 20

BEE 2_1 SNP profiles and assigned subspecies/variants

Sample ID	BEE 2_1						Assigned subspecies / variant
	1	2	3	4	5	6	
PBF7.1-2	A	C	T	T	T	C	*A. m. macedonica*
PBF12.1-2	A	C	T	T	T	C	Alpine carnica
PBF13.1-2	G	C	T	T	T	C	Pannonian carnica
PBF18.1-2	A	C	T	T	T	C	Alternative ligustica
PBF18.3	A	T	C	C	C	T	*A. m. mellifera*

Results for honey samples

Regarding the honey samples, several noteworthy results were observed (see Table 21 for nucleotide percentages at each SNP in representative Austrian and non-Austrian samples):

• PSQ with the BEE 2_1 assay was performed at least once on 50 honey samples originating from Austria. However, only four of these samples were sequenced using the most recent version of the assay including all six SNPs.

• A very high level of variability was observed at SNP1, where the proportions of A and G varied widely among the Austrian samples.

• In contrast, SNP2 and SNP4 showed limited variability. At SNP2, nucleotide C exceeded 80% in 79 of 91 amplicons (87%), with 12 (13%) exceptions. Similarly, at SNP4, nucleotide T exceeded 80% in 80 amplicons (88%), with 11 (12%) exceptions. Counts are based on sequenced amplicons rather than unique samples, as some samples were analyzed more than once.

• Higher variability was again observed at SNP6. However, this is likely related to reduced sequencing efficiency toward the end of the PSQ reaction rather than true biological variation.

• SNP3 and SNP5 showed a consistent pattern with T detected at both positions. However, only a limited number of amplicons were sequenced for these SNPs, and additional data would be required for validation.

• Among EU/non-EU honey samples analyzed with BEE 2_1, only 8 of 24 amplicons (33%) reached the 80% threshold at SNP2 and 13 of 24 (54%) at SNP4 (see Table 21), suggesting the presence of honey bee subspecies distinguishable from *A. m. carnica* at these SNP positions. Greater caution is required when interpreting SNP6 due to reduced sequencing efficiency at later positions. No EU/non-EU honey samples were analyzed for SNP3 and SNP5.

• All honey samples reported to originate from Spain (HP5, P18, P101), Nigeria (P105), Yemen (P106), and Brazil (P22) clearly showed T at SNP2 and C at SNP4, indicating the presence of DNA from honey bee subspecies different from *A. m. carnica*. This combination is characteristic of *A. m. iberiensis* and several African subspecies such as *A. m. capensis* and *A. m. scutellata*, consistent with the origin of the samples and with the spread of Africanized honey bees in Brazil following the introduction of *A. m. scutellata* in the 1950s (Calfee et al., 2020).

Table 21

Nucleotide percentages at each SNP for selected honey samples (BEE 2_1, first version with only 4 SNPs), showing variability at SNP1 and limited variability at SNPs 2 and 4 in Austrian samples, contrasting patterns in non-Austrian samples, and apparent variability at SNP6 likely caused by reduced sequencing efficiency at the end of the PSQ run

Sample ID	Origin	SNP1		SNP2		SNP3		SNP4		SNP5		SNP6	
		% A	% G	% C	% T	% C	% T	% C	% T	% C	% T	% C	% T
P9	Austria (Styria)	44.2	55.8	98.8	1.2			0.0	100			100	0.0
P60	Austria (Vienna)	3.7	96.3	98.0	2.0			0.0	100			88.2	11.8
P85	Austria	29.4	70.6	95.7	4.3			0.0	100			96.9	3.1
HP1	EU/non-EU	55.7	44.3	61.9	38.1			27.9	72.1			81.3	18.7
HP5	Spain/Greece	98.0	2.0	5.0	95.0			79.7	20.3			0.0	100
HP22	EU/non-EU	46.8	53.2	74.3	25.7			17.8	82.2			80.1	19.9
P18	Spain	96.8	3.2	2.5	97.5			70.4	29.6			0.0	100
P105	Nigeria	98.9	1.1	3.1	96.9			75.5	24.5			0.0	100

Discussion

Overall, these results support the hypothesis that the majority of Austrian honey samples contain DNA from *A. m. carnica*, either in the Alpine variant, the Pannonian variant, or a mixture of the two. According to the BEE 2_1 assay, the two variants differ only at SNP1, while the remaining SNPs (SNP2–6) are identical. Specifically, Alpine carnica carries an A at SNP1, whereas Pannonian carnica carries a G. Honey produced from mixed Alpine and Pannonian populations is expected to contain both nucleotides at SNP1, with proportions reflecting the relative contributions of each variant. Consequently, SNP1 allows discrimination between Alpine and Pannonian variants, while SNPs 2–6 provide internal consistency and can reveal the potential presence of other subspecies.

At this stage, PSQ results were also compared with observations from HRM analysis. Although it is not possible to compare all HRM curves with PSQ results within this thesis, selected examples illustrate the relationship between the two approaches. Figure 59 shows four honey samples analyzed with the BEE 2_1 assay including four SNPs. Sample P15 from Austria appears from PSQ analysis to contain approximately equal proportions of Alpine and Pannonian *A. m. carnica*. The corresponding HRM peak displays a shouldered profile, consistent with the presence of mixed *A. m. carnica* variants.

Sample P115, also from Austria, appears to contain only Pannonian carnica according to PSQ, and the HRM peak is a single well-defined peak clearly distinct from that of another honey sample, P18, from Spain. PSQ analysis of P18 suggests the presence of *A. m. iberiensis* DNA, although information on SNP3 and SNP5 is not available. This could reveal the involvement of additional subspecies, as suggested by a small shoulder on the HRM peak. Finally, sample P23, an EU/non-EU honey, exhibits an HRM peak indistinguishable from that of P15. Nevertheless, PSQ reveals the presence of non-carnica honey bee subspecies, indicated by the 52.2% T observed at SNP2. This highlights the complementary value of combining HRM and PSQ for subspecies detection.

Sample ID	Origin	SNP1		SNP2		SNP4		SNP6	
		% A	% G	% C	% T	% C	% T	% C	% T
P15	Austria	49.4	50.6	97.5	2.5	0.0	100	95.6	4.4
P18	Spain	97.0	3.0	1.9	98.1	78.9	21.1	0.0	100
P23	EU/non-EU	64.7	35.3	47.8	52.2	5.0	95.0	40.9	59.1
P115	Austria	97.0	3.0	95.3	4.7	0.0	100	76.0	24.0

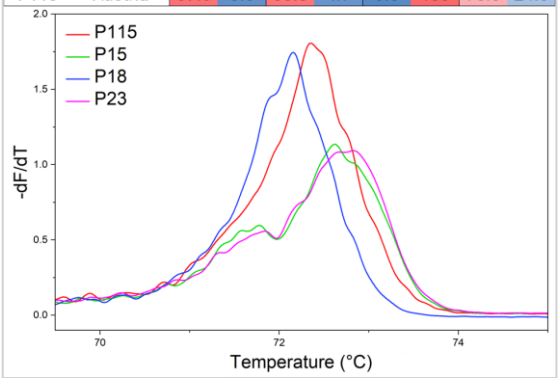

Figure 59
Comparison of derivative melting plots and PSQ SNP analysis for four honey samples (single replicate) from Austria, Spain, and EU/non-EU (BEE 2_1 assay) (exported from Rotor-Gene Q to Origin)

Overall, the BEE 2_1 PSQ assay proved reliable and informative for analyzing both bee and honey samples. It can discriminate between the Alpine and Pannonian variants of *A. m. carnica* and detect DNA from other bee subspecies when clear SNP patterns are present. Repeatability was generally satisfactory, although reduced sequencing efficiency at later positions (particularly SNP6) and limited data for SNP3 and SNP5 represent notable limitations. In honey samples, the assay distinguished Austrian honey dominated by *A. m. carnica* from EU/non-EU honeys containing other subspecies, including *A. m. iberiensis* and African lineages. Combined with HRM, which reflects allelic mixtures through melting behavior, PSQ provides precise quantitative SNP information and enables a more confident assessment of subspecies composition.

5.6.2. PSQ results for the BEE 3_2 assay

The PSQ analysis using the BEE 3_2 assay was performed on 167 amplicons from DNA extracted from bee and honey samples (140 honey-derived and 27 bee-derived), analyzed across multiple PSQ runs. The full dataset, presented as tabular heatmap showing the percentage of each nucleotide at every SNP position, is available in Table 36 (Section 9.4.), with percentages calculated from pyrogram peak heights as described in Section 4.6. To assess repeatability, 46 DNA extracts were sequenced in multiple runs, each providing independent confirmation of HRM-inferred polymorphisms. Results were considered repeatable if all measurements fell within ±5 percentage points of the mean value.

Within this subset, 74% of the samples (n=34) showed consistent results across all SNPs, while 9% (n=4) were repeatable for all positions except SNP6. Finally, 17% of the samples (n=8) displayed discrepancies at SNPs other than SNP6. These observations indicate that, while the assay is generally robust, some variability is expected, mostly in honey-derived samples and at later sequencing positions.

Results for bee specimens

With regard to the *A. mellifera* samples analyzed with BEE 3_2, all bees reported by the beekeepers as pure *A. m. carnica* (n=6) yielded sequences consistent with the BLAST reference sequences summarized in Table 18, confirming the results obtained with BEE 2_1. The sequences from bees explicitly identified as Alpine (PBF12.1 and PBF12.2) and Pannonian (PBF13.1 and PBF13.2) variants also matched the expected profiles, validating their use as reference specimens in this study. Although the two *A. m. carnica* variants were not clearly distinguishable by HRM using BEE 3_2, PSQ allowed their differentiation. In fact, both variants carry a single C within the amplicon, but at different positions (see Table 18).

In contrast to BEE 2_1, where bees from North Macedonia reported as *A. m. macedonica* (PBF7.1 and PBF7.2) yielded sequences identical to Alpine carnica, BEE 3_2 produced a sequence distinct from both *A. m. carnica* variants. Since no BLAST reference sequences were available for *A. m. macedonica*, a direct comparison was not possible. Based on these results, the BEE 3_2 assay can distinguish *A. m. macedonica* from both *A. m. carnica* variants, addressing a limitation of the BEE 2_1 assay.

The bee sample PBF10.2, reported by the beekeeper as a hybrid between *A. m. carnica* and *A. m. ligustica*, showed the expected sequence for Pannonian carnica, which is entirely plausible. However, as with BEE 2_1, the sequence for Pannonian carnica is identical to that of Reference ligustica (see Table 18), so the result for this bee could correspond to either subspecies.

PSQ analysis with the BEE 3_2 assay also confirmed the results for bees from the Italian region of Lazio. Samples PBF18.1 and PBF18.2 yielded sequences compatible with Alternative ligustica. Unlike BEE 2_1, BEE 3_2 can distinguish Alternative ligustica from Alpine carnica, resolving a limitation of BEE 2_1. The distinction between Alternative ligustica and *A. m. macedonica* remains impossible with BEE 3_2. This is not unexpected given the close phylogenetic relationship between *A. m. ligustica* and *A. m. macedonica*, both belonging to the C lineage (Ilyasov et al., 2020). Genetically distinguishing these two subspecies would require a different assay, which was beyond the scope of this study.

Finally, PSQ with BEE 3_2 clearly confirmed the assignment of sample PBF18.3 to *A. m. mellifera*, as indicated by BEE 2_1. Overall, the sequences obtained with BEE 3_2 validated the suitability of the bee samples listed in Table 20 as reference individuals for their respective subspecies/variants and resolved several uncertainties that remained when using BEE 2_1 alone.

Representative nucleotide percentages for selected bee samples are shown in Table 22. The corresponding SNP profiles and their assigned subspecies or variants are summarized in Table 23, which provides a compact overview of the bee samples that can serve as reference individuals based on PSQ results obtained with the BEE 3_2 assay (and confirming the BEE 2_1 results).

Table 22

Nucleotide percentages at each SNP for selected bee samples (BEE 3_2)

Sample ID	Origin	SNP1		SNP2		SNP3		SNP4		SNP5		SNP6	
		% C	% T	% A	% T	%C	%T	% C	% T	% A	% G	% C	% T
PBF7.2	North Macedonia	1.5	98.5	0.0	100	9.4	90.6	0.0	100	93.6	6.4	4.2	95.8
PBF12.2	Austria (Carinthia)	1.9	98.1	0.0	100	11.7	88.3	0.0	100	87.9	12.1	92.1	7.9
PBF13.2	Austria (Salzburg)	100	0.0	0.0	100	9.3	90.7	0.0	100	92.9	7.1	5.0	95.0
PBF18.2	Italy (Lazio)	2.7	97.3	0.0	100	9.1	90.9	0.0	100	93.6	6.4	3.8	96.2
PBF18.3	Italy (Lazio)	1.7	98.3	0.0	100	10.9	89.1	100	0.0	90.6	9.4	7.1	92.9

Table 23

BEE 3_2 SNP profiles and assigned subspecies/variants

Sample ID	BEE 3_2						Assigned Subspecies / variant
	1	2	3	4	5	6	
PBF7.2	T	T	T	T	A	T	*A. m. macedonica*
PBF12.2	T	T	T	T	A	C	Alpine carnica
PBF13.2	C	T	T	T	A	T	Pannonian carnica
PBF18.2	T	T	T	T	A	T	Alternative ligustica
PBF18.3	T	T	T	C	A	T	*A. m. mellifera*

Results for honey samples

Regarding the honey samples, several noteworthy results were observed (see Table 24 for nucleotide percentages at each SNP in representative Austrian and non-Austrian samples):

• PSQ with the BEE 3_2 assay was performed at least once on 36 honey samples originating from Austria. However, only 28 of these samples were analyzed using the most recent version of the assay including all six SNPs.

• In Austrian samples, SNPs 2–5 showed limited variability and mostly matched the expected sequence of *A. m. carnica* (see Table 18). Counts are based on sequenced amplicons rather than unique samples, as some samples were analyzed more than once.
At SNP2, nucleotide T exceeded 80% in 47 of 50 amplicons (94%).
At SNP3, T exceeded 80% in 42 amplicons (84%).
At SNP4, T exceeded 80% in 48 amplicons (96%).
At SNP5, nucleotide A exceeded 80% in 44 amplicons (88%).
Only a small number of honey samples deviated from the expected *A. m. carnica* sequence at SNPs 2–5. Notably, among these deviating samples, only two originated from federal states where this subspecies is protected.

• Among amplicons resulting from Austrian honey samples showing the expected *A. m. carnica* sequence at SNPs 2–5, a characteristic mirror pattern was observed between SNP1 and SNP6 in 71% of cases (25 of 35 amplicons). In this pattern, the nucleotide proportions at the two positions are approximately reversed. Representative examples are shown in Table 24. For example, in amplicon P58, 55.8% C and 44.2% T were observed at SNP1, while 42.5% C and 57.5% T were observed at SNP6. The mirror pattern was considered present when the percentage of C at SNP1 differed by less than 10 percentage points from the percentage of T at SNP6, or when the percentage of T at SNP1 differed by less than 10 percentage points from the percentage of C at SNP6.

• In contrast, 10 of 12 honey samples (83%) with mixed EU/non-EU origin deviated from the expected *A. m. carnica* sequence at SNPs 2–5. Certain alternative nucleotides occurred repeatedly in these samples. An A at SNP2 was frequently observed in EU/non-EU samples, but also occurred in samples from Spain (HP5, P18), Brazil (P22), and Nigeria (P105). Similarly, a C at SNP4 was frequently detected in EU/non-EU samples and in samples from Spain (HP5, P101). At SNP5, a G was frequently observed in EU/non-EU samples and in samples from Spain (HP5, P18).

Table 24

Nucleotide percentages at each SNP for selected honey samples (BEE 3_2), showing the mirror pattern at SNPs 1 and 6 and limited variability at SNPs 2–5 in Austrian samples, and contrasting patterns in non-Austrian samples

Sample ID	Origin	SNP1		SNP2		SNP3		SNP4		SNP5		SNP6	
		%C	%T	%A	%T	%C	%T	%C	%T	%A	%G	%C	%T
P58	Austria (Burgenland)	55.8	44.2	0.0	100	11.4	88.6	0.0	100	88.7	11.3	42.5	57.5
P60	Austria (Vienna)	100	0.0	0.0	100	10.6	89.4	0.0	100	94.1	5.9	4.8	95.2
P85	Austria	75.2	24.8	0.0	100	10.3	89.7	0.0	100	90.3	9.7	28.3	71.7
HP1	EU/non-EU	40.4	59.6	30.1	69.9	9.3	90.7	9.8	90.2	53.5	46.5	4.9	95.1
HP5	Spain/Greece	2.3	97.7	41.6	58.4	10.6	89.4	48.7	51.3	53.1	46.9	6.5	93.5
P18	Spain	2.7	97.3	74.8	25.2	10.3	89.7	13.0	87.0	52.8	47.2	4.6	95.4
P101	Spain	5.6	94.4	27.8	72.2	13.5	86.5	70.8	29.2	72.7	27.3	9.8	90.2
P105	Nigeria	6.9	93.1	90.9	9.1	12.4	87.6	6.3	93.7	63.7	36.3	7.7	92.3

Discussion

Overall, these results support the hypothesis that the majority of the Austrian honey samples contain DNA from *A. m. carnica*, either in the Alpine variant, the Pannonian variant, or a mixture of the two.

In honeys produced exclusively by *A. m. carnica*, SNPs 2–5 are expected to show the characteristic nucleotides of this subspecies with very high proportions, whereas SNPs 1 and 6 differentiate the two main *A. m. carnica* variants present in Austria, namely the Alpine and the Pannonian variant (see Table 18).

Alpine carnica is characterized by T at SNP1 and C at SNP6, whereas Pannonian carnica shows the opposite combination (C at SNP1 and T at SNP6). Consequently, honey produced exclusively by Alpine populations is expected to display the sequence TTTTAC, while honey produced by Pannonian populations should show CTTTAT. In honey derived from mixed Alpine and Pannonian populations, both nucleotides are expected at SNPs 1 and 6, with proportions reflecting their relative contributions.

When both variants contribute to honey production, the nucleotide proportions at SNPs 1 and 6 are therefore expected to show a reciprocal relationship. For example, a honey sample containing approximately 75% Alpine carnica and 25% Pannonian carnica would be expected to show roughly 75% T and 25% C at SNP1, and approximately 75% C and 25% T at SNP6. This reciprocal relationship results in a characteristic mirror pattern between the two SNPs, which can serve as an internal consistency check when interpreting BEE 3_2 results. In honey produced exclusively by *A. m. carnica*, similar relative proportions of the variant-specific nucleotides are therefore expected at these two positions. Conversely, marked discrepancies between SNP1 and SNP6 may indicate either technical inconsistencies or the contribution of additional bee subspecies.

The results obtained for Austrian honey samples were largely consistent with these expectations. Most samples showed limited variability at SNPs 2–5 and high proportions of the nucleotides characteristic of *A. m. carnica*, supporting the assumption that these honeys were predominantly produced by this subspecies. Furthermore, among amplicons showing the expected *A. m. carnica* profile at SNPs 2–5, the mirror relationship between SNP1 and SNP6 was observed in the majority of cases, further supporting the internal consistency of the assay and the contribution of Alpine and Pannonian *A. m. carnica* populations to Austrian honey production.

SNPs 2–5 of the BEE 3_2 assay are highly informative for detecting the involvement of subspecies other than *A. m. carnica* in honey. In honey derived exclusively from *A. m. carnica*, these SNPs are expected to show minimal variation; the presence of alternative nucleotides provides strong evidence for additional subspecies (see Table 18 for SNP positions and subspecies).

An A at SNP2 indicates African A-lineage subspecies, including *A. m. intermissa*, *A. m. ruttneri*, and *A. m. capensis*, or populations with introgression, such as *A. m. iberiensis* and *A. m. siciliana*, while *A. m. carnica* consistently shows T. A C at SNP3 is typical of *A. m. carpatica*, sometimes considered a local *A. m. carnica* population. At SNP4, C indicates M-lineage subspecies such as *A. m. mellifera* and *A. m. iberiensis*, whereas *A. m. carnica* (C lineage) shows T. G at SNP5 is characteristic of African A-lineage subspecies and absent in *A. m. carnica*.

The geographic patterns observed match expected population genetics. High A at SNP2 in Nigerian samples reflects the African lineage, while elevated A in Spanish and Brazilian samples likely reflects historical gene flow and africanization after the introduction of *A. m. scutellata* in the 1950s (Calfee et al., 2020). Mixed EU/non-EU samples also showed increased A at SNP2, indicating contributions from non-European populations. C at SNP3 appeared mainly in Italian honeys, likely reflecting imported Eastern European honey rather than local variation. High C at SNP4 in Spanish samples aligns with the endemic *A. m. iberiensis* (M lineage). G at SNP5 was detected in African, Spanish, and Sicilian honeys, reflecting the influence of *A. m. iberiensis* and *A. m. siciliana*; elevated G was also seen in mixed EU/non-EU samples. Overall, high proportions of nucleotides characteristic of non-carnica subspecies at SNPs 2–5 indicate their contribution to honey production and suggest non-compliance with regulations in several Austrian federal states safeguarding *A. m. carnica* genetic integrity.

PSQ results were also compared with HRM analysis. Although not all HRM curves could be compared in this thesis, selected examples illustrate the relationship between the two approaches (Figure 60). Austrian honey samples P60 and P85 both displayed the characteristic mirror pattern in PSQ. P60 appears to contain almost exclusively Pannonian carnica DNA (95% C at SNP1, 91% T at SNP6), whereas P85 shows a mixture of Pannonian (~70–75%) and Alpine (~25–30%) carnica. This difference is reflected in HRM profiles: P60 exhibits a single, well-defined peak, while P85 shows a double peak, with the higher peak aligning with P60 and a smaller peak at slightly lower Tm.

Samples HP1 and HP5, from mixed EU/non-EU and Spain/Greece, showed nucleotides characteristic of non-carnica subspecies at SNPs 2–5. The presence of additional subspecies produces more complex, often shouldered HRM peaks, making these samples clearly distinguishable from most Austrian honeys containing only *A. m. carnica* DNA.

Sample ID	Origin	SNP1		SNP2		SNP3		SNP4		SNP5		SNP6	
		% C	% T	% A	% T	% C	% T	% C	% T	% A	% G	% C	% T
HP1	EU/non-EU	40.4	59.6	30.1	69.9	9.3	90.7	9.8	90.2	53.5	46.5	4.9	95.1
HP5	Spain/Greece	2.3	97.7	41.6	58.4	10.6	89.4	48.7	51.3	53.1	46.9	6.5	93.5
P60	Austria	95.0	5.0	0.1	99.9	14.5	85.5	0.0	100	87.3	12.7	9.0	91.0
P85	Austria	75.2	24.8	0.0	100	10.3	89.7	0.0	100	90.3	9.7	28.3	71.7

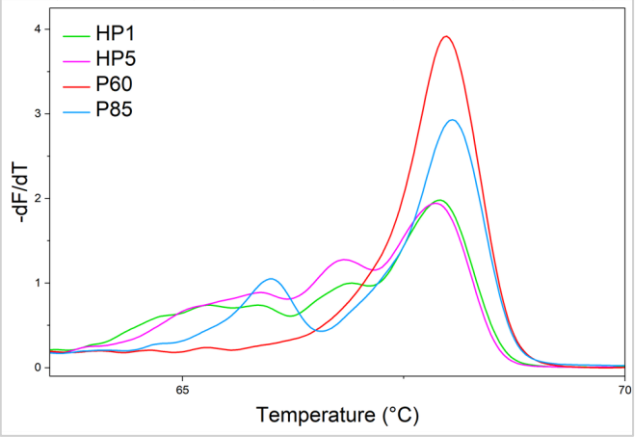

Figure 60
Comparison of derivative melting plots and PSQ SNP analysis for four honey samples (single replicate) from Austria, Spain/Greece, and EU/non-EU (BEE 3_2 assay) (exported from Rotor-Gene Q to Origin)

Overall, the BEE 3_2 PSQ assay proved to be a robust and informative tool for analyzing both bee and honey samples. It can distinguish the Alpine and Pannonian variants of *A. m. carnica* and resolve some limitations of BEE 2_1, such as differentiating *A. m. macedonica* from *A. m. carnica* variants and distinguishing Alternative ligustica from Alpine carnica. Repeatability was generally satisfactory, although slightly reduced sequencing efficiency at later positions (particularly SNP6) represents a minor limitation. In honey samples, the assay confirmed that most Austrian honeys are dominated by *A. m. carnica*, showing minimal variability at SNPs 2–5, while mixed EU/non-EU and non-Austrian samples revealed alternative nucleotides indicative of additional subspecies, such as African A-lineage subspecies or *A. m. iberiensis*. The characteristic mirror pattern between SNP1 and SNP6 in Austrian samples reflects the relative contributions of Alpine and Pannonian carnica, and is consistent with HRM profiles, where single or double peaks correspond to homogeneous or mixed variant contributions. Combined with HRM, PSQ provides precise quantitative SNP information, enabling confident assessment of subspecies composition and detection of non-carnica contributions in honey.

Nevertheless, an important limitation remains: Pannonian carnica and Reference ligustica produce identical sequences with both the BEE 2_1 (GCTTTC) and BEE 3_2 (CTTTAT) assays, making them indistinguishable from each other. This limitation prompted the development of the BEE 6 assay, which was specifically designed to differentiate Pannonian carnica from Reference ligustica.

5.6.3. PSQ results for the BEE 6 assay

The PSQ analysis using the BEE 6 assay was performed on 24 amplicons from DNA extracted from bee and honey samples (14 honey-derived and 10 bee-derived). All samples were analyzed in a single run, so repeatability of the method could not be assessed. The BEE 6 primers were received very late in the study, limiting the opportunity for additional replicates. The full dataset, presented as tabular heatmap showing the percentage of each nucleotide at every SNP position, is available in Table 37 (Section 9.4.), with percentages calculated from pyrogram peak heights as described in Section 4.6.

Results for bee specimens

The PSQ results obtained with the BEE 6 assay fully confirmed the patterns observed in the HRM analysis, with *A. mellifera* samples clearly separating into two well-defined clusters. However, the sequencing results differed substantially from the genotype expected based on BLAST data (Table 18). The calculated nucleotide percentages at the SNP for reference *A. mellifera* individuals are reported in Table 25. Sample PBF16.2 is also reported in the table as it becomes relevant later in this section.

The BEE 6 assay clearly divides *A. mellifera* samples into two clusters that are detectable by both HRM and PSQ. Amplicons carrying an A at the single SNP form the lower-Tm cluster (69.5 °C), whereas those carrying a G form the higher-Tm cluster (70.3 °C).

A special case is represented by sample PBF16.2. Based on the PSQ results obtained with the BEE 2_1 and BEE 3_2 assays, this bee from Upper Austria – reported by the beekeeper as only probably *A. m. carnica* – would be compatible with assignment to either Pannonian carnica or Reference ligustica. However, in the PSQ analysis performed with BEE 6, sample PBF16.2 differs from PBF13.2, which was reported by the beekeeper as certainly Pannonian carnica. This observation suggests that PBF16.2 may represent an individual of Reference ligustica. Nevertheless, the discrepancies between the observed genotypes and those expected from BLAST remain considerable, and therefore caution is required before drawing conclusions.

Several factors may explain these discrepancies. First, BLAST reference sequences are typically derived from single specimens and may not capture the full genetic variability of natural populations. Consequently, samples such as PBF13.2, PBF16.2, and PBF18.2 (which did not yield the expected results) may show natural variation at the BEE 6 SNP while still belonging to the expected subspecies.

Second, *A. mellifera* colonies are frequently hybridized. Individuals that phenotypically match one subspecies may carry SNPs characteristic of another. This is particularly relevant for mitochondrial markers, which are not directly associated with the morphological traits traditionally used for subspecies identification. Hybrids between *A. m. carnica* and *A. m. ligustica* are especially common because they combine high productivity with docile behavior, making these two subspecies the most widely used in European and global beekeeping.

Technical explanations appear unlikely. The discriminating SNP lies within the BEE 6 amplicon rather than in the primer-binding sites, making primer–template mismatches improbable. Efficient and consistent qPCR amplification further supports this interpretation, and the absence of long repeats within the amplicon excludes PSQ artifacts.

Overall, the discrepancies are most plausibly explained by intra-subspecies variability or hybridization. This interpretation is consistent with the results obtained with the BEE 2_1 and BEE 3_2 assays, the beekeepers' reports, and the geographic origin of the samples. Accordingly, assigning PBF13.2 to Pannonian carnica and PBF18.2 to Alternative ligustica appears scientifically justified, whereas sample PBF16.2 remains ambiguous and may belong either to Reference ligustica or to Pannonian carnica.

Table 25

A. mellifera subspecies assignment and BEE 6 expected vs. observed SNP results

Sample ID	Most likely subspecies	% A	% G	BEE 6 Observed	BEE 6 Expected
PBF7.2	*A. m. macedonica*	97.6	2.4	A	-
PBF12.2	Alpine carnica	98.3	1.7	A	A
PBF13.2	Pannonian carnica	1.7	98.3	G	A
PBF18.2	Alternative ligustica	98.5	1.5	A	G
PBF16.2	Pannonian carnica / Reference ligustica	97.9	2.1	A	A/G

Results for honey samples

PSQ analysis using the BEE 6 assay was performed on 7 Austrian and 7 non-Austrian honey samples. Consistent with the HRM results, PSQ did not reveal clearly separated clusters among the honey samples based on the single SNP targeted by this assay.

The mean percentage of A at the SNP was lower in Austrian samples (51.8%) compared with non-Austrian samples (73.7%). However, a Mann–Whitney U test indicated that this difference was not statistically significant ($U = 14.0$, $n_1 = n_2 = 7$, $p > 0.01$). These results indicate that, within the dataset analyzed, the BEE 6 SNP did not allow a statistically supported separation between Austrian and non-Austrian honeys.

Discussion

The BEE 6 assay clearly differentiates two clusters of *A. mellifera* in bee specimens, detectable by both HRM and PSQ. The concordance between HRM clustering and PSQ nucleotide calls confirms that the polymorphism targeted by this assay is reliably detected. However, discrepancies between the observed genotypes and those expected from BLAST reference sequences indicate that this SNP cannot be considered fully diagnostic for distinguishing Pannonian carnica from Reference ligustica in natural populations. For bee specimens, these differences are most plausibly explained by intra-subspecies variability or hybridization rather than technical artifacts.

In honey, a clear cluster separation was not observed. The relatively small number of samples analyzed with the BEE 6 assay limits the statistical power to detect potential differences based on honey geographical origin. While the BEE 6 SNP reveals variability among samples, it does not provide a clear separation between Austrian and non-Austrian honeys under the conditions tested. These findings are consistent with the HRM results and likely reflect the complex and mixed genetic origin of honey DNA.

6. CONCLUSION

This study aimed to develop and evaluate molecular methods capable of identifying *A. mellifera* subspecies DNA in honey, with particular focus on *A. m. carnica*, a subspecies native to Austria and legally protected in several federal states. The results demonstrate that the combined application of mtDNA markers, qPCR, HRM analysis, and PSQ represents a reliable approach for detecting *A. mellifera* subspecies signatures in honey and for indirectly assessing the geographic origin of honey products.

The development of the BEE 3_2 assay proved to be a key outcome of this study. By targeting a short mtDNA region containing six informative SNPs, this assay enabled discrimination of *A. m. carnica* from most other subspecies, including differentiation between its Alpine and Pannonian variants. The assay showed satisfactory amplification performance in both bee- and honey-derived DNA, despite the challenges posed by honey as a complex, low-yield matrix, which required testing a more efficient extraction kit. Overall, these results confirm the greater applicability of mitochondrial markers over nuclear markers for phylogenetic assignment. The assay proved effective for practical application, achieving a success rate of approximately 91% in honey samples. Sufficient amplification was defined as the absence of warnings indicating that genotype determination was not possible due to low peak heights in subsequent PSQ.

The development of the BEE 6 assay was motivated by a limitation observed in the BEE 2_1 and BEE 3_2 assays, namely the difficulty in distinguishing Pannonian carnica from Reference ligustica. By targeting a single diagnostic SNP, BEE 6 showed potential to improve this distinction. However, PSQ results did not fully match expectations derived from BLAST analyses, indicating that further validation is required. BEE 6 therefore represents a promising complementary assay whose robustness for unequivocal discrimination should be evaluated on larger datasets.

HRM analysis proved to be a valuable rapid screening tool, showing high repeatability across runs and consistency between DNA extraction methods. Characteristic melting profiles were observed for honey samples of different geographic origins, particularly enabling differentiation between Austrian honeys and blended EU/non-EU products. PSQ was then used to confirm HRM-inferred polymorphisms at the nucleotide level and provided detailed characterization of SNP patterns. Application of correction factors to account for adenine signal bias and consecutive nucleotide incorporations allowed accurate quantification of nucleotide proportions, overcoming software limitations in interpreting mixed DNA signals commonly found in honey. These results confirmed that honey frequently contains DNA mixtures from multiple subspecies, reflecting the biological complexity of this product.

Overall, the study confirms that mtDNA-based methods are effective tools for identifying bee subspecies in honey. The developed workflow shows strong potential for applications in honey authenticity verification, geographic origin assessment, and support of conservation strategies for protected *A. mellifera* subspecies such as *A. m. carnica*. Future research should focus on expanding reference sequence databases, including additional honey samples from underrepresented federal states such as Tyrol, and further validating the methods on larger sample sets.

7. MATERIALS

7.1. Laboratory equipment

Name	*Manufacturer*
Centrifuge 5424	Eppendorf
Centrifuge 5910 Ri	Eppendorf
Classic Advanced Vortex Mixer	VELP Scientifica
FastPrep-24 5G Homogenizer	MP Biomedicals
Galaxy Mini Centrifuge	VWR International
Galaxy Mini Centrifuge (28 J)	VWR International
Lab Dancer Vortex Mixer (S000)	IKA
MiniStar Mini Centrifuge	VWR International
PCR Workstation Pro (PEQLAB 90-UV)	VWR International
PyroMark Q48 Autoprep System	QIAGEN
Qubit 4 Fluorimeter	Invitrogen (Thermo Fisher Scientific)
QuantStudio 5 Real-Time PCR System	Applied Biosystems (Thermo Fisher Scientific)
Rotor-Gene Q 5plex HRM System	QIAGEN
Sartorius Talent Analytical Balance (TE214S)	Sartorius
ThermoMixer C	Eppendorf
Vortex-Genie 2 Mixer	Scientific Industries
Xplorer Electronic Pipette (0.5–10 µL)	Eppendorf
Xplorer Electronic Pipette (1–20 µL)	Eppendorf
Xplorer Electronic Pipette (10–200 µL)	Eppendorf
Xplorer Electronic Pipette (50–1000 µL)	Eppendorf

7.2. Chemicals, solutions, and kits

Name	*Manufacturer*
BioSPE PureGenNucleo cfDNA Kit	Affinisep
Chloroform	Merck
DNA-ExitusPlus IF	PanReac AppliChem ITW Reagents
DNeasy mericon Food Kit	Qiagen
Deionized water (ELGA water)	Department of Analytical Chemistry, University of Vienna (AG Köllensperger)
Ethanol abs.	ChemSolute
Primers (lyophilized form)	Sigma-Aldrich
2x Type-It HRM PCR Kit	Qiagen
PyroMark Annealing Buffer	Qiagen
PyroMark Denaturation Solution	Qiagen
PyroMark Enzyme Mix	Qiagen
PyroMark Nucleotide Mix	Qiagen
PyroMark Substrate Mix	QIAGEN
Qubit dsDNA HS Assay Kit	Invitrogen (Thermo Fisher Scientific)
Rnase-free water	Qiagen
Streptavidin-coated beads (PyroMark)	Qiagen

7.3. Consumables and other materials

Name	*Manufacturer*
6-tube strip PCR tubes with attached caps	Applied Biosystems (Thermo Fisher Scientific)
Eppendorf Tubes (200 µL, 1.5 mL, 2 mL, 5 mL)	Eppendorf
Filter tips (10-1000 µL)	Sarstedt
Lysing Matrix tubes (FastPrep-24 5G, with beads)	MP Biomedicals
PyroMark Q48 absorber strips	Qiagen
PyroMark Q48 cartridges	Qiagen
PyroMark Q48 sample disc	Qiagen
Qubit Assay Tubes	Invitrogen
Rotor-Gene 4-tube strip PCR tubes	Qiagen
Screw-cap tubes (50 mL)	Sarstedt
Single-channel micropipettes (10-200-1000 µL)	Eppendorf (Research Plus)
duoSHIELD PFT Nitrile 240 gloves	SHIELD Scientific

7.4. Software

Name	*Developer*
Excel spreadsheet	Microsoft
OriginPro 2024 10.1.0.170	OriginLab
Pyromark Q48 Autoprep Software	Qiagen
QuantStudio Design & Analysis Software 1.4.3	Thermo Fisher
Rotor-Gene Q Series Software	Qiagen

7.5. Webservers

Name	*Link*
NCBI – Nucleotide BLAST	https://blast.ncbi.nlm.nih.gov/Nucleotide BLAST
OligoAnalyzer	https://www.idtdna.com/calc/analyzer
Oligonucleotide Properties Calculator	https://oligocalc.eu/
RNAfold Webserver	http://rna.tbi.univie.ac.at/RNAfold

8. REFERENCES

Alexander, A. M., Pecoraro, C., Styche, A., Rudert, W. A., Benos, P. V., Ringquist, S., & Trucco, M. (2005). SOP3: A web based tool for selection of oligonucleotide primers for single nucleotide polymorphism analysis by pyrosequencing. *BioTechniques, 38*(1), 87–94. https://doi.org/10.2144/05381RR01

Allio, R., Donega, S., Galtier, N., & Nabholz, B. (2017). Large variation in the ratio of mitochondrial to nuclear mutation rate across animals: Implications for genetic diversity and the use of mitochondrial DNA as a molecular marker. *Molecular Biology and Evolution, 34*(11), 2762–2772. https://doi.org/10.1093/molbev/msx197

Balazs, R., Molnar, T. G., Meleg, E. E., Hidas, A., Zajacz, E., Racz, T., & Palinkas-Bodzsar, N. (2025). Evolutionary origin and genetic diversity of the Pannonian ecotype of *Apis mellifera carnica* colonies in Hungary based on mitochondrial DNA and microsatellite markers. *Biology, 14*, 475. https://doi.org/10.3390/biology14050475

Barhate, R. S., Subramanian, R., Nandini, K. E., & Hebbar, H. U. (2003). Processing of honey using polymeric microfiltration and ultrafiltration membranes. *Journal of Food Engineering, 60*(1), 49–54. https://doi.org/10.1016/S0260-8774(03)00017-7

Bermek, O., Grindley, N. D. F., & Joyce, C. M. (2011). Distinct roles of the active-site Mg^{2+} ligands, Asp882 and Asp705, of DNA polymerase I (Klenow fragment) during the prechemistry conformational transitions. *Journal of Biological Chemistry, 286*(5), 3755–3766. https://doi.org/10.1074/jbc.M110.167593

Beyene, D. (2014). The state of knowledge in designing primer of interest for successful polymerase chain reaction: A review. *Advanced Journal of Biological Sciences Research, 2*(3), 1–12.

Bogenhagen, D. F. (2012). Mitochondrial DNA nucleoid structure. *Biochimica et Biophysica Acta (BBA) – Gene Regulatory Mechanisms, 1819*, 914–920. https://doi.org/10.1016/j.bbagrm.2011.11.005

Boom, R., Sol, C. J. A., Salimans, M. M. M., Jansen, C. L., Wertheim-van Dillen, P. M. E., & van der Noordaa, J. (1990). Rapid and simple method for purification of nucleic acids. *Journal of Clinical Microbiology, 28*(3), 495–503. https://doi.org/10.1128/jcm.28.3.495-503.1990

Bovo, S., Utzeri, V. J., Ribani, A., Taurisano, V., Schiavo, G., & Fontanesi, L. (2022). A genotyping-by-sequencing approach can disclose *Apis mellifera* population genomic information contained in honey environmental DNA. *Scientific Reports, 12*, 1–12. https://doi.org/10.1038/s41598-022-24101-z

Buck, G. A., Fox, J. W., Gunthorpe, M., Hager, K. M., & Rush, J. (1999). Design strategies and performance of custom DNA sequencing primers. *BioTechniques, 27*(3), 528–536. https://doi.org/10.2144/99273RR01

Bustin, S. A., Benes, V., Garson, J. A., Hellemans, J., Huggett, J., Kubista, M., Mueller, R., Nolan, T., Pfaffl, M. W., Shipley, G. L., Vandesompele, J., & Wittwer, C. T. (2009). The MIQE guidelines: Minimum information for publication of quantitative real-time PCR experiments. *Clinical Chemistry, 55*(4), 611–622. https://doi.org/10.1373/clinchem.2008.112797

Bustin, S., & Huggett, J. (2017). qPCR primer design revisited. *Biomolecular Detection and Quantification, 14*, 19–28. https://doi.org/10.1016/j.bdq.2017.11.001

Calfee, E., Agra, M. N., Palacio, M. A., Ramírez, S. R., & Coop, G. (2020). Selection and hybridization shaped the rapid spread of African honey bee ancestry in the Americas. *PLOS Genetics, 16*(10), e1009038. https://doi.org/10.1371/journal.pgen.1009038

Dhatterwal, P., Mehrotra, S., & Mehrotra, R. (2017). Optimization of PCR conditions for amplifying an AT-rich amino acid transporter promoter sequence with high number of tandem repeats from *Arabidopsis thaliana*. *BMC Research Notes, 10*(1), 638. https://doi.org/10.1186/s13104-017-2982-1

Dodd, S., Kevei, Z., Karimi, Z., Parmar, B., Franklin, D., Koidis, A., & Anastasiadi, M. (2025). Detection of sugar syrup adulteration in UK honey using DNA barcoding. *Food Control, 167*, 110772. https://doi.org/10.1016/j.foodcont.2024.110772

Dong, Z., Wang, Y., Li, C., Li, L., & Men, X. (2021). Mitochondrial DNA as a molecular marker in insect ecology: Current status and future prospects. *Annals of the Entomological Society of America, 114*(4), 470–476. https://doi.org/10.1093/aesa/saab020

Druml, B., & Cichna Markl, M. (2014). High resolution melting (HRM) analysis of DNA – its role and potential in food analysis. *Food Chemistry, 158*, 245–254. https://doi.org/10.1016/j.foodchem.2014.02.111

Elkins, K. M. (2013). *Forensic DNA biology: A laboratory manual*. Academic Press, pp. 39–52, 72–74, 81–87. https://doi.org/10.1016/C2011-0-06748-0

Erali, M., Voelkerding, K. V., & Wittwer, C. T. (2008). High resolution melting applications for clinical laboratory medicine. *Experimental and Molecular Pathology, 85*(1), 50–58. https://doi.org/10.1016/j.yexmp.2008.03.012

Erali, M., Voelkerding, K. V., & Wittwer, C. T. (2010). High resolution melting analysis for gene scanning. *Methods, 50*(3), 250–261. https://doi.org/10.1016/j.ymeth.2010.01.013

Evans, M. F. (2009). The polymerase chain reaction and pathology practice. *Diagnostic Histopathology, 15*(7), 344–356. https://doi.org/10.1016/j.mpdhp.2009.04.001

Fontana, P., Costa, C., Di Prisco, G., Ruzzier, E., Annoscia, D., Battisti, A., Caoduro, G., Carpana, E., Contessi, A., Dal Lago, A., Dall'Olio, R., De Cristofaro, A., Felicioli, A., Floris, I., Fontanesi, L., Gardi, T., Lodesani, M., Malagnini, V., Manias, L., … Segrè, A. (2018). Appeal for biodiversity protection of native honey bee subspecies of *Apis mellifera* in Italy (San Michele all'Adige declaration). *Bulletin of Insectology, 71*(2), 257–271.

Fraser, A. J., Greenland Bews, C., Kelly, D., Williams, C. T., CONDOR Steering Group, LSTM Diagnostics Group, Body, R., Adams, E. R., Cubas Atienzar, A., Edwards, T., Allen, D. J., & Dark, P. (2023). A high resolution melt curve toolkit to identify lineage defining SARS CoV 2 mutations. *Scientific Reports, 13*(1), 3887. https://doi.org/10.1038/s41598-023-30754-1

Ghemrawi, M., Tejero, N. F., Duncan, G., & McCord, B. (2023). Pyrosequencing: Current forensic methodology and future applications – a review. *Electrophoresis, 44*(1–2), 298–312. https://doi.org/10.1002/elps.202200177

Gupta, N. (2019). DNA extraction and polymerase chain reaction. *Journal of Cytology, 36*(2), 116–117. https://doi.org/10.4103/JOC.JOC_110_18

Guertler, P., Eicheldinger, C., Muschler, O., Goerlich, O., & Busch, U. (2014). Automated DNA extraction from pollen in honey. *Food Chemistry, 149*, 302–306. https://doi.org/10.1016/j.foodchem.2013.10.129

Henriques, D., Parejo, M., Vignal, A., Wragg, D., Wallberg, A., Webster, M. T., & Pinto, M. A. (2018). Developing reduced SNP assays from whole-genome sequence data to estimate introgression in an organism with complex genetic patterns, the Iberian honeybee (*Apis mellifera iberiensis*). *Evolutionary Applications, 11*(8), 1270–1282. https://doi.org/10.1111/eva.12623

Henriques, D. S. M., Chávez Galarza, J., Quaresma, A., Neves, C. J. D., Lopes, A. R., Costa, C., Costa, F. O., Rufino, J., & Pinto, M. A. (2019). From the popular tRNAleu COX2 intergenic region to the mitogenome: Insights from diverse honey bee populations of Europe and North Africa. *Apidologie, 50*(2), 215–229. https://doi.org/10.1007/s13592-019-00632-9

Hoff-Olsen, P., Mevåg, B., Staalstrøm, E., Hovde, B., Egeland, T., & Olaisen, B. (1999). Extraction of DNA from decomposed human tissue: An evaluation of five extraction methods for short tandem repeat typing. *Forensic Science International, 105*(1), 171–183. https://doi.org/10.1016/S0379-0738(99)00128-0

Honrado, M., Lopes, A. R., Pinto, M. A., & Amaral, J. S. (2022). A novel real-time PCR coupled with high resolution melting analysis as a simple and fast tool for the entomological authentication of honey by targeting *Apis mellifera* mitochondrial DNA. *Food Research International, 161*, 111761. https://doi.org/10.1016/j.foodres.2022.111761

Hyink, O., Laas, F., & Dearden, P. K. (2013). Genetic tests for alleles of complementary-sex-determiner to support honeybee breeding programmes. *Apidologie, 44*(3), 306–313. https://doi.org/10.1007/s13592-012-0181-6

Ilyasov, R. A., Lee, M.-L., Takahashi, J.-I., Kwon, H. W., & Nikolenko, A. G. (2020). A revision of subspecies structure of western honey bee *Apis mellifera*. *Saudi Journal of Biological Sciences, 27*, 3615–3621. https://doi.org/10.1016/j.sjbs.2020.08.001

Ivády, G., Madar, L., Dzsudzsák, E., Koczok, K., Kappelmayer, J., Krulisova, V., Macek, M., Jr., Horváth, A., & Balogh, I. (2018). Analytical parameters and validation of homopolymer detection in a pyrosequencing-based next generation sequencing system. *BMC Genomics 19*, 158. https://doi.org/10.1186/s12864-018-4544-x

Katevatis, C., Fan, A., & Klapperich, C. M. (2017). Low concentration DNA extraction and recovery using a silica solid phase. *PLoS ONE, 12*(5), e0176848. https://doi.org/10.1371/journal.pone.0176848

Kek, S. P., Chin, N. L., Tan, S. W., & Yusof, Y. A. (2018). Comparison of DNA extraction methods for entomological origin identification of honey using a simple additive weighting method. *International Journal of Food Science & Technology, 53*(11), 2490–2499. https://doi.org/10.1111/ijfs.13840

Kim, N., Kwon, J.-S., Kang, W.-H., & Yeom, S.-I. (2023). High resolution melting (HRM) genotyping. In Y. Shavrukov (Ed.), *Plant genotyping: Methods and protocols* (Methods in Molecular Biology, Vol. 2638, pp. 337–349). Springer. https://doi.org/10.1007/978-1-0716-3024-2_24

Lalhmangaihi, R., Ghatak, S., Laha, R., Gurusubramanian, G., & Senthil Kumar, N. (2014). Protocol for optimal quality and quantity pollen DNA isolation from honey samples. *Journal of Biomolecular Techniques, 25*(4), 92–95. https://doi.org/10.7171/jbt.14-2504-001

Land Kärnten. (1992). *Kärntner Bienenwirtschaftsgesetz (K-BiWG)*. Kärntner Landesrecht. https://www.jusline.at/gesetz/k-biwg/gesamt

Land Niederösterreich. (2014). *Niederösterreichisches Bienenzuchtgesetz (LGBl. 6320)*. Niederösterreichisches Landesrecht. https://www.ris.bka.gv.at

Land Steiermark. (1998). *Steiermärkisches Bienenzuchtgesetz (LGBl. Nr. 18/1998)*. Steiermärkisches Landesrecht. https://www.ris.bka.gv.at

Land Wien. (2000). *Gesetz über die Haltung und Zucht von Bienen (LGBl. Nr. 56/2000)*. Wiener Landesgesetzblatt. https://www.wien.gv.at/recht/landesrecht-wien/rechtsvorschriften/pdf/l2740000.pdf

Lee, W., Zamudio-Ochoa, A., Buchel, G., Podlesniy, P., Marti Gutierrez, N., Puigròs, M., Calderon, A., Tang, H.-Y., Li, L., Mikhalchenko, A., Koski, A., Trullas, R., Mitalipov, S., & Temiakov, D. (2023). Molecular basis for maternal inheritance of human mitochondrial DNA. *Nature Genetics, 55*, 1632–1639. https://doi.org/10.1038/s41588-023-01505-9

Li, M., Palais, R. A., Zhou, L., & Wittwer, C. T. (2017). Quantifying variant differences in DNA melting curves: Effects of length, melting rate, and curve overlay. *Analytical Biochemistry, 539*, 90–95. https://doi.org/10.1016/j.ab.2017.10.015

Lorenz, R., Bernhart, S. H., Höner zu Siederdissen, C., Tafer, H., Flamm, C., Stadler, P. F., & Hofacker, I. L. (2011). ViennaRNA Package 2.0. *Algorithms for Molecular Biology, 6*, 26. https://doi.org/10.1186/1748-7188-6-26

Matissek, R., Fischer, M., & Steiner, G. (2018). *Lebensmittelanalytik* (6th ed.). Springer, pp. 200–204, 209–210. https://doi.org/10.1007/978-3-662-55722-8

Momeni, J., Parejo, M., Nielsen, R. O., Langa, J., Montes, I., Papoutsis, L., Farajzadeh, L., Bendixen, C., Căuia, E., Charrière, J.-D., Coffey, M. F., Costa, C., Dall'Olio, R., De la Rúa, P., Drazic, M. M., Filipi, J., Galea, T., Golubovski, M., Gregorc, A., … Estonba, A. (2021). Authoritative subspecies diagnosis tool for European honey bees based on ancestry informative SNPs. *BMC Genomics, 22*, 101. https://doi.org/10.1186/s12864-021-07379-7

Moškrič, A., Marinč, A., Ferk, P., Leskošek, B., Mosbech, M.-B., Bunikis, I., Pettersson, O. V., Soler, L., & Prešern, J. (2022). The Carniolan honeybee from Slovenia — a complete and annotated mitochondrial genome with comparisons to closely related *Apis mellifera* subspecies. *Insects, 13*, 403. https://doi.org/10.3390/insects13050403

Owczarzy, R., Moreira, B. G., You, Y., Behlke, M. A., & Walder, J. A. (2008). Predicting stability of DNA duplexes in solutions containing magnesium and monovalent cations. *Biochemistry, 47*(19), 5336–5347. https://doi.org/10.1021/bi702363u

Pathiraja, D., Cho, J., Kim, J., & Choi, I.-G. (2023). Metabarcoding of eDNA for tracking the floral and geographical origins of bee honey. *Food Research International, 164*, 112413. https://doi.org/10.1016/j.foodres.2022.112413

Parakatselaki, M.-E., & Larsson, N.-G. (2021). mtDNA heteroplasmy: Origin, detection, significance, and evolutionary consequences. *Life, 11*(7), 633. https://doi.org/10.3390/life11070633

Piriyapongsa, J., Ngamphiw, C., Assawamakin, A., Wangkumhang, P., Ruangrit, U., Agavatpanitch, G., & Tongsima, S. (2009). RExPrimer: An integrated primer designing tool increases PCR effectiveness by avoiding 3' SNP in primer and mispriming from structural variation. *BMC Genomics, 10*(Suppl. 3), S4. https://doi.org/10.1186/1471-2164-10-S3-S4

Ririe, K. M., Rasmussen, R. P., & Wittwer, C. T. (1997). Product differentiation by analysis of DNA melting curves during the polymerase chain reaction. *Analytical Biochemistry, 245*(2), 154–160. https://doi.org/10.1006/abio.1996.9916

Rocha, A. D. S., Amorim, I. S. S., Simão, T. A., Fonseca, A. S. d., Garrido, R. G., & Mencalha, A. L. (2018). High resolution melting (HRM) of hypervariable mitochondrial DNA regions for forensic science. *Journal of Forensic Sciences, 63*(2), 536–540. https://doi.org/10.1111/1556-4029.13552

Ronaghi, M., Karamohamed, S., Pettersson, B., Uhlén, M., & Nyrén, P. (1996). Real time DNA sequencing using detection of pyrophosphate release. *Analytical Biochemistry, 242*(1), 84–89. https://doi.org/10.1006/abio.1996.0460

Scott, M. F., Fradgley, N., Bentley, A. R., Brabbs, T., Corke, F., Gardner, K. A., Horsnell, R., & Mackay, I. J. (2021). Limited haplotype diversity underlies polygenic trait architecture across 70 years of wheat breeding. *Genome Biology, 22*, 137. https://doi.org/10.1186/s13059-021-02354-7

Sharma, M. (2020). Basic concepts of primer designing: A mini review. *International Journal of Latest Trends in Engineering and Technology, 17*(4), 10–12. https://doi.org/10.21172/1.174.03

Shokolenko, I. N., & Alexeyev, M. F. (2015). Mitochondrial DNA: A disposable genome? *Biochimica et Biophysica Acta, 1852*, 1805–1809. https://doi.org/10.1016/j.bbadis.2015.05.016

Słomka, M., Sobalska Kwapis, M., Wachulec, M., Bartosz, G., & Strapagiel, D. (2017). High resolution melting (HRM) for high throughput genotyping—Limitations and caveats in practical case studies. *International Journal of Molecular Sciences, 18*(11), 2316. https://doi.org/10.3390/ijms18112316

Smith, C. J., & Osborn, A. M. (2009). Advantages and limitations of quantitative PCR (qPCR) based approaches in microbial ecology. *FEMS Microbiology Ecology, 67*(1), 6–20. https://doi.org/10.1111/j.1574-6941.2008.00629.x

Soares, S., Amaral, J. S., Oliveira, M. B. P., & Mafra, I. (2015). Improving DNA isolation from honey for the botanical origin identification. *Food Control, 48*, 130–136. https://doi.org/10.1016/j.foodcont.2014.02.035

Soares, S., Grazina, L., Mafra, I., Costa, J., Pinto, M. A., Pham, D. H., Oliveira, M. B. P. P., & Amaral, J. S. (2018). Novel diagnostic tools for Asian (*Apis cerana*) and European (*Apis mellifera*) honey authentication. *Food Research International, 105*, 686–693. https://doi.org/10.1016/j.foodres.2017.11.081

Soares, S., Rodrigues, F., & Delerue-Matos, C. (2023). Towards DNA-based methods analysis for honey: An update. *Molecules, 28*, 2106. https://doi.org/10.3390/molecules28052106

Tan, S. C., & Yiap, B. C. (2009). DNA, RNA, and protein extraction: The past and the present. *Journal of Biomedicine and Biotechnology, 2009*, Article 574398. https://doi.org/10.1155/2009/574398

Tong, S. Y. C., & Giffard, P. M. (2012). Microbiological applications of high resolution melting analysis. *Journal of Clinical Microbiology, 50*(11), 3418–3421. https://doi.org/10.1128/JCM.01709-12

Utzeri, V. J., Ribani, A., Taurisano, V., Banqué, C. H. i., & Fontanesi, L. (2021). Distribution of the main *Apis mellifera* mitochondrial DNA lineages in Italy assessed using an environmental DNA approach. *Insects, 12*(7), 620. https://doi.org/10.3390/insects12070620

Utzeri, V. J., Ribani, A., Taurisano, V., & Fontanesi, L. (2022). Entomological authentication of honey based on a DNA method that distinguishes *Apis mellifera* mitochondrial C mitotypes: Application to honey produced by *A. m. ligustica* and *A. m. carnica*. *Food Control, 134*, 108713. https://doi.org/10.1016/j.foodcont.2021.108713

Van der Meulen, H., & Hellemans, J. (2021). Web-based LinRegPCR: Application for the visualization and analysis of (RT)-qPCR amplification and melting data. *BMC Bioinformatics, 22*, 1. https://doi.org/10.1186/s12859-021-04306-1

Vandeventer, P. E., Mejia, J., Nadim, A., Johal, M. S., & Niemz, A. (2013). DNA adsorption to and elution from silica surfaces. *The Journal of Physical Chemistry B, 117*(37), 10742–10749. https://doi.org/10.1021/jp405753m

Veeraragavan, S., Johansen, M., & Johnston, I. G. (2024). Evolution and maintenance of mtDNA gene content across eukaryotes. *Biochemical Journal, 481*, 1015–1042. https://doi.org/10.1042/BCJ20230415

Veisi, H., Nazemi-Rafie, J., Azizi, A., & Rajabi-Maham, H. (2020). Genetic characteristics of the Iranian honey bee, *Apis mellifera meda*, based on mitochondrial genes of ND4, ND4L and ND6 and their internal transcribed spacers. *Insectes Sociaux, 67*, 439–448. https://doi.org/10.1007/s00040-020-00769-2

von Ahsen, N., Wittwer, C. T., & Schütz, E. (2011). Monovalent and divalent salt correction algorithms for T_m prediction — Recommendations for Primer3 usage. *Briefings in Bioinformatics, 12*(5), 514–517. https://doi.org/10.1093/bib/bbq081

Wilczyńska, A. (2014). Effect of filtration on colour, antioxidant activity and total phenolics of honey. *LWT – Food Science and Technology, 57*(2), 767–774. https://doi.org/10.1016/j.lwt.2014.01.034

Wilson, I. G. (1997). Inhibition and facilitation of nucleic acid amplification. *Applied and Environmental Microbiology, 63*(10), 3741–3751. https://doi.org/10.1128/AEM.63.10.3741-3751.1997

Wittwer, C. T., Reed, G. H., Gundry, C. N., Vandersteen, J. G., & Pryor, R. J. (2003). High-resolution genotyping by amplicon melting analysis using LCGreen. *Clinical Chemistry, 49*(6), 853–860. https://doi.org/10.1373/49.6.853

Ye, J., Coulouris, G., Zaretskaya, I., Cutcutache, I., Rozen, S., & Madden, T. L. (2012). Primer BLAST: A tool to design target specific primers for polymerase chain reaction. *BMC Bioinformatics, 13*, 134. https://doi.org/10.1186/1471-2105-13-134

Zappe, K., & Cichna Markl, M. (2024). Temperature wise calibration increases the accuracy of DNA methylation levels determined by high-resolution melting (HRM). *International Journal of Molecular Sciences, 25*(10), 5082. https://doi.org/10.3390/ijms25105082

9. APPENDIX

9.1. List of abbreviations

A.	*Apis*
A. m.	*Apis mellifera*
A	adenine
APS	adenosine 5'-phosphosulfate
AT	adenine-thymine
ATP	adenosine triphosphate
Bio-Rev primer	biotinylated reverse primer
BLAST	Basic Local Alignment Search Tool
bp	base pair
C	cytosine
CTAB	cetyltrimethylammonium bromide
Ct	threshold cycle
DNA	deoxyribonucleic acid
dNTPs	deoxyribonucleoside triphosphates
dsDNA	double-stranded DNA
eDNA	environmental DNA
EU	European Union
Fw primer	forward primer
G	guanine
GC	guanine-cytosine
HPBF / PBF	bee sample codes
HP / P	honey sample codes
HRM	high-resolution melting
kb	kilobase
mtDNA	mitochondrial deoxyribonucleic acid
NCBI	National Center for Biotechnology Information
nDNA	nuclear DNA
NTC	no template control
PCR	polymerase chain reaction
PPi	pyrophosphate
PSQ	pyrosequencing
qPCR	real-time quantitative PCR
Seq primer	sequencing primer
SNP	single nucleotide polymorphism
ssDNA	single-stranded DNA
T	thymine
Ta	annealing temperature
Te	elongation temperature
Tm	melting temperature
ΔG	Gibbs free energy change

9.2. List of figures

9.3. List of tables

9.4. Supplementary data

Table 26

List of all honey samples analyzed in this study

Sample ID	Honey type	Geographic origin
P1	Organic Blossom Honey	EU/non-EU
P2	Organic Blossom Honey	Austria (Lower Austria)
P3	n. a.	Slovenia
P4	n. a.	Austria (Upper Austria)
P5	Blossom Honey with Honeydew Honey	Austria (Styria)
P6	Blossom Honey	Austria (Lower Austria)
P7	n. a.	Austria (Vienna)
P8	Organic Blossom Honey	Austria
P9	Blossom Honey	Austria (Styria)
P10	Summer Blossom Honey	Austria (Burgenland)
P11	Blossom Honey	EU/non-EU
P12	Blossom Honey	Austria
P13	Creamy Blossom Honey	EU/non-EU
P14	Viennese Organic Blossom Honey	Austria (Vienna)
P15	Organic Blossom Honey	Austria (Lower Austria)
P17	Blossom Honey	EU/non-EU
P18	Wildflower Honey	Spain
P20	Summer Blossom Honey	Romania/Hungary/Bulgaria
P21	Blossom Honey	n. a.
P22	Blossom Honey	Brazil
P23	Blossom Honey	EU/non-EU
P24	Blossom Honey with Linden Honey	Austria (Styria)
P25	Lavender Honey (Raw)	Bulgaria
P26	Organic Thistle Honey (Raw)	Bulgaria
P27	Organic Wild Flowers Honey (Raw)	Bulgaria
P28	Comb Honey	Turkey
P29	Northern German Honey	Germany
P30	Raspberry Honey	Germany
P31	Dandelion Honey	France
P32	Buckthorn Honey	n. a.
P33	Leatherwood Honey	Australia
P34	Honey with Chili	n. a.
P35	Heather Honey	n. a.
P36	Spring Honey	Germany
P37	Hawthorn Honey	France
P38	Sea Aster Honey	Germany
P39	Early Harvest Honey	Germany
P40	Summer Blossom	Germany

P41	Acacia Honey	Czech Republic
P42	Linden Honey	Romania
P43	Summer Blossom Honey	EU/non-EU
P44	Acacia Honey	EU/non-EU
P45	Linden Honey	Austria (Lower Austria)
P46	Sunflower Honey	Austria (Lower Austria)
P47	Vetch Honey	Austria (Lower Austria)
P48	Acacia Honey	Austria (Lower Austria)
P49	Blossom Honey from Acacias and Linden	Austria (Lower Austria)
P50	Linden-Currant Honey	Slovakia
P51	Forest Honey	North Macedonia
P52	Forest Honey	North Macedonia
P53	Wildflower Honey	North Macedonia
P54	Chestnut Honey	Italy
P55	Chestnut Honey	Italy
P56	Chestnut Honey	France
P57	Chestnut Honey	Austria (Burgenland)
P58	Acacia Honey	Austria (Burgenland)
P59	Sunflower Honey	Austria (Burgenland)
P60	Cruciferous Honey	Austria (Vienna)
P61	Blossom Honey Cream	Austria (Salzburg)
P62	Blossom Honey with Forest Honey	Austria (Salzburg)
P63	Blossom Honey with Forest Honey	Austria (Salzburg)
P64	Alpine Honey	Austria (Salzburg)
P65	High Mountain Honey	Austria (Salzburg)
P66	Acacia Honey	Croatia
P67	Mediterranean Honey	Croatia
P68	Blossom Honey	Austria (Lower Austria)
P69	Forest Honey	Austria (Lower Austria)
P70	Blossom Honey	Italy (Liguria)
P71	Blossom Honey	Italy (Trentino)
P72	Rhododendron Honey	Italy (Trentino)
P73	Blossom Honey	Italy (Veneto)
P74	*A. m. carnica* Honig	Austria (Carinthia)
P75	Blossom Honey	Austria (Carinthia)
P76	Forest Honey	Austria (Carinthia)
P77	Chestnut Honey	Italy
P78	Acacia Honey	Italy
P79	Sunflower Honey	Italy
P80	Cherry Blossom Honey	Italy
P81	Sweet chestnut honey	Italy
P82	Chestnut - Blossoms & Honeydew Honey	Italy
P83	Linden Honey	Romania
P84	Linden Honey	Germany
P85	Acacia Honey with Blossom Honey	Austria
P86	Acacia Honey	Austria
P88	Acacia Honey	Italy (Sicily)
P89	Chestnut Honey	Italy (Sicily)
P90	Acacia Honey	Austria
P91	Chestnut Honey	Austria (Upper Austria)
P92	Forest Honey	Austria (Upper Austria)
P93	Linden Honey	Hungary
P94	Chestnut Honey	Hungary
P96	n. a.	Austria (Upper Austria)
P97	Linden Honey	Russia
P98	Ailanthus Honey	Italy (Lazio)
P99	Honeydew Honey	Italy (Lazio)
P100	Manuka Honey	New Zealand
P101	Orange Blossom Honey	Spain

P102	Thyme Honey	Greece (Crete)
P103	Pine Honey	Greece (Rhodos)
P104	Raw Forest Honey	Latvia
P105	African Oyin	Nigeria
P106	Sidr Honey	Yemen
P114	Forest Honey	Austria (Vorarlberg)
P115	Forest Honey	Austria (Vorarlberg)
P116	Silver Fir Honey	Austria (Vorarlberg)
HP1	Forest Honey	EU/non-EU
HP3	Forest Honey	Austria (Upper Austria)
HP4	Forest Honey	Austria (Styria)
HP5	Forest Honey	Spain/Greece
HP6	Forest Honey	Austria (Styria)
HP7	Organic Forest Honey	Romania
HP16	Organic Forest Honey	Austria (Lower Austria)
HP17	Organic Forest Honey	EU/non-EU
HP18	Organic Forest Honey with Organic Blossom Honey	EU/non-EU
HP20	Forest Honey	Austria
HP22	Forest Honey	EU/non-EU
HP23	Forest Honey	EU/non-EU
HP24	Forest Honey	EU/non-EU
HP25	Forest Honey	Turkey
HP26	Forest Honey with Pine Thyme	Greece
HP27	Forest Honey with Heather	Greece
HP28	Forest Honey with Sage	Greece
HP29	Mountain Honey with White Thyme	Greece
HP35	Northern German Early Harvest Honey	Germany
HP36	Fennel in Honey	n. a.
HP37	Chestnut Honey	Italy
HP38	Linden Honey	Germany
HP39	Blossom Honey with Acacia Honey	Germany
HP40	Fir Honey	n. a.
HP41	Forest and Blossom Honey	n. a.
HP42	Honeydew Honey	Bulgaria
HP43	Organic Honeydew Honey	Bulgaria
HP44	Organic Acacia Honey	Bulgaria
HP45	Organic Linden Honey	Bulgaria
HP46	Raw Forest Honey	Estonia
HP47	Glucose-Fructose Syrup (90%) with Honey (10%)	n. a.
HP48	Blossom Honey	Hungary
HP49	Acacia Honey	Hungary
HP50	Goldenrod Honey	Hungary
HP51	Linden Honey	Hungary
HP55	Wildflower Honey	Bosnia and Herzegovina

Table 27

List of all A. mellifera specimens analyzed in this study

Sample ID	Beekeeper-reported subspecies	Geographic origin
PBF1.1	*A. m. carnica*	Austria (Lower Austria)
PBF1.2	*A. m. carnica*	Austria (Lower Austria)
PBF2.1	*A. m. carnica* - Drone	Austria (Lower Austria)
PBF2.2	*A. m. carnica* - Drone	Austria (Lower Austria)
PBF3.1	*A. m. carnica* (after an invasion)	Austria (Lower Austria)
PBF3.2	*A. m. carnica* (after an invasion)	Austria (Lower Austria)
PBF4.1	*A. m. carnica* (probably hybrid)	Austria (Lower Austria)
PBF4.2	*A. m. carnica* (probably hybrid)	Austria (Lower Austria)
PBF5.1	*A. m. carnica*	Austria (Lower Austria)
PBF5.2	*A. m. carnica*	Austria (Lower Austria)
PBF6.1	*A. m. carnica* with color defect	Austria (Lower Austria)
PBF6.2	*A. m. carnica* with color defect	Austria (Lower Austria)
PBF7.1	*A. m. macedonica*	North Macedonia
PBF7.2	*A. m. macedonica*	North Macedonia
PBF8.1	*A. m. ligustica*	Italy (Liguria)
PBF8.2	*A. m. ligustica*	Italy (Liguria)
PBF9.1	*A. m. carnica/ligustica* Hybrid	Italy (Trentino)
PBF9.2	*A. m. carnica/ligustica* Hybrid	Italy (Trentino)
PBF10.1	*A. m. carnica/ligustica* Hybrid	Italy (Trentino)
PBF10.2	*A. m. carnica/ligustica* Hybrid	Italy (Trentino)
PBF11.1	*A. m. carnica*	Austria (Carinthia)
PBF11.2	*A. m. carnica*	Austria (Carinthia)
PBF12.1	Alpine *A. m. carnica*	Austria (Carinthia)
PBF12.2	Alpine *A. m. carnica*	Austria (Carinthia)
PBF13.1	Pannonian *A. m. carnica* - Drone	Austria (Salzburg)
PBF13.2	Pannonian *A. m. carnica* - Worker	Austria (Salzburg)
PBF14.1	*A. mellifera* (subspecies n. a.)	Austria (Carinthia)
PBF14.2	*A. mellifera* (subspecies n. a.)	Austria (Carinthia)
PBF15.1	*A. mellifera* - Worker (subspecies n. a.)	Austria (Carinthia)
PBF15.2	*A. mellifera* - Drone (subspecies n. a.)	Austria (Carinthia)
PBF16.1	*A. m. carnica*	Austria (Upper Austria)
PBF16.2	*A. m. carnica*	Austria (Upper Austria)
PBF17	*A. mellifera* (subspecies n. a.)	Austria (Lower Austria)
PBF18.1	*A. m. ligustica* (hybridization not excluded)	Italy (Lazio)
PBF18.2	*A. m. ligustica* (hybridization not excluded)	Italy (Lazio)
PBF18.3	*A. m. ligustica* (hybridization not excluded)	Italy (Lazio)
HPBF	*A. m. carnica*	Austria (Styria)
HPBF2.1	*A. m. carnica*	Bosnia and Herzegovina
HPBF2.2	*A. m. carnica*	Bosnia and Herzegovina
HPBF3.1	*A. m. carnica*	Bosnia and Herzegovina
HPBF3.2	*A. m. carnica*	Bosnia and Herzegovina
HPBF4	*A. m. carnica*	Croatia
HPBF5.1	*A. m. carnica*	Austria (Salzburg)
HPBF5.1.1	*A. m. carnica*	Austria (Salzburg)
HPBF5.2	*A. m. carnica*	Austria (Salzburg)

Figure 61

Results for homodimer formation of the BEE 6 Fw primer using the OligoAnalyzer online tool (*https://www.idtdna.com/calc/analyzer*).

Figure 62

Results for homodimer formation of the BEE 6 Bio-Rev primer using the OligoAnalyzer online tool (*https://www.idtdna.com/calc/analyzer*).

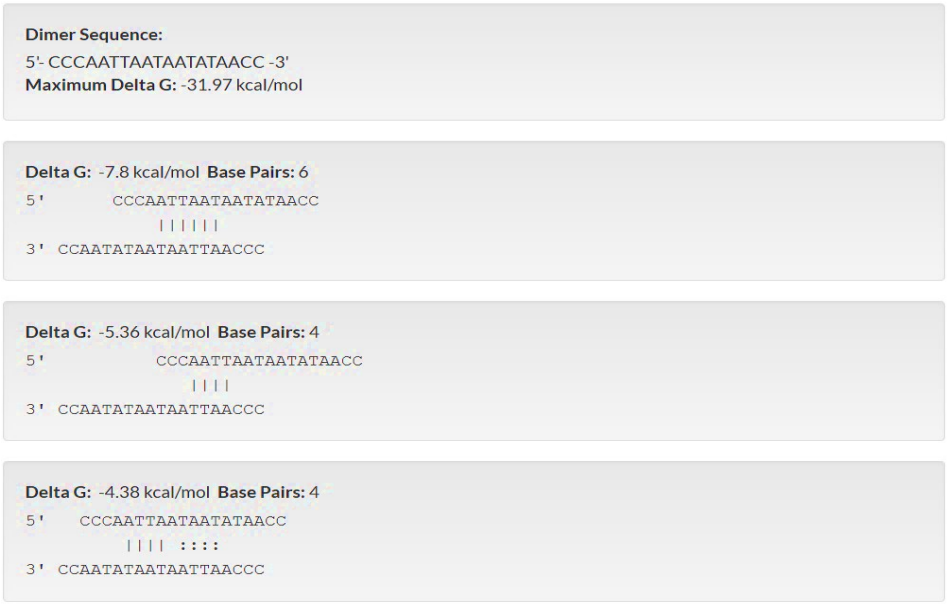

Figure 63

Results for homodimer formation of the BEE 6 Seq primer using the OligoAnalyzer online tool (*https://www.idtdna.com/calc/analyzer*).

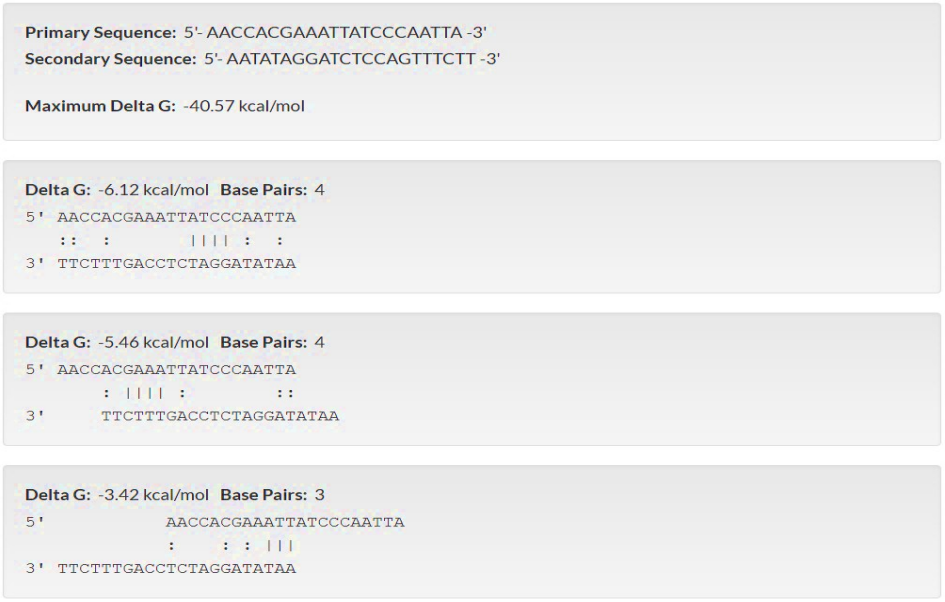

Figure 64

Results for heterodimer formation between the BEE 6 Fw and Bio-Rev primers using the OligoAnalyzer online tool (*https://www.idtdna.com/calc/analyzer*)

Table 28

HRM results for honey samples obtained with the BEE 2_1 assay

Sample ID	Geographic origin	Tm	Peak shape
P1	EU/non-EU	72.5	Shouldered peak
P2	Austria (Lower Austria)	73.0	Single peak
P3	Slovenia	72.5	Shouldered peak
P4	Austria (Upper Austria)	72.4	Single peak
P5	Austria (Styria)	72.9	Single peak
P6	Austria (Lower Austria)	72.9	Single peak
P7	Austria (Vienna)	72.7	Single peak
P8	Austria	72.8	Single peak
P10	Austria (Burgenland)	72.5	Single peak
P11	EU/non-EU	72.8	Shouldered peak
P12	Austria	72.6	Shouldered peak
P13	EU/non-EU	72.6	Shouldered peak
P14	Austria (Vienna)	72.8	Shouldered peak
P15	Austria (Lower Austria)	72.7	Shouldered peak
P17	EU/non-EU	73.1	Shouldered peak
P18	Spain	72.2	Single peak
P20	Romania/Hungary/Bulgaria	72.7	Shouldered peak
P21	n. a.	73.0	Single peak
P22	Brazil	72.3	Shouldered peak
P23	EU/non-EU	73.0	Shouldered peak
P24	Austria (Styria)	72.6	Single peak
P25	Bulgaria	72.5	Single peak
P26	Bulgaria	72.4	Single peak
P27	Bulgaria	72.4	Single peak
P28	Turkey	n. a.	No proper amplification
P29	Germany	72.7	Shouldered peak
P30	Germany	72.5	Single peak
P31	France	72.6	Single peak
P32	n. a.	72.5-73.3	Symmetrical double peak
P33	Australia	72.9	Shouldered peak
P34	n. a.	72.5	Shouldered peak
P35	n. a.	72.8	Double peak
P36	Germany	72.5	Shouldered peak
P37	France	72.7	Single peak
P38	Germany	72.5	Single peak
P39	Germany	72.5	Shouldered peak
P40	Germany	72.6	Single peak
P41	Czech Republic	72.6	Shouldered peak
P42	Romania	72.5	Single peak
P43	EU/non-EU	72.5	Shouldered peak
P44	EU/non-EU	72.6	Single peak
P45	Austria (Lower Austria)	73.0	Single peak
P46	Austria (Lower Austria)	72.8	Shouldered peak
P47	Austria (Lower Austria)	72.7	Single peak
P48	Austria (Lower Austria)	72.8	Single peak
P49	Austria (Lower Austria)	72.9	Single peak
P50	Slovakia	72.9	Shouldered peak
P51	North Macedonia	72.4	Single peak
P52	North Macedonia	72.5	Single peak
P53	North Macedonia	72.5	Single peak
P54	Italy	72.4	Shouldered peak
P55	Italy	72.5	Shouldered peak
P56	France	72.4	Shouldered peak
P57	Austria (Burgenland)	72.4	Shouldered peak
P58	Austria (Burgenland)	72.8	Shouldered peak
P59	Austria (Burgenland)	72.5	Shouldered peak
P60	Austria (Vienna)	72.8	Single peak
P61	Austria (Salzburg)	72.7	Single peak
P62	Austria (Salzburg)	72.6	Single peak
P63	Austria (Salzburg)	72.4	Shouldered peak

P64	Austria (Salzburg)	72.8	Shouldered peak
P65	Austria (Salzburg)	72.6	Shouldered peak
P66	Croatia	72.6	Shouldered peak
P67	Croatia	72.6	Shouldered peak
P68	Austria (Lower Austria)	72.6	Shouldered peak
P69	Austria (Lower Austria)	72.5	Shouldered peak
P70	Italy (Liguria)	72.6	Shouldered peak
P71	Italy (Trentino)	72.9	Shouldered peak
P72	Italy (Trentino)	72.6	Shouldered peak
P73	Italy (Veneto)	72.6	Shouldered peak
P74	Austria (Carinthia)	72.5	Shouldered peak
P75	Austria (Carinthia)	72.9	Shouldered peak
P76	Austria (Carinthia)	72.8	Double peak
P77	Italy	72.9	Single peak
P78	Italy	72.9	Single peak
P79	Italy	73.2	Shouldered peak
P80	Italy	72.8	Double peak
P81	Italy	72.9	Shouldered peak
P82	Italy	72.9	Shouldered peak
P83	Romania	72.8	Single peak
P84	Germany	72.8	Single peak
P85	Austria	73.1	Shouldered peak
P86	Austria	72.6	Double peak
P88	Italy (Sicily)	72.9	Shouldered peak
P89	Italy (Sicily)	72.7	Single peak
P90	Austria	72.7	Shouldered peak
P91	Austria (Upper Austria)	72.5	Double peak
P92	Austria (Upper Austria)	73.1	Single peak
P93	Hungary	72.1-73.1	Symmetrical double peak
P94	Hungary	73.0	Double peak
P96	Austria (Upper Austria)	73.2	Single peak
P97	Russia	72.8	Double peak
P98	Italy (Lazio)	72.4	Shouldered peak
P99	Italy (Lazio)	72.8	Shouldered peak
P100	New Zealand	72.8	Single peak
P101	Spain	72.1	Single peak
P102	Greece (Crete)	72.4	Single peak
P103	Greece (Rhodos)	72.4	Single peak
P104	Latvia	72.8	Shouldered peak
P105	Nigeria	72.1	Single peak
P106	Yemen	72.1	Single peak
P114	Austria (Vorarlberg)	72.5	Shouldered peak
P115	Austria (Vorarlberg)	72.4	Single peak
P116	Austria (Vorarlberg)	72.3	Double peak
HP35	Germany	72.6	Shouldered peak
HP36	n. a.	72.6	Shouldered peak
HP37	Italy	72.8	Single peak
HP38	Germany	72.6	Shouldered peak
HP39	Germany	72.5	Single peak
HP40	n. a.	72.9	Shouldered peak
HP41	n. a.	72.2	Single peak
HP42	Bulgaria	72.5	Single peak
HP43	Bulgaria	72.5	Single peak
HP44	Bulgaria	72.5	Single peak
HP45	Bulgaria	72.6	Single peak
HP46	Estonia	72.9	Shouldered peak
HP47	n. a.	72.6	Shouldered peak
HP48	Hungary	72.6	Single peak
HP49	Hungary	72.7	Shouldered peak
HP50	Hungary	72.9	Shouldered peak
HP51	Hungary	72.9	Shouldered peak
HP55	Bosnia and Herzegovina	72.2	Single peak

Note: Tm values represent the average Tm across runs, the Tm range in case of symmetrical double peaks, or the Tm of the major peak in case of double peaks.

Table 29

HRM results for bee samples obtained with the BEE 2_1 assay

Sample ID	Beekeeper-reported subspecies	Tm	Peak shape
PBF1.1	*A. m. carnica*	72.8	Single peak
PBF1.2	*A. m. carnica*	72.8	Single peak
PBF2.1	*A. m. carnica* - Drone	72.9	Single peak
PBF2.2	*A. m. carnica* - Drone	72.9	Single peak
PBF3.1	*A. m. carnica* (after an invasion)	72.9	Single peak
PBF3.2	*A. m. carnica* (after an invasion)	72.9	Single peak
PBF4.1	*A. m. carnica* (probably hybrid)	72.9	Single peak
PBF4.2	*A. m. carnica* (probably hybrid)	72.9	Single peak
PBF5.1	*A. m. carnica*	72.8	Single peak
PBF5.2	*A. m. carnica*	72.8	Single peak
PBF6.1	*A. m. carnica* with color defect	72.8	Single peak
PBF6.2	*A. m. carnica* with color defect	72.8	Single peak
PBF7.1	*A. m. macedonica*	72.4	Single peak
PBF7.2	*A. m. macedonica*	72.4	Single peak
PBF8.1	*A. m. ligustica*	73.4	Single peak
PBF8.2	*A. m. ligustica*	73.4	Single peak
PBF9.1	*A. m. carnica/ligustica* Hybrid	72.7	Single peak
PBF9.2	*A. m. carnica/ligustica* Hybrid	73.0	Single peak
PBF10.1	*A. m. carnica/ligustica* Hybrid	72.9	Single peak
PBF10.2	*A. m. carnica/ligustica* Hybrid	72.9	Single peak
PBF11.1	*A. m. carnica*	72.6	Single peak
PBF11.2	*A. m. carnica*	72.6	Single peak
PBF12.1	*Alpine A. m. carnica*	72.5	Single peak
PBF12.2	*Alpine A. m. carnica*	72.7	Single peak
PBF13.1	*Pannonian A. m. carnica* - Drone	72.9	Single peak
PBF13.2	*Pannonian A. m. carnica* - Worker	73.1	Single peak
PBF14.1	*A. mellifera* (subspecies n. a.)	72.6	Single peak
PBF14.2	*A. mellifera* (subspecies n. a.)	72.9	Single peak
PBF15.1	*A. mellifera* - Worker (subspecies n. a.)	73.0	Single peak
PBF15.2	*A. mellifera* - Drone (subspecies n. a.)	73.0	Single peak
PBF16.1	*A. m. carnica*	72.9	Single peak
PBF16.2	*A. m. carnica*	72.9	Single peak
PBF17	*A. mellifera* (subspecies n. a.)	73.3	Single peak
PBF18.1	*A. m. ligustica* (hybridization not excluded)	73.0	Single peak
PBF18.2	*A. m. ligustica* (hybridization not excluded)	73.0	Single peak
PBF18.3	*A. m. ligustica* (hybridization not excluded)	73.7	Single peak
HPBF	*A. m. carnica*	72.9	Single peak
HPBF2.1	*A. m. carnica*	72.4	Single peak
HPBF2.2	*A. m. carnica*	72.5	Single peak
HPBF3.1	*A. m. carnica*	72.4	Single peak
HPBF3.2	*A. m. carnica*	72.5	Single peak
HPBF4	*A. m. carnica*	72.8	Single peak

Note: Tm values represent the average Tm across runs.

Table 30

HRM results for honey samples obtained with the BEE 3_2 assay

Sample ID	Geographic origin	Tm	Peak shape
P9	Austria (Styria)	68.0	Double peak
P10	Austria (Burgenland)	67.5	Single peak
P12	Austria	68.1	Shouldered peak
P18	Spain	66.6-67.6	Symmetrical double peak
P20	Romania/Hungary/Bulgaria	67.4	Single peak
P21	n. a.	68.2	Single peak
P22	Brazil	67.5	Single peak
P26	Bulgaria	67.6	Single peak
P27	Bulgaria	67.5	Single peak
P29	Germany	68.1	Double peak

P33	Australia	67.5	Single peak
P34	n. a.	67.8	Shouldered peak
P36	Germany	67.0-67.8	Symmetrical double peak
P39	Germany	n. a.	No proper amplification
P41	Czech Republic	n. a.	No proper amplification
P45	Austria (Lower Austria)	67.6	Single peak
P46	Austria (Lower Austria)	67.9	Single peak
P47	Austria (Lower Austria)	67.6	Single peak
P48	Austria (Lower Austria)	68.0	Single peak
P49	Austria (Lower Austria)	68.2	Single peak
P50	Slovakia	67.4	Shouldered peak
P51	North Macedonia	67.6	Single peak
P52	North Macedonia	67.5	Single peak
P53	North Macedonia	67.3	Single peak
P54	Italy	67.4	Single peak
P55	Italy	67.4	Single peak
P56	France	67.7	Shouldered peak
P57	Austria (Burgenland)	66.9-67.9	Symmetrical double peak
P58	Austria (Burgenland)	68.2	Double peak
P59	Austria (Burgenland)	68.1	Shouldered peak
P60	Austria (Vienna)	67.9	Single peak
P61	Austria (Salzburg)	67.9	Double peak
P62	Austria (Salzburg)	67.9	Double peak
P63	Austria (Salzburg)	67.5	Double peak
P64	Austria (Salzburg)	67.9	Double peak
P65	Austria (Salzburg)	67.9	Double peak
P66	Croatia	67.4	Shouldered peak
P67	Croatia	68.0	Double peak
P68	Austria (Lower Austria)	67.8	Double peak
P69	Austria (Lower Austria)	67.7	Double peak
P70	Italy (Liguria)	n. a.	No proper amplification
P71	Italy (Trentino)	67.8	Double peak
P72	Italy (Trentino)	67.5	Single peak
P73	Italy (Veneto)	67.5	Single peak
P74	Austria (Carinthia)	67.7	Double peak
P75	Austria (Carinthia)	67.9	Single peak
P76	Austria (Carinthia)	67.9	Shouldered peak
P77	Italy	67.3	Single peak
P78	Italy	67.4	Single peak
P79	Italy	n. a.	No proper amplification
P80	Italy	67.5	Shouldered peak
P81	Italy	67.7	Shouldered peak
P82	Italy	67.7	Shouldered peak
P83	Romania	67.7	Shouldered peak
P84	Germany	67.6	Single peak
P85	Austria	68.0	Double peak
P86	Austria	67.6	Single peak
P88	Italy (Sicily)	67.4	Single peak
P89	Italy (Sicily)	n. a.	No proper amplification
P90	Austria	67.5	Shouldered peak
P91	Austria (Upper Austria)	67.7	Double peak
P92	Austria (Upper Austria)	68.0	Single peak
P93	Hungary	67.4	Shouldered peak
P94	Hungary	67.4	Single peak
P96	Austria (Upper Austria)	67.8	Single peak
P97	Russia	67.5	Double peak
P98 *	Italy (Lazio)	n. a.	No proper amplification
P99 *	Italy (Lazio)	n. a.	No proper amplification
P100 *	New Zealand	n. a.	No proper amplification
P101 *	Spain	67.4	Single peak
P102 *	Greece (Crete)	n. a.	No proper amplification
P103 *	Greece (Rhodos)	n. a.	No proper amplification
P104 *	Latvia	n. a.	No proper amplification
P105 *	Nigeria	67.3	Single peak

P106 *	Yemen	67.4	Single peak
P114 *	Austria (Vorarlberg)	n. a.	No proper amplification
P115 *	Austria (Vorarlberg)	n. a.	No proper amplification
P116 *	Austria (Vorarlberg)	n. a.	No proper amplification
HP1	EU/non-EU	67.9	Shouldered peak
HP3	Austria (Upper Austria)	68.0	Double peak
HP4	Austria (Styria)	68.0	Double peak
HP5	Spain/Greece	67.9	Shouldered peak
HP6	Austria (Styria)	68.0	Double peak
HP7	Romania	67.4	Shouldered peak
HP16	Austria (Lower Austria)	68.0	Double peak
HP17	EU/non-EU	67.9	Shouldered peak
HP18	EU/non-EU	67.9	Shouldered peak
HP20	Austria	67.6	Double peak
HP22	EU/non-EU	68.1	Shouldered peak
HP23	EU/non-EU	67.9	Shouldered peak
HP24	EU/non-EU	67.9	Shouldered peak
HP25	Turkey	67.9	Single peak
HP26	Greece	67.5	Single peak
HP27	Greece	67.6	Single peak
HP28	Greece	67.5	Single peak
HP29	Greece	67.7	Single peak
HP37	Italy	67.9	Single peak
HP42	Bulgaria	67.6	Single peak
HP43	Bulgaria	67.5	Single peak
HP44	Bulgaria	67.5	Shouldered peak
HP45	Bulgaria	67.5	Single peak
HP46	Estonia	67.9	Shouldered peak
HP48	Hungary	67.6	Single peak
HP49	Hungary	67.0-67.9	Symmetrical double peak
HP50	Hungary	67.8	Shouldered peak
HP51	Hungary	68.0	Shouldered peak

Note: Tm values represent the average Tm across runs, the Tm range in case of symmetrical double peaks, or the Tm of the major peak in case of double peaks. Samples marked with an asterisk (*) are from a run that showed consistently weak amplification and were excluded from the assay performance evaluation.

Table 31

HRM results for bee samples obtained with the BEE 3_2 assay

Sample ID	Beekeeper-reported subspecies	Tm	Peak shape
PBF5.2	*A. m. carnica*	67.9	Single peak
PBF7.2	*A. m. macedonica*	67.3	Single peak
PBF8.2	*A. m. ligustica*	67.9	Single peak
PBF10.2	*A. m. carnica/ligustica* Hybrid	67.7	Single peak
PBF12.2	Alpine *A. m. carnica*	67.8	Single peak
PBF13.2	Pannonian *A. m. carnica* - Worker	68.0	Single peak
PBF16.2	*A. m. carnica*	67.7	Single peak
PBF17	*A. mellifera* (subspecies n. a.)	67.6	Single peak
PBF18.1	*A. m. ligustica* (hybridization not excluded)	67.3	Single peak
PBF18.2	*A. m. ligustica* (hybridization not excluded)	67.3	Single peak
PBF18.3	*A. m. ligustica* (hybridization not excluded)	67.6	Single peak
HPBF5.1	*A. m. carnica*	67.7	Single peak
HPBF5.1.1	*A. m. carnica*	67.7	Single peak
HPBF5.2	*A. m. carnica*	67.7	Single peak

Note: Tm values represent the average Tm across runs.

Table 32
HRM results for honey samples obtained with the BEE 6 assay

Sample ID	Geographic origin	Tm	Peak shape
P18	Spain	69.5	Single peak
P46	Austria (Lower Austria)	70.2	Single peak
P51	North Macedonia	69.4	Shouldered peak
P57	Austria (Burgenland)	69.5	Shouldered peak
P58	Austria (Burgenland)	69.5	Shouldered peak
P60	Austria (Vienna)	70.0	Shouldered peak
P61	Austria (Salzburg)	69.5	Shouldered peak
P70	Italy (Liguria)	69.3	Single peak
P71	Italy (Trentino)	69.6	Shouldered peak
P72	Italy (Trentino)	69.3	Shouldered peak
P75	Austria (Carinthia)	69.6	Shouldered peak
P88	Italy (Sicily)	69.5	Shouldered peak
P99	Italy (Lazio)	70.2	Single peak
HP20	Austria	69.5	Shouldered peak

Note: Tm values represent the average Tm across runs.

Table 33
HRM results for bee samples obtained with the BEE 6 assay

Sample ID	Beekeeper-reported subspecies	Tm	Peak shape
PBF2.1	*A. m. carnica* - Drone	70.3	Single peak
PBF7.2	*A. m. macedonica*	69.5	Single peak
PBF8.2	*A. m. ligustica*	69.5	Single peak
PBF9.2	*A. m. carnica/ligustica* Hybrid	69.5	Single peak
PBF10.2	*A. m. carnica/ligustica* Hybrid	70.3	Single peak
PBF11.2	*A. m. carnica*	69.5	Single peak
PBF12.2	*Alpine A. m. carnica*	69.5	Single peak
PBF13.2	*Pannonian A. m. carnica* - Worker	70.3	Single peak
PBF16.2	*A. m. carnica*	69.5	Single peak
PBF18.2	*A. m. ligustica* (hybridization not excluded)	69.5	Single peak

Note: Tm values represent the average Tm across runs.

Table 34
Corrections applied to PSQ SNP measurements for BEE 2_1, BEE 3_2, and BEE 6 assays

Assay	SNP	Correction type	Calculation
BEE 2_1	1	Adenine signal correction and consecutive A incorporation	Dispensation 3 * 0.9 – Dispensation 2
	2	No correction needed	n. a.
	3	No correction needed	n. a.
	4	Consecutive C incorporation	Dispensation 34 – Dispensation 32
	5	No correction needed	n. a.
	6	Consecutive C incorporation	Dispensation 44 – Dispensation 40
		Consecutive T incorporation	Dispensation 43 – 2 * Dispensation 40
BEE 3_2	1	No correction needed	n. a.
	2	Adenine signal correction and consecutive A incorporation	Dispensation 17 * 0.9 – Dispensation 16
	3	No correction needed	n. a.
	4	Consecutive C incorporation	Dispensation 33 – Dispensation 32
		Consecutive T incorporation	Dispensation 34 – Dispensation 32
	5	Adenine signal correction and consecutive A incorporation	Dispensation 35 * 0.9 – 2 * Dispensation 32
	6	Consecutive T incorporation	Dispensation 37 – Dispensation 40
BEE 6	1	No correction needed	n. a.

Table 35

PSQ results for the BEE 2_1 assay

Sample ID	SNP1		SNP2		SNP3		SNP4		SNP5		SNP6	
	% A	% G	% C	% T	%C	%T	% C	% T	%C	%T	% C	% T
HP1	55.7	44.3	61.9	38.1			27.9	72.1			81.3	18.7
HP1	54.4	45.6	63.8	36.2			29.3	70.7			70.0	30.0
HP2	67.0	33.0	68.0	32.0			22.4	77.6			82.5	17.5
HP3	72.2	27.8	98.2	1.8			0.0	100			91.8	8.2
HP4	54.9	45.1	97.8	2.2			0.0	100			97.1	2.9
HP5	98.0	2.0	5.0	95.0			79.7	20.3			0.0	100
HP5	98.5	1.5	5.1	94.9			77.8	22.2			0.0	100
HP6	58.1	41.9	98.5	1.5			0.0	100			83.1	16.9
HP6	64.5	35.5	97.9	2.1			0.0	100			94.6	5.4
HP6	65.3	34.7	97.6	2.4			0.0	100			93.3	6.7
HP6	60.9	39.1	98.2	1.8			0.0	100			91.2	8.8
HP6	59.3	40.7	98.4	1.6			0.0	100			91.8	8.2
HP6	60.9	39.1	97.9	2.1			0.0	100			91.3	8.7
HP7	65.8	34.2	80.4	19.6			13.2	86.8			71.7	28.3
HP8	23.8	76.2	98.2	1.8			0.0	100			91.9	8.1
HP9	54.8	45.2	98.0	2.0			0.0	100			90.4	9.6
HP10	40.1	59.9	97.6	2.4			0.0	100			90.2	9.8
HP11	21.6	78.4	98.1	1.9			0.0	100			88.5	11.5
HP12	33.8	66.2	67.4	32.6			22.7	77.3			90.1	9.9
HP13	49.4	50.6	64.1	35.9			29.9	70.1			64.8	35.2
HP14	9.1	90.9	98.0	2.0			0.0	100			20.8	79.2
HP15	28.4	71.6	98.3	1.7			0.0	100			98.5	1.5
HP16	33.5	66.5	98.2	1.8			0.0	100			97.2	2.8
HP17	96.3	3.7	15.7	84.3			70.1	29.9			49.6	50.4
HP18	79.0	21.0	46.1	53.9			44.6	55.4			83.5	16.5
HP19	70.4	29.6	69.1	30.9			22.8	77.2			92.0	8.0
HP20	28.5	71.5	97.8	2.2			0.0	100			86.1	13.9
HP21	16.6	83.4	97.6	2.4			0.0	100			95.0	5.0
HP22	46.8	53.2	74.3	25.7			17.8	82.2			80.1	19.9
HP23	40.9	59.1	76.3	23.7			14.7	85.3			69.2	30.8
HP24	45.6	54.4	64.0	36.0			28.3	71.7			62.2	37.8
HP25	82.5	17.5	97.9	2.1			0.0	100			86.1	13.9
HP25	40.7	59.3	97.9	2.1			0.4	99.6			95.8	4.2
HP25	40.9	59.1	97.6	2.4			0.0	100			95.0	5.0
HP25	81.5	18.5	97.8	2.2			0.0	100			85.4	14.6
HP25	81.0	19.0	98.8	1.2			0.0	100			87.9	12.1
HP25	92.9	7.1	98.2	1.8			0.0	100			89.1	10.9
HP26	98.8	1.2	98.4	1.6			0.0	100			90.7	9.3
HP26	99.0	1.0	98.2	1.8			0.0	100			88.7	11.3
HP27	98.7	1.3	97.9	2.1			0.0	100			87.6	12.4
HP28	99.0	1.0	98.3	1.7			0.0	100			87.8	12.2
HP29	98.8	1.2	98.2	1.8			0.0	100			84.3	15.7
HP30	84.5	15.5	72.7	27.3			19.8	80.2			65.6	34.4
HP31	48.7	51.3	98.4	1.6			0.0	100			86.5	13.5
HP32	43.4	56.6	98.4	1.6			0.0	100			86.0	14.0
HP33	11.9	88.1	98.3	1.7			0.0	100			44.4	55.6
HP34	90.6	9.4	98.2	1.8			0.0	100			82.3	17.7
HP35	49.9	50.1	97.7	2.3			0.0	100			81.6	18.4
HP36	70.1	29.9	97.2	2.8			0.0	100			83.6	16.4
HP37	9.2	90.8	98.0	2.0			0.9	99.1			95.6	4.4
HP37	1.4	98.6	98.2	1.8			0.0	100			79.9	20.1
HP38	46.9	53.1	95.8	4.2			0.0	100			81.8	18.2
HP39	95.1	4.9	97.8	2.2			0.0	100			78.8	21.2
HP40	21.7	78.3	97.3	2.7			0.0	100			75.6	24.4
HP41	98.3	1.7	3.5	96.5			77.4	22.6			0.0	100
HP42	88.8	11.2	98.0	2.0			0.0	100			86.6	13.4
HP43	89.2	10.8	97.2	2.8			0.0	100			80.7	19.3

HP44	93.1	6.9	92.0	8.0	3.4	96.6	79.9	20.1
HP45	94.7	5.3	97.6	2.4	0.0	100	83.9	16.1
HP45	93.7	6.3	97.7	2.3	0.0	100	79.9	20.1
HP46	27.8	72.2	96.5	3.5	0.0	100	n. a.	n. a.
HP46	29.1	70.9	97.7	2.3	0.0	100	86.3	13.7
HP47	67.5	32.5	97.2	2.8	0.0	100	72.5	27.5
HP48	93.6	6.4	98.2	1.8	0.0	100	79.3	20.7
HP49	71.7	28.3	98.1	1.9	0.0	100	84.6	15.4
HP50	26.7	73.3	94.8	5.2	1.2	98.8	91.4	8.6
HP51	44.3	55.7	97.6	2.4	0.0	100	91.2	8.8
HP55	99.1	0.9	97.0	3.0	0.0	100	74.2	25.8
HP56	98.6	1.4	96.2	3.8	0.0	100	94.2	5.8
P1	98.4	1.6	8.0	92.0	72.1	27.9	62.2	37.8
P1	97.2	2.8	8.3	91.7	73.1	26.9	64.4	35.6
P2	14.2	85.8	97.5	2.5	0.0	100	82.9	17.1
P2	5.6	94.4	97.7	2.3	0.0	100	89.2	10.8
P9	43.5	56.5	98.7	1.3	0.0	100	88.4	11.6
P9	44.2	55.8	98.8	1.2	0.0	100	100	0.0
P9	47.6	52.4	98.4	1.6	0.0	100	93.2	6.8
P10	95.3	4.7	96.7	3.3	0.0	100	77.3	22.7
P10	94.2	5.8	96.7	3.3	0.0	100	83.5	16.5
P10	95.4	4.6	97.5	2.5	0.0	100	75.0	25.0
P10	94.9	5.1	97.7	2.3	0.0	100	93.5	6.5
P11	55.0	45.0	65.3	34.7	22.3	77.7	67.5	32.5
P11	67.5	32.5	44.5	55.5	21.7	78.3	46.5	53.5
P12	44.9	55.1	92.0	8.0	6.7	93.3	87.4	12.6
P12	40.9	59.1	86.4	13.6	0.0	100	78.1	21.9
P13	86.8	13.2	75.2	24.8	15.0	85.0	74.2	25.8
P13	87.1	12.9	77.8	22.2	9.0	91.0	84.3	15.7
P14	41.7	58.3	97.6	2.4	0.0	100	75.1	24.9
P15	59.7	40.3	97.5	2.5	0.0	100	82.5	17.5
P15	49.4	50.6	97.5	2.5	0.0	100	95.6	4.4
P17	32.6	67.4	93.2	6.8	0.5	99.5	82.5	17.5
P17	40.0	60.0	92.3	7.7	0.0	100	84.0	16.0
P17	33.7	66.3	88.4	11.6	0.0	100	82.4	17.6
P18	96.8	3.2	2.5	97.5	70.4	29.6	0.0	100
P18	97.0	3.0	1.9	98.1	78.9	21.1	0.0	100
P19	91.5	8.5	49.3	50.7	42.1	57.9	41.5	58.5
P19	91.2	8.8	47.3	52.7	41.6	58.4	40.8	59.2
P19	91.5	8.5	48.2	51.8	40.1	59.9	39.1	60.9
P19	91.8	8.2	48.2	51.8	40.0	60.0	42.7	57.3
P19	92.4	7.6	49.2	50.8	40.2	59.8	40.4	59.6
P20	47.5	52.5	97.2	2.8	0.0	100	74.4	25.6
P20	49.9	50.1	97.9	2.1	0.0	100	88.4	11.6
P21	13.2	86.8	95.8	4.2	0.0	100	82.5	17.5
P21	17.1	82.9	82.7	17.3	0.0	100	89.3	10.7
P22	98.2	1.8	4.3	95.7	70.0	30.0	40.6	59.4
P23	32.5	67.5	84.7	15.3	2.9	97.1	73.5	26.5
P23	64.7	35.3	47.8	52.2	5.0	95.0	40.9	59.1
P24	89.4	10.6	97.5	2.5	0.0	100	70.9	29.1
P24	89.3	10.7	97.8	2.2	0.0	100	88.1	11.9
P25	90.2	9.8	97.5	2.5	0.0	100	85.5	14.5
P25	90.3	9.7	97.7	2.3	0.0	100	95.5	4.5
P26	98.5	1.5	97.9	2.1	0.0	100	78.9	21.1
P27	98.2	1.8	97.6	2.4	0.0	100	75.5	24.5
P28	98.9	1.1	97.0	3.0	0.0	100	88.7	11.3
P29	42.9	57.1	95.7	4.3	0.0	100	60.3	39.7
P29	39.7	60.3	96.0	4.0	0.0	100	61.3	38.7
P30	95.3	4.7	93.4	6.6	0.0	100	83.0	17.0
P31	90.6	9.4	95.0	5.0	0.0	100	73.6	26.4
P31	89.5	10.5	95.8	4.2	0.0	100	85.6	14.4
P32	70.0	30.0	62.2	37.8	0.0	100	33.8	66.2

P33	34.6	65.4	97.9	2.1	0.0	100	100	0.0
P33	39.7	60.3	97.3	2.7	0.0	100	94.3	5.7
P34	41.4	58.6	97.3	2.7	0.0	100	72.9	27.1
P35	87.2	12.8	50.8	49.2	34.1	65.9	37.9	62.1
P35	89.3	10.7	39.9	60.1	39.9	60.1	34.4	65.6
P36	62.8	37.2	96.7	3.3	0.0	100	71.7	28.3
P37	95.0	5.0	80.0	20.0	1.5	98.5	59.7	40.3
P37	96.7	3.3	22.3	77.7	2.0	98.0	14.4	85.6
P38	97.4	2.6	96.3	3.7	0.0	100	78.3	21.7
P38	91.4	8.6	95.0	5.0	0.0	100	89.3	10.7
P39	79.8	20.2	98.3	1.7	0.0	100	83.8	16.2
P40	97.0	3.0	94.4	5.6	0.0	100	77.7	22.3
P41	23.0	77.0	92.8	7.2	0.5	99.5	89.0	11.0
P42	88.4	11.6	85.6	14.4	4.0	96.0	66.3	33.7
P42	87.6	12.4	86.3	13.7	2.0	98.0	84.0	16.0
P43	73.9	26.1	96.3	3.7	1.2	98.8	94.9	5.1
P43	72.2	27.8	95.6	4.4	0.0	100	78.9	21.1
P44	82.7	17.3	93.7	6.3	0.0	100	76.7	23.3
P44	81.2	18.8	94.2	5.8	0.0	100	81.7	18.3
P45	3.3	96.7	97.9	2.1	0.0	100	89.5	10.5
P45	0.0	100	97.5	2.5	0.0	100	86.4	13.6
P45	2.2	97.8	97.8	2.2	0.0	100	92.0	8.0
P46	28.0	72.0	98.1	1.9	0.0	100	75.6	24.4
P46	5.5	94.5	97.6	2.4	0.0	100	76.2	23.8
P47	8.9	91.1	98.3	1.7	0.0	100	89.1	10.9
P47	6.5	93.5	97.5	2.5	0.0	100	84.3	15.7
P48	14.3	85.7	97.9	2.1	0.0	100	87.6	12.4
P49	8.5	91.5	98.4	1.6	0.0	100	94.6	5.4
P49	7.2	92.8	97.6	2.4	0.0	100	91.1	8.9
P49	0.0	100	97.6	2.4	0.0	100	90.1	9.9
P49	11.0	89.0	97.7	2.3	0.0	100	93.1	6.9
P50	34.8	65.2	98.2	1.8	0.0	100	93.1	6.9
P50	37.4	62.6	97.6	2.4	0.0	100	80.0	20.0
P51	97.4	2.6	98.1	1.9	0.0	100	78.4	21.6
P52	98.6	1.4	98.1	1.9	0.0	100	84.4	15.6
P53	98.9	1.1	98.2	1.8	0.0	100	81.6	18.4
P54	74.5	25.5	86.4	13.6	5.1	94.9	69.4	30.6
P55	91.1	8.9	88.9	11.1	4.1	95.9	66.2	33.8
P56	93.2	6.8	86.7	13.3	7.4	92.6	67.5	32.5
P56	93.0	7.0	85.7	14.3	4.2	95.8	67.8	32.2
P57	79.9	20.1	96.6	3.4	0.0	100	68.7	31.3
P57	78.5	21.5	96.6	3.4	0.0	100	73.5	26.5
P58	49.3	50.7	97.6	2.4	0.0	100	54.1	45.9
P59	74.1	25.9	96.4	3.6	0.5	99.5	61.8	38.2
P60	4.7	95.3	97.8	2.2	0.0	100	85.2	14.8
P60	3.7	96.3	98.0	2.0	0.0	100	88.2	11.8
P61	9.7	90.3	98.2	1.8	0.0	100	79.3	20.7
P61	6.3	93.7	97.8	2.2	0.0	100	90.2	9.8
P62	14.5	85.5	97.7	2.3	0.0	100	84.5	15.5
P63	24.7	75.3	98.0	2.0	0.0	100	61.6	38.4
P63	25.7	74.3	97.1	2.9	0.0	100	85.4	14.6
P64	22.3	77.7	98.4	1.6	0.0	100	85.4	14.6
P64	19.9	80.1	97.7	2.3	0.0	100	81.5	18.5
P65	11.1	88.9	97.7	2.3	0.0	100	73.1	26.9
P65	11.6	88.4	97.4	2.6	0.0	100	80.8	19.2
P66	64.8	35.2	96.3	3.7	0.0	100	83.7	16.3
P67	63.4	36.6	96.7	3.3	0.0	100	81.0	19.0
P68	84.6	15.4	95.9	4.1	0.0	100	63.6	36.4
P69	80.1	19.9	97.0	3.0	0.0	100	81.8	18.2
P69	79.7	20.3	98.0	2.0	0.0	100	76.5	23.5
P70	67.4	32.6	71.0	29.0	0.0	100	51.9	48.1
P71	7.4	92.6	94.6	5.4	0.0	100	19.8	80.2

P71	10.4	89.6	92.9	7.1			0.0	100			12.8	87.2
P72	53.9	46.1	83.8	16.2			2.8	97.2			65.1	34.9
P72	57.8	42.2	78.5	21.5			11.0	89.0			54.7	45.3
P73	74.0	26.0	95.2	4.8			0.0	100			82.0	18.0
P73	75.4	24.6	95.9	4.1			0.0	100			80.5	19.5
P74	80.4	19.6	95.9	4.1			0.0	100			79.7	20.3
P74	82.2	17.8	97.6	2.4			0.0	100			78.9	21.1
P75	93.2	6.8	89.3	10.7			2.9	97.1			74.8	25.2
P76	97.7	2.3	69.6	30.4			18.8	81.2			56.5	43.5
P77	96.3	3.7	95.5	4.5	6.1	93.9	1.0	99.0	4.3	95.7	87.7	12.3
P78	91.3	8.7	95.0	5.0	6.9	93.1	0.0	100	3.5	96.5	85.3	14.7
P79	21.8	78.2	97.2	2.8	4.7	95.3	0.0	100	3.6	96.4	100	0.0
P80	60.5	39.5	71.2	28.8	3.0	97.0	18.5	81.5	3.4	96.6	78.8	21.2
P81	67.5	32.5	90.0	10.0			0.0	100			86.5	13.5
P81	70.0	30.0	91.3	8.7			0.0	100			93.1	6.9
P82	74.9	25.1	92.4	7.6			0.0	100			81.0	19.0
P82	71.0	29.0	92.7	7.3			0.0	100			87.2	12.8
P83	93.8	6.2	95.4	4.6			0.0	100			81.1	18.9
P83	92.3	7.7	96.3	3.7			0.0	100			82.2	17.8
P84	90.1	9.9	92.3	7.7			3.7	96.3			79.2	20.8
P84	95.1	4.9	92.5	7.5			0.8	99.2			75.9	24.1
P85	29.4	70.6	95.7	4.3			0.0	100			96.9	3.1
P85	31.5	68.5	94.7	5.3			0.0	100			87.0	13.0
P86	93.9	6.1	40.2	59.8			45.9	54.1			31.5	68.5
P86	89.9	10.1	32.4	67.6			52.9	47.1			22.7	77.3
P88	72.9	27.1	92.3	7.7			0.0	100			81.5	18.5
P88	68.4	31.6	89.3	10.7			0.0	100			72.2	27.8
P89	97.9	2.1	88.0	12.0			2.0	98.0			75.9	24.1
P89	98.6	1.4	93.3	6.7			0.0	100			83.0	17.0
P90	87.5	12.5	93.4	6.6			0.0	100			72.3	27.7
P90	89.0	11.0	94.2	5.8	5.5	94.5	0.0	100	2.9	97.1	89.4	10.6
P91	88.5	11.5	35.7	64.3	3.4	96.6	50.8	49.2	4.0	96.0	34.7	65.3
P91	87.8	12.2	37.5	62.5			43.9	56.1			27.4	72.6
P92	10.6	89.4	97.3	2.7			0.0	100			80.9	19.1
P92	8.8	91.2	97.6	2.4	2.5	97.5	0.0	100	4.1	95.9	94.4	5.6
P93	61.5	38.5	97.5	2.5	5.2	94.8	0.0	100	3.4	96.6	99.6	0.4
P94	92.7	7.3	88.2	11.8	6.0	94.0	2.1	97.9	3.8	96.2	83.9	16.1
P96	8.4	91.6	98.0	2.0	2.3	97.7	0.0	100	3.6	96.4	97.5	2.5
P97	66.8	33.2	66.9	33.1	3.4	96.6	21.7	78.3	3.5	96.5	66.8	33.2
P98	70.3	29.7	94.7	5.3			0.0	100			72.9	27.1
P99	14.3	85.7	96.6	3.4			0.0	100			84.2	15.8
P100	5.0	95.0	97.7	2.3			0.0	100			87.5	12.5
P101	98.8	1.2	3.1	96.9			71.5	28.5			0.0	100
P102	98.7	1.3	96.5	3.5			0.0	100			79.1	20.9
P103	97.3	2.7	97.6	2.4			0.0	100			80.8	19.2
P104	35.4	64.6	94.3	5.7			0.0	100			84.4	15.6
P105	98.9	1.1	3.1	96.9			75.5	24.5			0.0	100
P106	98.8	1.2	2.3	97.7			75.2	24.8			0.0	100
P114	86.8	13.2	86.2	13.8			6.8	93.2			68.8	31.2
P115	97.0	3.0	95.3	4.7			0.0	100			76.0	24.0
P116	93.1	6.9	58.2	41.8			28.6	71.4			42.5	57.5
HPBF	4.5	95.5	98.1	1.9			0.0	100			90.3	9.7
HPBF	1.7	98.3	98.3	1.7			0.0	100			96.1	3.9
HPBF	7.1	92.9	98.5	1.5			0.0	100			100	0.0
HPBF	0.4	99.6	97.8	2.2			0.0	100			83.1	16.9
HPBF	9.7	90.3	98.3	1.7			0.0	100			91.2	8.8
HPBF	8.9	91.1	98.2	1.8			0.0	100			94.3	5.7
HPBF	6.3	93.7	98.4	1.6			0.0	100			97.7	2.3
HPBF2.1	98.5	1.5	98.1	1.9			0.0	100			65.9	34.1
HPBF2.1	98.7	1.3	97.9	2.1			0.0	100			75.6	24.4
HPBF2.2	98.5	1.5	98.3	1.7			0.0	100			77.7	22.3
HPBF3.1	99.0	1.0	97.6	2.4			0.0	100			38.6	61.4

HPBF3.1	98.7	1.3	97.2	2.8			0.0	100			74.8	25.2
HPBF3.2	98.8	1.2	97.8	2.2			0.0	100			81.5	18.5
HPBF4	12.4	87.6	96.7	3.3			0.0	100			95.4	4.6
HPBF4	1.3	98.7	98.0	2.0			0.0	100			86.9	13.1
HPBF5.1	7.1	92.9	97.8	2.2			0.0	100			91.8	8.2
HPBF5.1.1	99.0	1.0	98.1	1.9			0.0	100			85.7	14.3
HPBF5.2	98.7	1.3	97.9	2.1			0.0	100			87.0	13.0
PBF1.1	11.7	88.3	98.0	2.0			0.0	100			90.9	9.1
PBF1.1	3.7	96.3	97.6	2.4			0.0	100			90.5	9.5
PBF1.1	0.4	99.6	97.8	2.2			0.0	100			90.7	9.3
PBF1.1	0.0	100	97.9	2.1			0.0	100			90.6	9.4
PBF1.2	12.8	87.2	97.9	2.1			0.0	100			93.2	6.8
PBF2.1	6.9	93.1	98.3	1.7			0.0	100			89.0	11.0
PBF2.2	5.9	94.1	97.8	2.2			0.0	100			90.4	9.6
PBF3.1	9.6	90.4	98.3	1.7			0.0	100			93.6	6.4
PBF3.2	6.7	93.3	98.4	1.6			0.0	100			94.3	5.7
PBF4.1	10.1	89.9	98.0	2.0			0.0	100			90.5	9.5
PBF4.2	11.0	89.0	98.2	1.8			0.0	100			94.5	5.5
PBF5.1	6.8	93.2	97.7	2.3			0.0	100			98.9	1.1
PBF6.1	6.7	93.3	97.7	2.3			0.0	100			93.6	6.4
PBF7.1	98.5	1.5	97.8	2.2			0.0	100			83.1	16.9
PBF7.2	98.8	1.2	97.8	2.2			0.0	100			85.0	15.0
PBF7.2	98.8	1.2	98.2	1.8	7.4	92.6	0.0	100	2.6	97.4	89.1	10.9
PBF8.1	98.6	1.4	6.7	93.3			0.0	100			0.0	100
PBF9.1	9.1	90.9	95.3	4.7			0.0	100			0.0	100
PBF9.2	2.2	97.8	97.1	2.9			0.0	100			83.0	17.0
PBF10.1	6.0	94.0	95.9	4.1			0.0	100			83.2	16.8
PBF11.1	98.9	1.1	97.3	2.7			0.0	100			82.4	17.6
PBF12.1	98.5	1.5	95.6	4.4			0.0	100			84.4	15.6
PBF12.2	98.3	1.7	98.1	1.9	7.4	92.6	0.0	100	3.1	96.9	89.4	10.6
PBF13.1	5.4	94.6	97.2	2.8			0.0	100			85.9	14.1
PBF13.2	3.8	96.2	97.6	2.4	2.2	97.8	0.0	100	2.4	97.6	99.0	1.0
PBF14.1	98.1	1.9	96.0	4.0			0.0	100			87.4	12.6
PBF14.2	9.7	90.3	97.1	2.9			0.0	100			81.6	18.4
PBF15.1	5.5	94.5	96.1	3.9			0.0	100			87.8	12.2
PBF16.1	0.0	100	96.9	3.1			0.0	100			88.3	11.7
PBF17	4.6	95.4	98.2	1.8	2.5	97.5	0.0	100	3.0	97.0	100	0.0
PBF18.1	98.8	1.2	97.9	2.1	7.3	92.7	0.0	100	2.4	97.6	84.7	15.3
PBF18.2	98.5	1.5	98.2	1.8	4.7	95.3	0.0	100	3.4	96.6	91.6	8.4
PBF18.3	99.0	1.0	2.6	97.4	94.6	5.4	81.6	18.4	75.3	24.7	0.0	100

Table 36

PSQ results for the BEE 3_2 assay

Sample ID	SNP1		SNP2		SNP3		SNP4		SNP5		SNP6	
	%C	%T	%A	%T	%C	%T	%C	%T	%A	%G	%C	%T
HP1	41.0	59.0	29.2	70.8	11.0	89.0					10.0	90.0
HP1	40.4	59.6	30.1	69.9	9.3	90.7	9.8	90.2	53.5	46.5	4.9	95.1
HP3	26.9	73.1	0.0	100	13.1	86.9					60.2	39.8
HP4	30.7	69.3	0.0	100	13.8	86.2					15.9	84.1
HP5	3.2	96.8	38.9	61.1	12.7	87.3					11.9	88.1
HP5	2.3	97.7	41.6	58.4	10.6	89.4	48.7	51.3	53.1	46.9	6.5	93.5
HP6	38.9	61.1	0.0	100	13.5	86.5					59.3	40.7
HP7	28.0	72.0	7.7	92.3	12.2	87.8					8.0	92.0
HP16	73.9	26.1	0.0	100	11.9	88.1					29.1	70.9
HP17	4.2	95.8	65.4	34.6	12.9	87.1					15.0	85.0
HP17	3.1	96.9	70.2	29.8	9.7	90.3	10.1	89.9	36.9	63.1	4.4	95.6
HP18	16.4	83.6	52.2	47.8	16.0	84.0					14.7	85.3
HP18	15.2	84.8	50.5	49.5	10.2	89.8	5.7	94.3	31.6	68.4	4.9	95.1
HP20	78.0	22.0	0.0	100	12.4	87.6					23.5	76.5
HP22	48.5	51.5	13.8	86.2	14.2	85.8					9.6	90.4

HP22	47.3	52.7	18.3	81.7	9.9	90.1	1.5	98.5	62.8	37.2	5.4	94.6
HP23	52.1	47.9	14.9	85.1	14.2	85.8					10.9	89.1
HP23	51.0	49.0	19.3	80.7	8.7	91.3	0.0	100	57.0	43.0	4.9	95.1
HP24	47.5	52.5	24.9	75.1	12.6	87.4					8.7	91.3
HP24	49.2	50.8	26.8	73.2	9.6	90.4	1.9	98.1	69.7	30.3	4.0	96.0
HP25	8.0	92.0	0.0	100	15.1	84.9					20.4	79.6
HP26	2.2	97.8	0.0	100	16.6	83.4					8.5	91.5
HP27	2.5	97.5	0.0	100	12.1	87.9					8.4	91.6
HP28	2.7	97.3	0.0	100	14.1	85.9					7.7	92.3
HP29	1.9	98.1	0.0	100	14.6	85.4					9.0	91.0
HP37	97.0	3.0	0.0	100	10.6	89.4					8.2	91.8
HP42	10.9	89.1	0.0	100	13.8	86.2					21.2	78.8
HP43	10.6	89.4	0.0	100	16.3	83.7					9.5	90.5
HP44	8.8	91.2	0.0	100	13.9	86.1					14.7	85.3
HP45	8.9	91.1	0.0	100	15.2	84.8					9.1	90.9
HP46	81.4	18.6	0.0	100	13.1	86.9					9.7	90.3
HP46	79.8	20.2	0.0	100	9.7	90.3	0.0	100	92.4	7.6	5.2	94.8
HP48	7.3	92.7	0.0	100	13.6	86.4					7.7	92.3
HP49	27.3	72.7	0.0	100	15.7	84.3					27.2	72.8
HP50	73.2	26.8	0.0	100	17.3	82.7					11.7	88.3
HP50	75.9	24.1	0.0	100	14.0	86.0					10.5	89.5
HP51	60.6	39.4	0.0	100	12.8	87.2					24.7	75.3
P9	48.6	51.4	0.0	100	11.6	88.4	0.0	100	86.2	13.8	53.0	47.0
P10	8.0	92.0	0.0	100	14.9	85.1	0.0	100	87.2	12.8	82.3	17.7
P12	61.7	38.3	0.0	100	11.1	88.9	0.0	100	86.4	13.6	9.0	91.0
P18	3.1	96.9	72.6	27.4	13.8	86.2					12.6	87.4
P18	2.6	97.4	75.8	24.2	13.2	86.8					8.8	91.2
P18	2.7	97.3	74.8	25.2	10.3	89.7	13.0	87.0	52.8	47.2	4.6	95.4
P20	37.7	62.3	0.0	100	17.3	82.7					8.3	91.7
P20	36.8	63.2	0.0	100	14.4	85.6	0.0	100	92.8	7.2	7.6	92.4
P21	100	0.0	0.0	100	10.5	89.5	0.0	100	87.6	12.4	6.7	93.3
P22	2.4	97.6	93.5	6.5	12.4	87.6					14.4	85.6
P26	1.6	98.4	0.0	100	11.8	88.2	0.0	100	90.1	9.9	4.7	95.3
P27	2.1	97.9	0.0	100	11.6	88.4	0.0	100	89.4	10.6	5.3	94.7
P29	50.2	49.8	0.0	100	11.1	88.9	0.0	100	88.2	11.8	40.7	59.3
P33	70.5	29.5	0.0	100	12.3	87.7					5.8	94.2
P34	67.4	32.6	0.0	100	11.5	88.5	0.0	100	89.6	10.4	8.9	91.1
P36	42.9	57.1	0.0	100	11.5	88.5	0.0	100	88.7	11.3	24.5	75.5
P39	17.3	82.7	0.0	100	13.0	87.0	0.0	100	69.3	30.7	6.8	93.2
P45	100	0.0	0.0	100	16.1	83.9					10.1	89.9
P45	100	0.0	0.0	100	9.3	90.7	0.0	100	93.6	6.4	5.1	94.9
P46	94.8	5.2	0.0	100	11.6	88.4					8.2	91.8
P47	98.4	1.6	0.0	100	12.0	88.0					6.5	93.5
P47	100	0.0	2.7	97.3	25.2	74.8	0.0	100	40.4	59.6	48.0	52.0
P48	99.5	0.5	0.0	100	11.7	88.3	0.0	100	87.3	12.7	6.6	93.4
P49	100	0.0	0.0	100	15.3	84.7	0.0	100	86.9	13.1	6.7	93.3
P50	59.8	40.2	0.0	100	14.2	85.8	0.0	100	88.5	11.5	8.0	92.0
P50	61.7	38.3	0.0	100	11.7	88.3					5.5	94.5
P51	9.4	90.6	0.0	100	11.9	88.1					11.6	88.4
P51	7.3	92.7	0.0	100	13.6	86.4	0.0	100	75.9	24.1	7.5	92.5
P52	3.2	96.8	0.0	100	12.2	87.8					7.2	92.8
P53	2.1	97.9	0.0	100	13.1	86.9					7.0	93.0
P54	26.8	73.2	4.1	95.9	19.4	80.6					22.2	77.8
P55	9.2	90.8	0.0	100	11.4	88.6					7.1	92.9
P56	7.6	92.4	1.2	98.8	12.7	87.3	0.0	100	79.2	20.8	6.4	93.6
P56	9.4	90.6	1.7	98.3	16.4	83.6	0.0	100	80.0	20.0	8.7	91.3
P57	24.5	75.5	0.0	100	14.3	85.7	0.0	100	81.3	18.7	49.0	51.0
P57	26.7	73.3	0.0	100	20.0	80.0	0.0	100	80.8	19.2	49.9	50.1
P58	55.8	44.2	0.0	100	11.4	88.6	0.0	100	88.7	11.3	42.5	57.5
P59	26.5	73.5	0.0	100	12.7	87.3	0.0	100	87.1	12.9	47.5	52.5
P60	100	0.0	0.0	100	10.6	89.4	0.0	100	94.1	5.9	4.8	95.2
P60	95.0	5.0	0.1	99.9	14.5	85.5	0.0	100	87.3	12.7	9.0	91.0

P61	97.6	2.4	0.0	100	11.5	88.5	0.0	100	89.0	11.0	10.3	89.7
P61	90.6	9.4	0.0	100	19.4	80.6	27.8	72.2	86.8	13.2	17.2	82.8
P62	94.6	5.4	0.0	100	11.6	88.4	0.0	100	89.6	10.4	10.9	89.1
P63	74.0	26.0	0.0	100	10.7	89.3	0.0	100	87.7	12.3	26.8	73.2
P63	70.2	29.8	0.0	100	16.4	83.6	0.0	100	73.8	26.2	31.7	68.3
P64	87.2	12.8	0.0	100	10.5	89.5	0.0	100	89.7	10.3	20.3	79.7
P64	77.7	22.3	1.4	98.6	20.2	79.8	0.0	100	80.5	19.5	32.6	67.4
P65	97.0	3.0	0.0	100	11.1	88.9	0.0	100	87.4	12.6	11.5	88.5
P65	89.3	10.7	0.0	100	23.3	76.7	0.0	100	46.1	53.9	23.3	76.7
P66	33.8	66.2	0.0	100	12.3	87.7					22.4	77.6
P67	33.8	66.2	0.0	100	12.4	87.6	0.0	100	91.5	8.5	48.3	51.7
P68	14.2	85.8	0.0	100	13.0	87.0					75.0	25.0
P68	14.5	85.5	0.0	100	15.8	84.2	0.0	100	81.3	18.7	77.7	22.3
P69	20.6	79.4	0.0	100	11.8	88.2					63.1	36.9
P69	23.8	76.2	0.0	100	12.6	87.4	0.0	100	89.2	10.8	73.6	26.4
P70	36.0	64.0	4.0	96.0	16.3	83.7	5.0	95.0	66.6	33.4	8.2	91.8
P71	91.9	8.1	0.0	100	10.9	89.1					7.8	92.2
P71	90.9	9.1	0.0	100	15.4	84.6	0.0	100	87.2	12.8	8.9	91.1
P72	41.1	58.9	10.0	90.0	13.7	86.3					11.3	88.7
P72	59.7	40.3	0.3	99.7	30.8	69.2	0.0	100	28.1	71.9	80.3	19.7
P73	23.4	76.6	0.0	100	15.1	84.9					10.8	89.2
P73	36.5	63.5	0.0	100	21.0	79.0	0.0	100	72.8	27.2	31.8	68.2
P74	17.8	82.2	0.0	100	12.3	87.7					74.1	25.9
P74	17.6	82.4	0.0	100	13.6	86.4	0.0	100	87.3	12.7	73.0	27.0
P75	6.6	93.4	0.0	100	15.1	84.9	0.0	100	86.6	13.4	13.2	86.8
P76	3.3	96.7	6.2	93.8	11.5	88.5	0.0	100	75.0	25.0	6.6	93.4
P77	4.1	95.9	0.0	100	11.6	88.4					12.4	87.6
P78	7.4	92.6	0.0	100	12.3	87.7					6.7	93.3
P79	75.8	24.2	0.0	100	12.5	87.5	0.0	100	76.1	23.9	5.5	94.5
P80	38.3	61.7	20.2	79.8	12.2	87.8					8.6	91.4
P80	38.4	61.6	17.2	82.8	11.4	88.6	0.0	100	50.7	49.3	5.6	94.4
P81	36.8	63.2	0.0	100	16.9	83.1	0.0	100	82.3	17.7	10.3	89.7
P82	32.1	67.9	0.0	100	10.2	89.8	0.0	100	78.7	21.3	14.6	85.4
P83	10.9	89.1	0.0	100	12.7	87.3	0.0	100	87.7	12.3	21.9	78.1
P84	6.8	93.2	0.0	100	14.3	85.7	0.0	100	73.2	26.8	5.4	94.6
P85	75.2	24.8	0.0	100	10.3	89.7	0.0	100	90.3	9.7	28.3	71.7
P86	11.4	88.6	64.2	35.8	11.8	88.2	0.0	100	87.5	12.5	6.4	93.6
P88	29.0	71.0	0.0	100	10.0	90.0	0.0	100	92.6	7.4	7.9	92.1
P88	27.9	72.1	0.0	100	14.0	86.0					9.9	90.1
P88	36.8	63.2	3.9	96.1	17.7	82.3	0.0	100	88.6	11.4	14.1	85.9
P89	21.1	78.9	0.0	100	19.6	80.4					9.3	90.7
P89	74.2	25.8	0.0	100	27.0	73.0	6.8	93.2	48.7	51.3	90.2	9.8
P90	13.4	86.6	0.0	100	21.0	79.0					51.8	48.2
P90	15.1	84.9	0.0	100	22.3	77.7	0.0	100	88.9	11.1	48.9	51.1
P91	15.3	84.7	57.9	42.1	12.1	87.9					9.1	90.9
P91	31.1	68.9	51.8	48.2	17.2	82.8	0.0	100	31.3	68.7	18.8	81.2
P92	91.1	8.9	0.0	100	11.9	88.1					10.3	89.7
P92	96.4	3.6	0.0	100	19.1	80.9	1.3	98.7	56.6	43.4	44.3	55.7
P93	40.9	59.1	0.0	100	11.6	88.4					6.6	93.4
P94	9.1	90.9	1.5	98.5	12.8	87.2					8.3	91.7
P96	94.1	5.9	0.0	100	11.9	88.1					6.4	93.6
P97	34.4	65.6	18.6	81.4	16.6	83.4					22.5	77.5
P98	91.7	8.3	0.0	100	32.0	68.0	0.0	100	50.3	49.7	49.6	50.4
P99	99.0	1.0	0.0	100	25.0	75.0	0.0	100	50.3	49.7	77.5	22.5
P100	94.2	5.8	0.9	99.1	19.3	80.7	0.0	100	79.4	20.6	16.0	84.0
P101	5.6	94.4	27.8	72.2	13.5	86.5	70.8	29.2	72.7	27.3	9.8	90.2
P102	20.6	79.4	0.0	100	14.8	85.2	0.0	100	74.9	25.1	16.6	83.4
P103	7.7	92.3	0.0	100	13.4	86.6	0.0	100	88.9	11.1	9.2	90.8
P104	50.3	49.7	0.0	100	22.7	77.3	33.6	66.4	81.1	18.9	18.0	82.0
P105	6.9	93.1	90.9	9.1	12.4	87.6	6.3	93.7	63.7	36.3	7.7	92.3
P114	50.0	50.0	0.0	100	22.7	77.3	0.0	100	50.0	50.0	100	0.0
P115	100	0.0	0.0	100	36.6	63.4	66.1	33.9	100	0.0	100	0.0

P116	100	0.0	0.0	100	38.5	61.5	0.0	100	9.8	90.2	100	0.0
HPBF5.1	100	0.0	0.0	100	10.4	89.6					9.5	90.5
HPBF5.1	97.9	2.1	0.0	100	9.8	90.2	0.0	100	92.2	7.8	9.4	90.6
HPBF5.1.1	1.9	98.1	0.0	100	10.0	90.0					88.3	11.7
HPBF5.1.1	1.8	98.2	0.0	100	9.7	90.3	0.0	100	91.7	8.3	92.3	7.7
HPBF5.2	1.5	98.5	0.0	100	11.8	88.2					84.4	15.6
HPBF5.2	1.1	98.9	0.0	100	9.8	90.2	0.0	100	91.5	8.5	92.9	7.1
PBF5.2	100	0.0	0.0	100	9.7	90.3					7.1	92.9
PBF5.2	100	0.0	0.0	100	8.5	91.5	0.0	100	93.6	6.4	4.6	95.4
PBF7.2	1.7	98.3	0.0	100	10.6	89.4					5.6	94.4
PBF7.2	1.5	98.5	0.0	100	9.4	90.6	0.0	100	93.6	6.4	4.2	95.8
PBF8.2	1.5	98.5	0.0	100	12.9	87.1					11.8	88.2
PBF10.2	100	0.0	0.0	100	9.4	90.6					5.9	94.1
PBF10.2	100	0.0	0.0	100	9.8	90.2	0.0	100	92.9	7.1	5.3	94.7
PBF12.2	2.3	97.7	0.0	100	11.9	88.1					85.5	14.5
PBF12.2	1.9	98.1	0.0	100	11.7	88.3	0.0	100	87.9	12.1	92.1	7.9
PBF13.2	100	0.0	0.0	100	6.4	93.6					6.5	93.5
PBF13.2	100	0.0	0.0	100	9.3	90.7	0.0	100	92.9	7.1	5.0	95.0
PBF16.2	100	0.0	0.0	100	8.7	91.3					5.2	94.8
PBF16.2	100	0.0	0.0	100	8.1	91.9	0.0	100	94.1	5.9	4.3	95.7
PBF17	100	0.0	0.0	100	11.0	89.0					5.5	94.5
PBF17	99.7	0.3	0.0	100	8.1	91.9	0.0	100	94.1	5.9	4.3	95.7
PBF18.1	2.2	97.8	0.0	100	11.8	88.2					5.2	94.8
PBF18.1	2.4	97.6	0.0	100	8.6	91.4	0.0	100	92.2	7.8	3.8	96.2
PBF18.2	3.2	96.8	0.0	100	10.9	89.1					5.0	95.0
PBF18.2	2.7	97.3	0.0	100	9.1	90.9	0.0	100	93.6	6.4	3.8	96.2
PBF18.3	1.8	98.2	0.0	100	12.9	87.1					10.1	89.9
PBF18.3	1.7	98.3	0.0	100	10.9	89.1	100	0.0	90.6	9.4	7.1	92.9

Table 37

PSQ results for the BEE 6 assay

Sample ID	SNP1	
	%A	%G
HP20	35.9	64.1
P18	99.1	0.9
P46	5.7	94.3
P51	88.6	11.4
P57	60.8	39.2
P58	62.9	37.1
P60	44.1	55.9
P61	68.0	32.0
P70	94.9	5.1
P71	63.0	37.0
P72	81.1	18.9
P75	85.4	14.6
P88	65.6	34.4
P99	23.3	76.7
PBF2.1	2.6	97.4
PBF7.2	97.6	2.4
PBF8.2	98.5	1.5
PBF9.2	98.4	1.6
PBF10.2	2.6	97.4
PBF11.2	98.5	1.5
PBF12.2	98.3	1.7
PBF13.2	1.7	98.3
PBF16.2	97.9	2.1
PBF18.2	98.5	1.5